

**Acid Sphingomyelinase
is a critical regulator in cytotoxic granule
secretion of primary T lymphocytes**

Inaugural-Dissertation

zur

Erlangung des Doktorgrades

an der Mathematisch-Naturwissenschaftlichen Fakultät

der Universität zu Köln

vorgelegt von

Jasmin Herz

aus Bergisch Gladbach

Köln 2008

Berichterstatter: **Prof. Dr. Martin Krönke**
Prof. Dr. Jens Brüning

Tag der Disputation: 01. Juli 2008

Table of Contents

1. Introduction	1
2. Material and Methods	8
2.1 Material	
2.1.1 Mice	8
2.1.2 Virus	8
2.1.3 Cell lines	8
2.1.4 Peptide	9
2.1.5 Oligonucleotides (<i>Primer</i>)	9
2.1.6 Chemicals, media, buffers and solutions	10
2.1.7 Antibodies	12
2.1.8 Technical equipment	14
2.1.9 Kits	14
2.2 Methods	
2.2.1 Infection of adult mice with the LCMV	15
2.2.2 Preparation of LCMV-specific CD8 ⁺ T cells from spleens	15
2.2.3 Cell culture	16
2.2.4 Infection or peptide loading of target cells with LCMV	16
2.2.5 Assay for virus-specific cytotoxicity of CD8 ⁺ T cells	17
2.2.6 Stimulation or inhibition of virus-specific T lymphocytes	18
2.2.7 Flow cytometry	19
2.2.8 Assays for secretion of cytotoxic granules	20
2.2.9 pRT-PCR analysis of <i>perf</i> -, <i>gzmA</i> - and <i>B</i> -specific mRNA transcripts	22
2.2.10 Immunoblotting	23
2.2.11 Immunological synapse formation	23
2.2.12 Immunofluorescence microscopy	24
2.2.13 Electron Microscopy	24
2.2.14 Measurement of ASMase activity	25
2.2.15 Thin-layer chromatography	25
2.2.16 Measurement of the intracellular calcium-response	26
2.2.17 Measurement of intragranular pH	26
2.2.18 Two-Photon vital microscopy	27
2.2.19 Radiolabeling of CD8 ⁺ T cells with [³⁵ S]-sulfate	27
2.2.20 Patch-clamp technique	27
2.2.21 Statistical analysis	29
3. Results	30
3.1 CD8 ⁺ T cells of ASMase-deficient mice are severely impaired in perforin-dependent but not in Fas Ligand-mediated cytotoxicity	30
3.2 Impaired secretion of cytotoxic effector molecules by ASMase ^{-/-} virus-specific CTL	33
3.3 ASMase localises to lytic granules of CTL	36

3.4	Selective secretory defects of ASMase ^{-/-} CD8 ⁺ T cells.....	40
3.5	Specific inhibition of ASMase in CD8 ⁺ T cells with imipramine mimics the phenotype of ASMase ^{-/-} CTL.....	43
3.6	Membrane-lipid composition is not altered in ASMase ^{-/-} CD8 ⁺ T cells.....	46
3.7	Calcium-dependent signalling is normal in ASMase ^{-/-} T cells.....	48
3.8	Normal intragranular pH in ASMase ^{-/-} CD8 ⁺ T cells.....	50
3.9	Intracellular transport of cytotoxic granules: Polarisation to the immunological synapse and fusion with the plasma membrane.....	52
3.9	Characterisation of cytotoxic granule exocytosis in ASMase ^{-/-} CD8 ⁺ T cells.....	56
3.10	Deficiency in ASMase impairs cytotoxicity of CTL independent of the molecular size of granular matrix.....	63
3.11	Monitoring exocytosis by patch-clamp experiments reveals in ASMase ^{-/-} CD8 ⁺ T cells larger gains in membrane area than in wt T cells.....	66
4.	Discussion.....	68
5.	References.....	73
6.	Abstract.....	80
7.	Zusammenfassung.....	81
	Curriculum Vitae.....	82
	Danksagung.....	83
	Erklärung.....	84

Abbreviations

mAb	monoclonal antibody
ASMase	acid sphingomyelinase
ASMase ^{-/-}	acid sphingomyelinase deficient mice
APC	antigen presenting cell
cpm	counts per minute
CD	cluster of differentiation
CMA	concanamycin A
CTL	cytotoxic T lymphocytes
DTH	delayed type hypersensitivity reaction
EM	electron microscopy
E:T	effector : target
ELISA	enzyme linked immunosorbent assay
FACS	fluorescence activated cell sorting
FasL	Fas Ligand
Fig.	figure
GAG	glycosaminoglycane
gzm	granzyme
HPRT	hypoxanthin:guanine phosphoribosyltransferase
IFM	immunofluorescence microscopy
IFN- γ	interferon-gamma
IS	immune serum
IU	infectious unit
kDa	kilodalton
Lamp	lysosome-associated membrane protein
LCMV	Lymphocytic Choriomeningitis virus
LPC	lysophosphatidylcholine
MACS	magnetic cell sorting
MEF	mouse embryonic fibroblasts
MHC	major histocompatibility complex
MOI	multiplicity of infection
MTOC	microtubule organizing center
mRNA	messenger RNA

NK cells	natural killer cells
PBS	phosphate buffered saline
PC	phosphatidylcholine
PE	phosphatidylethanolamine
perf	perforin
PFA	paraformaldehyde
PFU	plaque forming unit
PS	phosphatidylserine
RT-PCR	reverse transcriptase PCR
SDS	sodium dodecylsulfate
SG	serglycin
SM	sphingomyelin
SMase	sphingomyelinase
SNARE	soluble N-ethylmaleimide-sensitive factor attachment receptor protein
SRB	sulforhodamine B
SV	Simian virus
TCR	T cell receptor
TEP	two-photon extracellular polar-tracer imaging
TNF	tumor necrosis-factor
WB	western blot
wt	wild type

1. Introduction

1.1 The Acid Sphingomyelinase

Sphingomyelinases catalyse the hydrolysis of sphingomyelin into ceramide and phosphorylcholine. Seven sphingomyelinases (SMases) are currently known and classified with regard to their pH-optimum, their cellular localisation or their dependency of bivalent metal ions. The Acid Sphingomyelinase (ASMase) is the most intensely characterised among the SMases (Levade and Jaffrezou 1999). ASMase is expressed ubiquitously in most mammalian cell types. Its name refers to its pH-optimum of about pH 5 and it localises to the extracellular leaflet of the plasma membrane and to the luminal leaflet of lysosomes, phagosomes and endosomes (Kanfer, Young et al. 1966; Krönke 1999; Grassmé, Schwarz et al. 2001; Schneider-Brachert, Tchikov et al. 2004). The ASMase is activated by a number of extracellular ligands binding to their specific cell-surface receptors, e.g. tumour necrosis-factor (TNF), Fas-ligand (FasL or CD95L) or interleukin (IL)-1 β (Schütze, Potthoff et al. 1992; Cifone, Roncaioli et al. 1995). Deficiency in ASMase results in accumulation of sphingomyelin in multilamellar bodies in a variety of cells, among them macrophages and neuronal cells of the cerebellum (Otterbach and Stoffel 1995). Loss of cerebellar cells leads in ASMase^{-/-} humans to Niemann-Pick Disease, type A or B, lethal in early childhood or late and adolescence, respectively. In ASMase^{-/-} mice first clinical symptoms of Niemann-Pick Disease show up at about three months and the mice die at about 9 month of age (Horinouchi, Erlich et al. 1995; Lozano, Morales et al. 2001).

Agonist-induced sphingomyelin hydrolysis by SMases is a major source of ceramide in cells. During recent years, ceramide has received great attention as a possible mediator of various cellular signalling pathways, e.g. programmed cell death, cell differentiation and proliferation (Futerman and Hannun 2004), which, however, has been disputed (Hofmann and Dixit 1998; Hofmann and Dixit 1999; Kolesnick and Hannun 1999; Perry and Hannun 1999; Watts, Aebersold et al. 1999). In fact, although direct ceramide interacting partners have been identified *in vitro* including protein kinases, protein phosphatase 2A, phospholipase A2, and cathepsin D (Zhang, Yao et al. 1997; Huwiler, Fabbro et al. 1998; Heinrich, Wickel et al. 2000; Chalfant, Szulc et al. 2004), the respective physical interaction has not been demonstrated in intact cells. In light of both, the biophysical properties of ceramide

predicting strict association with the membrane bilayer and the subcellular topology of ceramide generation, the functional consequences of possible interactions of ceramide with specific signalling proteins, especially interactions with cytosolic proteins, remained elusive.

1.2 Effects of ASMase on lipid bilayers

In consideration of the biophysical impact of sphingomyelin hydrolysis on membrane bilayers, the involvement of ASMase in cellular signalling is likely to be indirect. Sphingomyelin and cholesterol interact with each other to form detergent-resistant domains in the plasma membrane, also known as lipid rafts, which are central for the spatial organization of cell-surface receptors. Sphingomyelin hydrolysis within lipid rafts alters the composition of lipid rafts, because ceramide spontaneously self-associates and has the tendency to form ceramide-enriched membrane microdomains (Holopainen, Subramanian et al. 1998). Ceramide generation by ASMase may thus indirectly and non-specifically impact on many signalling pathways through reorganization of cell-surface receptors and their signalosomes (Bollinger, Teichgraber et al. 2005).

Moreover, for comprehensive appreciation of the impact of ASMase activity, it is important to stress that its substrate, sphingomyelin, is an important component of the outer leaflet of the plasma membrane or the intraluminal leaflet of endo-lysosomal vesicles (Futerman and Riezman 2005; Holthuis and Levine 2005). Due to this asymmetric distribution of sphingomyelin and the tendency of ceramide to separate into domains, ASMase-generated ceramide will spontaneously form negative curvatures that in turn lead to membrane invagination (**Fig. 1**) and budding as previously shown with synthetic liposomes (Holopainen, Angelova et al. 2000). The impact of ASMase activity and ceramide generation on basic membrane architecture has been implicated by our workgroup as well as by others as a possible mechanism modifying cellular signalling (Krönke 1999; Goni and Alonso 2002; Bollinger, Teichgraber et al. 2005) and was the conceptual framework of the present study.

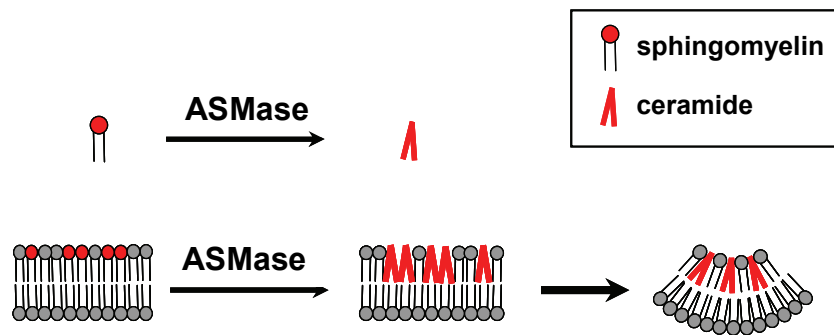


Fig. 1 Effects of ASMase on lipid bilayers

Acid Sphingomyelinase (ASMase) hydrolyses sphingomyelin into ceramide. In lipid bilayers the lipid distribution is asymmetric and generation of the cone-shape ceramide within one leaflet leads to increased surface tension, result in budding of the whole membrane with a negative curvature of the ceramide-containing leaflet.

1.3 Involvement of ASMase in immune responses

ASMase is activated by a number of pro-inflammatory cytokines like TNF, IL-1 β or IFN- γ (Schütze, Potthoff et al. 1992; Cifone, Roncaioli et al. 1995) and localises to phagosomes, lysosomes and endosomes, i.e. those organelles that are essential for bacterial uptake, inactivation and degradation as well as the processing and presentation of antigens. It has been previously shown in our workgroup that ASMase deficient macrophages are strongly impaired in their capacity to kill intracellular bacteria, which results in an increased susceptibility of ASMase^{-/-} mice to infections with e.g. *Listeria monocytogenes* or *Salmonella typhimurium* (Utermöhlen, Karow et al. 2003). On the other hand, Grassmé *et al.* showed that ASMase is required for the uptake of *Neisseria gonorrhoeae in vitro* (Grassmé, Gulbins et al. 1997) and *Pseudomonas aeruginosa in vivo* (Grassmé, Jin et al. 2006). Thus, depending on specific characteristics of pathogens, ASMase appears to contribute to various mechanisms of antibacterial defence.

1.4 Acute infection of ASMase^{-/-} mice with the Lymphocytic Choriomeningitis virus

The consequences of ASMase-deficiency on an adaptive immune response *in vivo* were studied in mice acutely infected with the Lymphocytic Choriomeningitis

virus (LCMV). The infection of mice with LCMV is one of the best characterised animal models of virus-induced cell-mediated immune responses (Buchmeier, Welsh et al. 1980; Butz and Bevan 1998; Oldstone 2002; Zinkernagel 2002). ASMase-deficient ($ASMase^{-/-}$) mice cleared acute infection with the LCMV with a significant delay from the spleen (**Fig. 2**; our unpublished observation). In adult immunocompetent mice, $CD8^{+}$ cytotoxic T lymphocytes (CTL) are necessary and sufficient to eliminate the LCMV from the spleen during acute primary infection (Buchmeier, Welsh et al. 1980; Moskophidis, Cobbold et al. 1987). Thus, the delayed elimination of LCMV suggested an impaired effector function of $CD8^{+}$ virus-specific CTL in $ASMase^{-/-}$ mice.

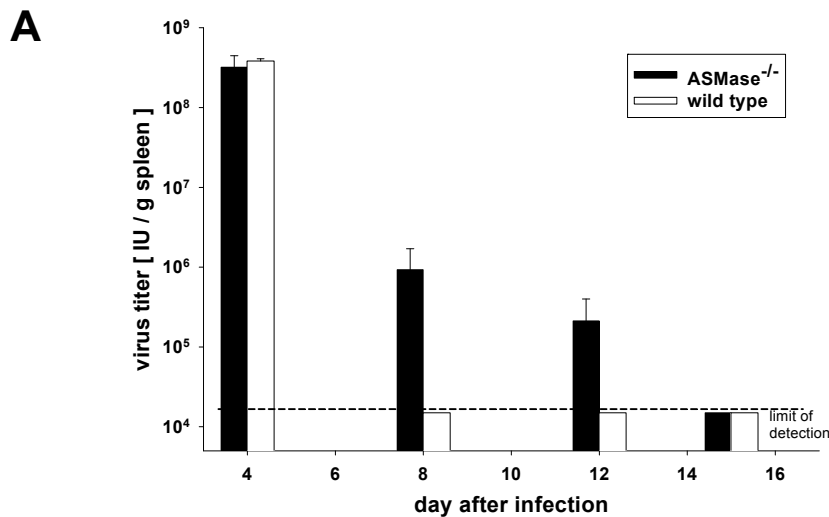


Fig. 2 Delayed clearance of the LCMV from the spleen of acutely infected $ASMase^{-/-}$ mice (unpublished data)

Mice were infected i.v. with 10^5 IU of the LCMV. At the indicated days after infection, the virus load in the spleen was measured as PFU/g spleen and converted to IU as described in Methods. Shown are the means and standard errors for groups of three mice per day. The limit of detection of the LCMV was 2×10^4 IU/g.

In my Diploma project I found, the virus-specific cytotoxic activity of $ASMase^{-/-}$ CTL to be severely impaired on day 8 after infection in comparison to wild type (wt) littermates (citation Diploma; **Fig. 3A**). Surprisingly, the absolute numbers of LCMV-specific $CD8^{+}$ T cells per spleen were found to be similar in wt and $ASMase^{-/-}$ mice on day 8 and 9 post infection (p.i.) (**Fig. 3B**). The aim of this study was to elucidate the ASMase dependent mechanism in virus-specific $CD8^{+}$ T cells.

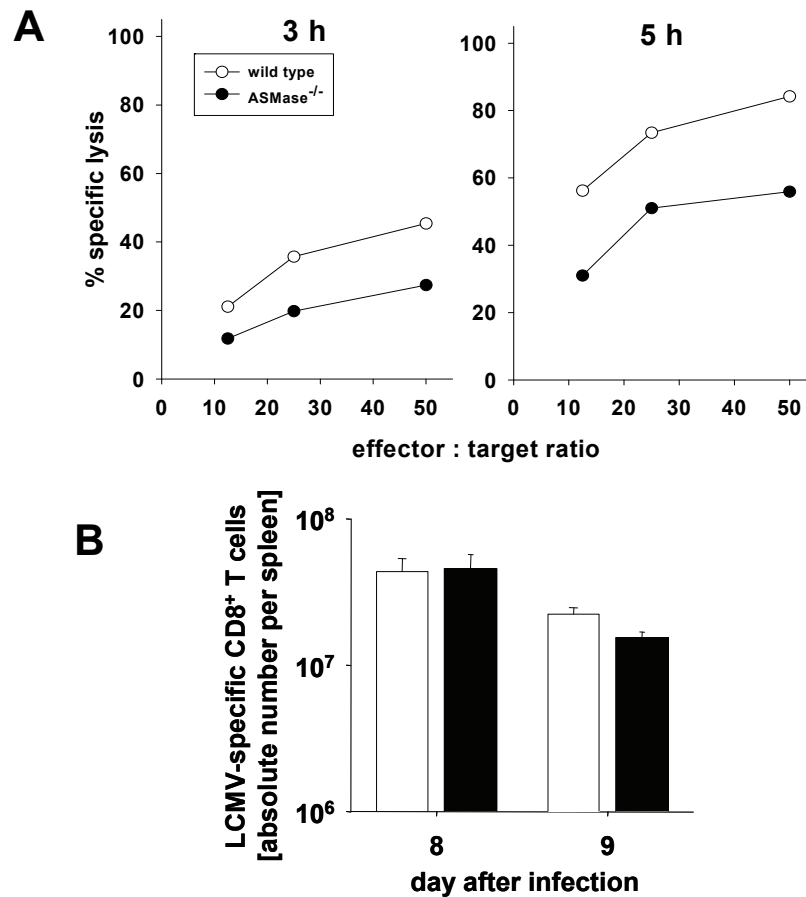


Fig. 3 LCMV-specific cytotoxic activity of ASMase^{-/-} CD8⁺ T cells is impaired despite equal numbers of LCMV-specific CD8⁺ T cells (Diploma)

Mice were infected i.v. with 10⁵ IU of the LCMV.

(A) At day 8 after infection, wild type or ASMase^{-/-} CD8⁺ T cells were enriched from splenic single cell suspensions. Cytotoxic activity of CD8⁺ T cells against LCMV infected C57BL/6 fibroblasts was determined in a 3 h or 5 h Chromium [⁵¹Cr] -release assay.

(B) Absolute numbers of CD8⁺ T cells per spleen expressing TCR-specific for the three major immunodominant epitopes gp₃₃₋₄₁, gp₂₇₆₋₂₈₆ and np₃₉₆₋₄₀₄ of the LCMV. Data were calculated from the total number of mononuclear spleen cells, the percentage of CD8⁺ spleen cells and the percentage of epitope-specific CD8⁺ spleen cells.

1.5 Cytotoxic activity of CD8⁺ T lymphocytes

CD8⁺ cytotoxic T lymphocytes induce target cell death by two distinct pathways: (i) the receptor-mediated pathway and (ii) the usually dominant granule exocytosis pathway. The receptor-mediated pathway involves activation of receptors of the TNF

family of receptors, such as Fas. Engagement of Fas receptor on the target cell surface by the Fas Ligand on the surface of the CTL leads to induction of apoptosis via multiple protein-protein interactions involving caspases. The details of the receptor-mediated pathway will not be described here (Kägi, Ledermann et al. 1994; Barry and Bleackley 2002).

The granule exocytosis pathway as major cytotoxic effector mechanism of CD8⁺ CTL depends on the exocytosis of cytotoxic granules at the immunological synapse leading to apoptosis of the target cell (Griffiths and Isaaz 1993; Henkart, Williams et al. 1997; Shresta, Pham et al. 1998; Stinchcombe and Griffiths 1999). Cytotoxic granules were identified as secretory lysosomes (Peters, Borst et al. 1991), a cellular compartment combining both, degradative as well as secretory functions. Within secretory lysosomes the major cytotoxic effector molecules perforin (perf), granzyme (gzm) A and -B are complexed to an acidified chondroitin sulfate proteoglycan matrix, which reduces the osmolarity allowing storage of cytotoxic effector molecules high concentrated (Raja, Metkar et al. 2003).

1.6 Secretion of cytotoxic granules: mechanistic steps identified so far

In CTL, exocytosis of cytotoxic granules is triggered by ligating the antigen specific T cell receptor (TCR). Upon TCR ligation, cytotoxic granules previously scattered all over the cytoplasm of the cell are polarised towards the immunological synapse, i.e. the contact zone between CTL and its target cell. Polarisation requires directed transport of cytotoxic granules, including the reorientation of the Golgi complex and the microtubule organizing center (MTOC) towards the immunological synapse. Adaptor protein 3 (AP-3) is required for the transport of cytotoxic granules along microtubules toward the MTOC close to the immunological synapse (Clark, Stinchcombe et al. 2003). The immunological synapse is comprised of an outer ring of adhesion molecules and an inner region containing signalling molecules, termed central supramolecular activation complex (cSMAC) (Stinchcombe, Bossi et al. 2001; Vyas, Maniar et al. 2002). Cytotoxic granules are secreted in the secretion zone of the inner region distinct from cSMAC.

Exocytosis of cytotoxic granules is thought to require at least four distinct steps and two molecules contributing to these have been identified so far. The first step is the release of cytotoxic granules from the microtubules. In the absence of the small GTPase Rab27a, cytotoxic granules remain connected to microtubules in the zone

directly adjacent to the immunologic synapse. This shows that Rab27a is involved in release of cytotoxic granules from microtubules (Menasche, Pastural et al. 2000; Haddad, Wu et al. 2001). After detachment from microtubules the granules are tethered and docked to the plasma membrane at the immunological synapse. Thereafter, the granule membrane fuses with the plasma membrane by virtue of soluble N-ethylmaleimide-sensitive fusion factor attachment protein receptors (SNARE) (Jahn, Lang et al. 2003). This process is regulated by Munc13-4, a member of the Munc13 family (Feldmann, Callebaut et al. 2003). It has been shown that in Munc13-4-deficient CTL, cytotoxic granules dock to the plasma membrane, but membrane fusion does not take place, completely blocking secretion of the granular contents. Finally, the contents of granules are secreted into the synaptic cleft (**Fig. 4**). Although the functions of AP-3, Rab27a, and Munc13-4 have been identified, the remaining molecular machinery responsible for this specialised secretory mechanism is by far not completely understood (Stinchcombe and Griffiths 2007).

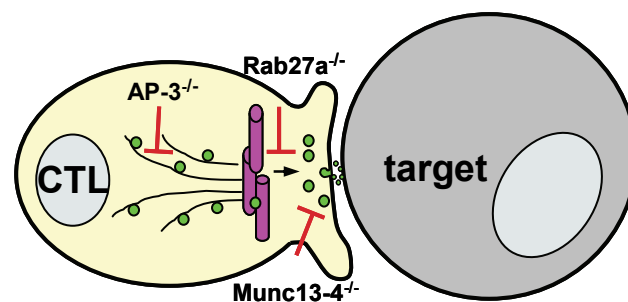


Fig. 4 Molecules involved in the polarised secretion of cytotoxic granules in CTL

In CTL (left) cytotoxic granules (green) move in a minus-end direction along microtubules towards the MTOC (purple), localised beneath the immunological synapse. Granules dock and tether to the membrane at the immunological synapse and fuse with the plasma membrane, before releasing their contents into the synaptic cleft. The illustration indicates the side of action of AP-3, Rab27a and Munc13-4. In AP-3^{-/-} CTL, cytotoxic granules do not move along microtubules. In Rab27a^{-/-} CTL, cytotoxic granules remain aligned along the microtubules. In Munc13-4^{-/-} CTL, cytotoxic granules cannot fuse with the plasma membrane.

1.8 Aim of this work

The aim of this study is to elucidate the mechanism by which ASMase contributes to effective secretion of cytotoxic granules in CD8⁺ cytotoxic T lymphocytes.

2. Material and Methods

2.1 Material

2.1.1 Mice

Breeding pairs of heterozygous Acid Sphingomyelinase-deficient ($ASMase^{-/-}$) mice were kindly provided by Richard Kolesnick (Memorial Sloan-Kettering Cancer Center, New York) and originally obtained by Prof. Edward H. Schuchmann (Mount Sinai School of Medicine, New York). $ASMase^{-/-}$ mice already backcrossed six times to the C57BL/6 background were obtained from Douglas R. Green and Tesu Lin, La Jolla Institute of Allergy and Immunology, San Diego and further backcrossed to the 10th generation. Their genotypes were analysed as described (Diploma).

Perforin-deficient ($perf^{-/-}$) C57BL/6 mice were kindly provided by Hans Hengartner, Institute of Experimental Immunology, University Hospital Zürich, Switzerland and serglycin-deficient ($SG^{-/-}$) C57BL/6 mice by Magnus Abrink, University of Agricultural Sciences, Department of Molecular Biosciences, The Biomedical Centre, Uppsala, Sweden. $ASMase^{-/-}$ mice were crossed either with $perf^{-/-}$ or $SG^{-/-}$ C57BL/6 to generate $ASMase^{-/-}/perf^{-/-}$ or $ASMase^{-/-}/SG^{-/-}$ mice.

All mice were bred and maintained under specific pathogen-free (SPF) conditions and experiments were performed in accordance with the Animal Protection Law of Germany in compliance with the Ethics Committee at the University of Cologne.

2.1.2 Virus

Lymphocytic Choriomeningitis virus (LCMV), strain WE, was propagated and titrated as plaque forming units (PFU) on murine L929 cells (Lehmann-Grube and Ambrassat 1977).

2.1.3 Cell lines

Simian virus (SV) 40 transformed C57BL/6 murine embryonic fibroblasts (MEF), EL4.F15 T cell lymphoma, MBL.2 and MBL.Fas thymic lymphoma, L1210.3 lymphocytic leukaemia (DBA subline 212 origin) and the CTL line 1.3E6 SN, are murine cell lines of C57BL/6 origin and were used as target cells or controls.

Cell lines were propagated in Dulbecco's minimal essential medium (DMEM) supplemented with 10% heat-inactivated fetal calf serum (FCS) at 37°C and 5% CO₂. For 1.3E6 SN cells, medium was supplemented with 10% rat Concanavalin A supernatant (ConA SN) and MBL.Fas were cultivated in the presence 1 mg/ml G418 for Fas-transfected cell selection. The cells were regularly treated to be free of mycoplasmas.

MBL.2, MBL.Fas, L1210.3 and 1.3E6 SN cell lines were a gift from Markus M. Simon, Max-Planck Institute for Immunobiology, University of Freiburg.

2.1.4 Peptide

The H2-D^b-restricted, LCMV glycoprotein derived peptide gp₃₃₋₄₁ (KAVYNFATC) was obtained from Biosynthan, Berlin. The lyophilised peptide was dissolved in dimethylsulfoxid (DMSO) to a 20 mg/ml stock solution.

2.1.5 Oligonucleotides (*Primer*)

The following primers were purchased from Sigma-Aldrich (Munich) or Hermann (Freiburg):

gene		sequenz
HPRT	sense:	5'GCT GGT GAA AAG GAC CTC T 3'
	antisense:	5'CAC AGG ACT AGA ACA CCT GC 3'
		amplifying a 249-bp segment
perforin	sense:	5'ACA TTC TCA AAG TCC ATC T 3'
	antisense:	5'GGG GAT CTA CAA CTT GTA CGG 3'
		amplifying a 380-bp segment
granzyme A	sense:	5'GGG GAT CTA CAA CTT GTA CGG 3'
	antisense:	5'ATT GCA GGA GTC CTT TCC ACC AC 3'
		amplifying a 291-bp segment
granzyme B	sense:	5'TCA GGC TGC TGA TCC TTG ATC G 3'
	antisense:	5'ATG AAG ATC CTC CTG CTA C 3'
		Amplifying a 135-bp segment.

2.1.6 Chemicals, media, buffers and solutions

All chemicals were of research grade and purchased from Applichem (Darmstadt), MERCK (Darmstadt), Roth (Karlsruhe) or Sigma-Aldrich (Munich) if not otherwise specified. All buffers and solutions were prepared by using deionised or bidistilled water from an EASYpure[®] UV/UF water purification unit (Werner Reinstwassersysteme, Leverkusen), sterilised by autoclaving or sterile-filtered with a 0.2 µm filter if necessary and stored at room temperature.

β-mercaptoethanol (β-ME)	0.02 M in water, stored at 4°C
bath solution for patch-clamp	145 mM NaCl, 10 mM KCl, 10 mM HEPES, 2.5 mM CaCl ₂ , 1 mM MgCl ₂ adjusted to pH 7.4 with NaOH
blocking buffer for IFM	PBS with 3% BSA and 0.1% saponin
blocking buffer for WB	5% skim milk (Oxoid, Hampshire, UK), 2% BSA in 1 x TBST, stored at -20°C
cell sorting buffer for MACS	PBS with 0.5% BSA and 2 mM EDTA
chromogenic substrates	gzmA: HD-Pro-Phe-Arg-pNA gzmB: Ac-Ile-Glu-Pro-Asp-pNA β-hexosaminidase: 4-methylbelliferyl-2-acetamido-2-deoxy-β-D-glycopyranoside (Bachem, Weil am Rhein)
concanamycin A (CMA)	0.1 mg/ml in DMSO, stored at -20°C
cultivation medium for target cells	DMEM (1 x Dulbecco's modified Eagle medium, Biochrom AG, Berlin) supplemented with 5 or 10% FCS, stored at 4°C
cultivation of splenic T cells	standard medium: RPMI (1 x VLE RPMI-1640 Medium) supplemented with 10% FCS and 1% PS, stored at 4°C for enzymatic activity measurements: MEM (Minimal essential medium, Eagle's salt) without phenol red supplemented with 2 mg/ml BSA for [³⁵ S]-labelling: sulfate-free RPMI medium containing 10% FCS, 1% PS and 50 µM β-ME
cyclosporine A	5 mg in 1 ml ethanol, stored at -20°C
cytochalasin D	2 mg in DMSO, stored at -20°C
DNA standard	1 kb ladder (BioLabs, Frankfurt am Main)
erythrocyte lysis buffer	0.2% or 1.6% NaCl in water
FACS fixation buffer	PBS with 1% paraformaldehyde (PFA) and 0.5% BSA
fixation buffer for IFM	3% PFA in PBS, stored at -20°C
FK-506	2 mg in 1 ml DMSO, stored at -20°C

fetal calf serum (FCS)	heat-inactivated at 56°C for 30 min, stored at -20°C (Biochrom AG, Berlin)
Golgi Stop reagent	contains monensin (BD Pharmingen)
imipramine	500 mM in water, stored at -20°C
Indo-1	calcium sensitive fluorescent dye (Invitrogen)
ionomycin	1 M ready to use solution in DMSO, stored at -20°C
lymphocyte lysis buffer	10 mM Tris/HCl, adjust at room temperature pH to 7.5, 0.1% triton-X-100 (v/v), store at 4°C, add Complete protease inhibitor cocktail before use (Roché)
lysis buffer for ⁵¹ Cr-release	1.6% triton-X-100 (v/v) in water
MES calibration buffer	5 mM NaCl, 115 mM KCl, 1.2 mM MgSO ₄ and 25 mM MES; adjust pH 3, 4, 5, 6, 7 and 8
[N-methyl- ¹⁴ C]-sphingomyelin	0.2 µCi/ml, specific activity 56.6 mCi/ml (Amersham)
monensin	0.1 M in ethanol, stored at -20°C
PBS	1 x Dulbecco's phosphate buffered salt solution, pH 7.4 (Biochrom AG, Berlin)
PBS / EDTA	PBS with 0.5 M EDTA for target conjugate separation
penicillin/streptomycin (PS)	penicillin (10 000 U/ml) and streptomycin (10 ng/ml) in water, stored at -20°C (Biochrom AG, Berlin)
permeabilising buffer	PBS, 0.1% w/v saponin
phorbol 12-myristate 13-acetate (PMA)	2 mg were dissolved in 1 ml DMSO and stored in the dark at -20°C
protein standard	See blue plus 2 pre-stained standard (Invitrogen, Karlsruhe) or pre-stained protein ladder 10-180 kD (Fermentas)
10 x running buffer	1 x 25 mM Tris, 192 mM glycine, 1% SDS, pH 8.3 (Bio-Rad)
sample buffer (5 x laemmli)	60 mM Tris-HCl (pH 6.8), 2% SDS-solution, 25% glycerol, 0.2% bromphenol blue and 10% β-ME added before use
sheep-erythrocyte washing buffer	HBSS (Hanks balanced salt solution), 2 mg/ml BSA, 0.01 M HEPES (pH 7.4), 8 mM CaCl ₂
sodium chromate [⁵¹ Cr]	400 µl sodium chromate (Na ₂ CrO ₄), 2 mCi/ml (Hartmann Analytics, Braunschweig)
streptavidin-PE	IFM: diluted 1:500; FACS 1:100 (Becton Dickinson),
TBS (pH 7.4)	10 mM Tris-HCl, 150 mM NaCl
TBST (pH 7.4)	1 x TBS, 0.5% Tween-20
trypan blue solution	1 x ready to use solution (Sigma-Aldrich)
trypsin-EDTA solution	10 x trypsin-EDTA solution (Biochrom AG, Berlin), made up to 1 x using sterile water

western blot transfer buffer 25 mM Tris, 192 mM glycine, 20% methanol (Roth, Darmstadt) and 0.05% SDS pH 8.3, stored at 4°C

2.1.7 Antibodies

Rabbit against murine gzmA immune serum was a gift of Markus M. Simon, Max-Planck Institute for Immunobiology, Freiburg.

antigen	Specification	provider
primary		
β-actin	chicken anti-mouse monoclonal antibody (mAb) (clone AC-15), WB 1:10 000	Sigma-Aldrich
ASMase	affinity purified goat polyclonal anti-mouse (clone A-19), IFM 1:100	Santa Cruz
CD3ε	armenian hamster (IgG _{1, κ}) anti-mouse mAb (clone 145-2C11)	BD Pharmingen
CD8a (Ly-2)	rat anti-mouse APC-, PE- or FITC-conjugated mAb (clone 53-6.7), FACS 1:100	BD Pharmingen
CD28	conjugated to paramagnetic beads, MACS syrian hamster (IgG2 _{λ,1}) anti-mouse (clone 37.51)	Miltenyi Biotec BD Pharmingen
lamp1 (CD107a)	rat (IgG2 _{a, κ}) anti-mouse purified or FITC-conjugated mAb (clone 1D4B), FACS 1:100, IFM 1:1000	BD Pharmingen
gzmA	affinity-purified rabbit anti-mouse immune serum, FACS and IFM 1:100	Markus Simon
gzmB	rat (IgG2 _a) anti-mouse mAb (clone 216315), WB 1:500	R&D Systems
	mouse (IgG1) anti-human PE-conjugated mAb (clone GB11), FACS 1:20	CALTAG Laboratories
IFN-γ	rat (IgG1) anti-mouse FITC-conjugated mAb (clone XMG1.2), IFM 1:100	BD Pharmingen
perforin	rat (IgG2 _a) anti-mouse mAb (clone KM585), WB 1:1000	Kamiya
RANTES	rat anti-mouse biotinylated mAb (clone 53405), IFM 1:100	R&D Systems

isotype controls (IC)

rabbit IgG immune serum	whole IgG (H+L) rabbit immune serum	Dianova
hamster IgG1 _k	mouse (IgG2 _{b, κ}) anti-armenian and anti-syrian hamster IgG1 mAb (clone G94-56)	BD Pharmingen
mouse IgG1	mouse IgG1 PE-conjugated mAb	CALTAG

secondary

anti-mouse HRP	anti-mouse HRP-conjugated, WB 1:5 000	Amersham
anti-rat HRP	goat anti-rat HRP-conjugated, WB 1:10 000	Amersham
anti-goat Alexa488 or -555	donkey anti-goat IgG (H+L) conjugated with Alexa-488, IFM 1:1000	Invitrogen
anti-mouse PE	affinity purified goat anti-mouse IgG1 polyclonal PE-conjugated Ab, FACS 1:100	Invitrogen
anti-rabbit Alexa594	chicken anti-rabbit IgG (H+L), conjugated with Alexa-594, IFM 1:1000	Invitrogen
anti-rabbit FITC	goat anti-rabbit IgG FITC-conjugated, intracellular FACS 1:500	Dianova
anti-rat Cy3	goat anti-rat IgG (H+L) Cy3-conjugated mAb, IFM 1:1000	Invitrogen
protein A 10 nm	protein A conjugated gold particles of 10 nm in diameter, EM	Amersham

2.1.8 Technical equipment

β -counter	1217 Rackbeta	Wallac
Blot and gel chambers	Criterion blotter	Bio-Rad
Centrifuge	5417 R	Eppendorf
	Megafuge 1.0 R	Heraeus
Confocal Microscope	DMIRE2	Leica
Developer	AGFA Curix	AGFA
ELISA-reader	MRX Tc	Dynex Technol.
ELISpot reader	System ELR02	AID Diagnostic
Flow cytometer	FACSCalibur	Becton Dickinson
Fluorescence Microscope	IX81	Olympus
Gel-photosystem	Gel-doc 2000	Bio-Rad
γ -counter	COBRA II	Canberra-Packard
Incubator	Heracell	Heraeus
Magnetic separator	Quadro MACS	Miltenyi Biotec
Microscope	Axiovert 25	Zeiss
Power supply	Power Pac 3000	Bio-Rad
Spectrophotometer	SpectraMax 190	Molecular Devices

2.1.9 Kits

BD Cytofix/Cytoperm kit	Becton Dickinson
BCA-protein assay kit	Thermo Scientific
CD8 ⁺ T cell isolation kit	Miltenyi Biotec
Diacylglycerol-kinase assay kit	GE Healthcare
ECL western blotting detection kit	GE Healthcare
ELISA mouse IFN- γ OptEIA set	Becton Dickinson
ELISA mouse RANTES DuoSet	R&D Systems
ELISpot mouse IFN- γ detection kit	R&D Systems
RNase-free DNase kit	Qiagen
RNeasy mini kit	Qiagen
SpectraMax 190	Molecular Devices
Thermocycle PTC-200 DNA-Engine	MJ Research,
UV-transluminator	Vilber Lourmat

2.2 Methods

2.2.1 Infection of adult mice with the Lymphocytic Choriomeningitis virus

For acute infection of adult mice (6 to 8 weeks of age) with the LCMV, strain WE, plaque-forming units (PFU) were converted into infectious units (IU) by multiplying PFU with a factor of 10. Mice were infected by intravenous (i.v.) inoculation of 1×10^5 IU of the LCMV in 0.3 ml PBS with 5% penicillin/streptomycin (PS) and 1% fetal calf serum (FCS) into the tail vein.

2.2.2 Preparation of LCMV-specific CD8⁺ T cells from spleens

2.2.2.1 Splenic single cell suspensions

On day 8, 9 or 30 post infection (p.i.), animals were sacrificed and their spleens were removed under sterile conditions. Single cell suspensions were obtained by gently squeezing the spleen and passing cell suspensions through a 70 μ m nylon mesh with the plunger of a 2 ml syringe. Cells were centrifuged at 1200 rpm, for 5 min at 4°C and cell pellets were resuspended in 10 ml ice cold 0.2% NaCl to lyse red blood cells. After 30 seconds, isotonic conditions were reconstituted by adding the same volume 1.6% NaCl solution to the cells. Cells were then centrifuged, the pellet resuspended in 1 ml medium and viable cells were counted by using trypan blue exclusion in a Neubauer chamber.

2.2.2.2 Magnetic cell sorting (MACS)

For positive selection, CD8⁺ T cells were enriched by MACS from splenic cell suspensions, using a CD8-specific monoclonal antibody (mAb) conjugated to paramagnetic particles following the manufacturer's instructions (Miltenyi Biotec). After 20 min the cells were washed twice and resuspended in sorting buffer. The magnetically labelled cells were retained in LS-columns, while unlabelled cells were washed out by several rinses. The retained cells were eluted from the column after removal from the magnetic field, centrifuged, resuspended in medium and counted in trypan blue solution using Neubauer chambers.

In some instances, negative selection of CD8⁺ T cells was performed by depletion of undesired cells. Non-CD8⁺ T cells were labelled and eliminated from the cell suspension according to the instructions. The non-magnetic cell fraction containing

the CD8⁺ T cells was collected and the purity of selected CD8⁺ cells was assessed by flow cytometry to be between 94–98%.

2.2.2.3 Preparations of cell-lysates

CD8⁺ T cells or control cells were washed twice in ice-cold PBS and a total of 5×10^7 cells were lysed in 1 ml lymphocyte lysis buffer, containing protease inhibitors, on ice for 60 min. Thereafter, cell lysates were cleared by centrifugation for 15 min at 2500 g and 4°C for removal of nuclei and intact cells. The protein concentration was determined by using the BCA-protein assay kit according to instructions of the manufacturer (Thermo Scientific). The supernatants were resuspended in 5 x SDS sample buffer and run on a SDS-gel (2.2.10), tested for perforin, gzmA, gzmB, hexosaminidase enzymatic activity (2.2.8) or stored at -80°C.

2.2.3 Cell culture

Cells lines were grown and maintained in incubators at 37°C, 5% CO₂ and water vapour saturated atmosphere.

Adherent SV40-transformed C57BL/6 MEF, MBL.2 and MBL.Fas lymphoma cells were maintained in tissue culture flasks and passaged weekly after trypsin-EDTA-treatment. A small number of cells was passaged in a ratio of one to five every 3 to 5 days.

For L1210.3, EL4.15 and 1.3E6 SN suspension cells, medium was removed and a fraction of the cell pellet was resuspended in fresh medium every 3 to 5 days.

To produce concanamycin A (ConA) supernatant (SN), rat spleen cells were stimulated with 5 µg/ml ConA for 2 days. Subsequently the spleen cells were treated with 20 mg/ml α-methyl-D-mannopyranosid to block residual ConA activity and the SN was prepared.

2.2.4 Infection or peptide loading of target cells with LCMV

As target cells in cytotoxicity assays, C57BL/6-SV fibroblasts infected with the LCMV strain WE were used. Cells were plated in cell culture dishes at a density of 1×10^6 and 0.5×10^6 . After 3 h adhesion, the cells were infected with LCMV at a multiplicity of infection (MOI) of 0.01 and incubated for 48 h before being used in the

assay. At the experimental day the target cells were harvested and counted in trypan blue solution using Neubauer chambers.

In some instances target cells were loaded with synthetic peptide corresponding to the major immunodominant D^b-restricted epitope (gp₃₃₋₄₁, KAVYNTATC) of the LCMV glycoprotein at a final concentration of 10⁻⁶ M for 60 min prior to the assay. The cells were frequently resuspended by pipetting to avoid aggregation.

L1210.3 B cells lymphoma were used as target cells in assays of “re-directed cytotoxicity” in the presence of anti-CD3 and anti-CD28 mAb.

2.2.5 Assay for virus-specific cytotoxicity of CD8⁺ T cells

The virus-specific cytotoxic activity of splenic CD8⁺ T cells was measured in ⁵¹Chromium ([⁵¹Cr]) -release assays according to Brunner *et al.* (Brunner, Mael *et al.* 1968) with modifications (Lehmann-Grube, Lohler *et al.* 1993).

CD8⁺ T cells were immunomagnetically enriched from splenic single cell suspensions of mice acutely infected with LCMV on day 8 p.i. as described in (2.2.2). CD8⁺ effector cells were adjusted to 3 x 10⁶ /ml in RPMI medium and 200 µl were dispensed in 96-U bottom microtiterplates in replicates of four and furthermore diluted 3-times two-fold to achieve effector to target ratios of 100:1, 50:1, 25:1 and 12.5:1.

1 x 10⁶ target cells either infected with LCMV or loaded with gp₃₃, were incubated with 50 µCi [⁵¹Cr] sodium chromate (Hartmann Analytics) for 60 min at 37°C, washed and adjusted to a density of 3 x 10⁴ cells/ml. 100 µl of target cell suspension were added to each well with effector cells. As negative controls fibroblasts without antigen were used. The spontaneous release of each [⁵¹Cr]-labelled target cells was determined in 8 wells without effector cells. In these samples the spontaneous release was less than 9% of the maximum release.

The maximal release was determined by total target cell lysis in 1.6% Triton-X-100 in water. The virus-specific cytotoxic activity of CD8⁺ T cells was determined after 4 h incubation at 37°C. For the determination of the Fas Ligand dependent lysis, the supernatants were harvested after 9.5 h incubation time. Cells were spun down and 100 µl cell-free supernatants were harvested. Supernatants from each well were measured in a gamma-counter to detect the amount of [⁵¹Cr] as counts per minute (cpm). Mean of the 4 replicates were calculated before the virus-specific lysis of

target cells was calculated with correction for background lysis, as followed for each effector to target ratio:

$$\% \text{ specific lysis} = (\text{cpm}_{\text{sample}} - \text{cpm}_{\text{spontan}}) / (\text{cpm}_{\text{maximal}} - \text{cpm}_{\text{spontan}}) \times 100$$

2.2.6 Stimulation or inhibition of virus-specific T lymphocytes

2.2.6.1 Antigen-specific stimulation of CD8⁺ T cells

For measurement of the intracellular accumulation of IFN- γ (2.2.7), the frequency of IFN- γ secreting cells (2.2.8) and the amount of secreted cytokine into the supernatant was determined (2.2.8). Splenocytes were stimulated with LCMV infected C57BL/6-SV target cells at an effector to target ratio of 10:1.

2.2.6.2 TCR-triggered degranulation of CD8⁺ T cells

For analysing gzmA secretion and polarisation of cytotoxic granules towards the target cell, enriched CD8⁺ T cells from LCMV infected mice were incubated with L1210.3 cells in the presence or absence of increasing concentrations of anti-CD3 mAb plus the same amount anti-CD28 mAb.

2.2.6.3 PMA and ionomycin induced secretion

For some experiments, CD8⁺ T cells were stimulated for different periods of time with 10 ng phorbol 12-myristate 13-acetate (PMA) and 500 ng ionomycin per ml.

2.2.6.4 Specific inhibition of perforin

To inhibit perforin, CD8⁺ T cells were pre-treated in some experiments with 200 nM concanamycin A (CMA) for 2 h before being added to target cells in the continued presence of the drug.

2.2.6.5 Inhibition of ASMase with imipramine

CD8⁺ T cells were pre-treated with graded concentrations (5-50 μ M) and for defined periods of time (1-120 min) with the specific inhibitor of ASMase, imipramine. The cells were washed three times and counted before used in experiments.

2.2.6.6 Inhibition of exocytosis

To inhibit exocytosis, CD8⁺ T cells were stimulated with PMA/ionomycin in the presence of 0.5 μ g/ml cytochalasin D, 100 nM cyclosporin A or 100 nM FK-506.

2.2.7 Flow cytometry

2.2.7.1 Surface staining

The frequency of CD8⁺ T cells among spleen cells was determined by flow cytometry. A total of 1×10^6 splenocytes was washed with PBS, 0.5% BSA and stained for 15 min with 1 μ g of fluorochrom-labelled monoclonal antibodies specific for CD8 or isotype control antibody diluted in PBS with 0.5% BSA at 4°C in the dark.

For the detection of extracellular gzmB, CD8⁺ T cells were incubated for 45 min at 4°C with a PE-conjugated mAb to human and mouse gzmB or isotype control mAb, diluted 1:20. After incubation, the cells were washed twice with cold PBS, 0.5% BSA, stained with a PE-conjugated amplifying antibody, fixated and analysed using a FACSCalibur flow cytometer (Becton Dickinson).

2.2.7.2 Intracellular staining of IFN- γ and gzmA

The accumulation of intracellular IFN- γ in CD8⁺ T cells triggered by TCR-mediated recognition of MHC-restricted epitopes of the LCMV was measured according to Assenmacher *et al.* (Assenmacher, Schmitz *et al.* 1994). 1×10^6 splenocytes of a single cell suspension of mice day 8 and 9 p.i. were incubated with the LCMV epitope gp₃₃ for 5 h. After 1 h of incubation, monensin (Golgi Stop reagent, Becton Dickinson) was added to block the secretion of vesicles loaded with IFN- γ . In the following, splenocytes were stained with antibodies specific for CD8 (2.2.7). Afterwards the cells were fixed and permeabilised with the BD Cytofix/Cytoperm kit according to the instructor's manual.

For analysis of intracellular gzmA, day 8 immune splenocytes were stained with surface markers as described above and fixed with PBS containing 2.5% PFA for 15 min at 4°C. Subsequently, cells were incubated in 100 μ l permeabilising buffer for 10 min at 4°C, then stained for 45 min at 4°C with rabbit anti-mouse gzmA immune serum or rabbit IgG isotype control (Dianova) and washed with permeabilising buffer. Afterwards, cells were stained with FITC-labelled goat anti-rabbit IgG as secondary antibody (Dianova), diluted 1:500 in permeabilising buffer and washed twice. The cells were fixed in PBS with 1% PFA, 0.5% BSA and analysed by flow cytometry.

2.2.7.3 Detection of Lamp1 (CD107a) exposure on the cell surface

Surface expression of Lamp1 (CD107a) was measured by flow cytometry as described previously (Rubio, Stuge et al. 2003). Briefly, splenic single cell suspensions of mice on day 8 after LCMV infection were co-incubated with L1210.3 target cells at a ratio of 1:1 with or without anti-CD3 mAb for 10 min at 37°C in U-bottom microtiterplates. To avoid quenching of FITC fluorescence intensity, 1 µM monensin in ethanol was given per well. 1 µl of FITC-conjugated anti-Lamp1 (CD107a) or FITC-conjugated isotype control mAb was added. Cells were harvested and washed once using PBS with 0.5 M EDTA to dissociate effector-target cell conjugates at the indicated time points. CD8⁺ T cells were stained with APC-conjugated mAb and exposure of Lamp1 on the cell surface of CD8⁺ T cells with FITC-conjugated Lamp1 monoclonal antibody. Finally, the cells were fixed using FACS fixation buffer and measured by flow cytometry.

2.2.8 Assay for secretion of cytotoxic granules

2.2.8.1 Quantifying enzymatic activity of gzmA, gzmB, β-hexosaminidase or perforin

Enzymatic activity of gzmA, gzmB and β-hexosaminidase in CD8⁺ LCMV-immune T cells was analysed by cleavage of the chromogenic substrate HD-Pro-Phe-Arg-pNA, Ac-Ile-Glu-Pro-Asp-pNA and 4-methylumbelliferyl-2-acetamido-2-deoxy-β-D-glycopyranoside (Bachem, Weil am Rhein) (Ebnet, Hausmann et al. 1995; Martin, Wallich et al. 2005) in cooperation with Julian Pardo, MPI Freiburg by spectrophotometer (SpectraMax 190, Molecular Devices, Munich) as described above at wavelength 405 nm/690 nm.

The activity of gzmA secreted by serial dilutions of wt and ASMase^{-/-} CD8⁺ T cells in response to target cells was determined after incubation with L1210.3 cells in the presence or absence of 2 µg/ml anti-CD3 monoclonal antibody at an effector to target ratio of 20:1. The cells were cultured in MEM without phenol red, supplemented with 2 mg/ml BSA to avoid FCS-mediated inhibition of released gzmA. Cell-free supernatants were harvested after 6 h.

The activity of β-hexosaminidase activity in supernatant was measured with the substrate 4-methylumbelliferyl-2-acetamido-2-deoxy-β-D-glycopyranoside in 400 mM acetate buffer, pH 4.4 containing 250 mM sucrose. The released product 4-

methylumbelliferone was measured with a fluorescence microtiterplate reader at excitation and emission wavelengths of 355 nm and 460 nm, respectively.

The lytic activity of perforin was determined by the release of haemoglobin from sheep-erythrocytes as described (Shresta, Graubert et al. 1999; Fruth, Prester et al. 1987). Serial dilutions of lysates of CD8⁺ T cells from d8 p.i LCMV infected mice were prepared by resuspending 1×10^7 CD8⁺ T cells in 100 μ l PBS with 1 mM EDTA. The cells were subjected to repeated freeze / thaw cycles and ultrasonicated 3 times for 30 sec with a break of 30 sec. The cellular debris were removed by centrifugation (5 min at 10 000 rpm at 4°C). Sheep-erythrocytes were washed twice in PBS and resuspended in HBSS buffer at 3×10^7 cells/ml. 50 μ l of CTL lysates and 150 μ l of sheep-erythrocytes in HBSS buffer were incubated in a round-bottom microtiterplate for 20 min at 37°C. After centrifugation for 10 min at 1200 rpm at 4°C, 100 μ l cell-free supernatant per well were transferred into a flat-bottom microtiterplate and the haemoglobin in the SN was quantified at 405 nm in a microtiterplate reader.

2.2.8.2 Quantification of cytokines secreted by CD8⁺ T cells

IFN- γ and RANTES secreted into the supernatant by 1×10^6 LCMV-specific CD8⁺ T cells/ml on day 8 or 9 p.i. in response to antigen-specific stimulation, were quantified in the culture supernatants after 24 h by specific enzyme-linked immunosorbent assays (ELISA) according to the instructions of the manufacturer (R&D Systems or Becton Dickinson).

2.2.8.3 Measuring the frequency of IFN- γ secreting T cells via ELISpot

1×10^6 enriched LCMV-immune CD8⁺ T cells/ml were seeded by ten-fold dilution series in polyvinyliden-difluorid (PVDF)-coated microtiterplates of a mouse IFN- γ ELISpot (R&D Systems). For antigen-specific stimulation of CD8⁺ T cells, 1×10^6 / ml of naïve wt splenocytes, pre-incubated 1 h with the gp₃₃₋₄₁ epitope at a concentration of 10^{-6} M or LCMV infected C57BL/6-SV target cell, were added. After 24 h, the cells were washed off the membrane to detect spots of IFN- γ according to the instructions of the manufacturer.

2.2.8.4 Pulse/chase labelling of cytotoxic granules with fluid phase markers

CD8⁺ T cells were enriched from the spleen on day 8 p.i. from wt and ASMase^{-/-} mice. Lysosomes were pulsed with fluid phase markers dextran of graded size i.e. 3,

70 or 500 kDa molecular weight, Alexa488-, Texas Red (TR)-, Oregon Green- or FITC- conjugated (Invitrogen, Karlsruhe) by incubating the CD8⁺ T cells with 10 µM of dextrans at a density of 1 x 10⁶ cells/ml in DMEM with 10% FCS for 2 h. Non-endocytosed fluid phase marker were removed by washing three times with PBS. Fluid phase markers were chased into cytotoxic granules by incubation in fresh culture medium for 2 h at a density of 1 x 10⁶ cells/ml. Afterwards intracellular localisation of dextrans in lysosomes was verified after staining cells specific for Lamp1 by confocal microscopy. Secretion of dextran from lysosomes was monitored after stimulation with PMA/ionomycin by flow cytometry.

Formation of conjugates between CTL and target cell was assessed after incubation of L1210.3 cells with CD8⁺ T cells for 10 min by immune-fluorescence microscopy.

2.2.9 qRT-PCR analysis of perf-, gzmA- and gzmB-specific mRNA transcripts

2.2.9.1 RNA isolation

Total RNA was extracted from LCMV-infected splenic CD8⁺ T cells, using the QIAshredder spin columns and extracted RNA was further cleaned up by using the RNeasy mini kit and the RNase-free DNase kit (all from Qiagen, Hilden).

2.2.9.2 cDNA synthesis

mRNA was transcribed by incubating total RNA with random hexamer primer (33 mM, Pharmacia, Freiburg), RNasin inhibitor (20 U, Promega, Madison, USA), dNTPs (0,5 mM, Qbiogene, Heidelberg) and Omniscript RT (4U, Qiagen, Hilden) as advised by the manufacturers and in cooperation with Julian Pardo, MPI Freiburg. The reverse transcription was performed in a Thermocycle PTC-200 DNA-Engine (MJ Research, Waltham, MA, USA). The transcription reaction profile was as follows: 37°C for 60 min and 70°C for 10 min. The resulting cDNA was used as a template for qRT-PCR hypoxanthin:guanine phosphoribosyltransferase (HPRT)-, perf-, gzmA- and gzmB-amplification.

2.2.9.3 qRT-PCR

PCR-reaction was carried out in a Thermocycler PTC-200. The PCR reaction profiles were as follows: 1 cycle at 94°C for 2.5 min as an initial denaturation step, then denaturation at 94°C for 20 sec, annealing at 56°C for HPRT or 55°C for perf,

gzmA and gzmB for 20 sec; extension at 72°C for 20 sec for HPRT or 30 sec for perf, gzmA and gzmB (35 cycles), followed by further incubation for 3 min at 72°C (1 cycle). Specific sense and antisense primers shown in **2.1.5**, were used for HPRT, perf-, gzmA- and gzmB-specific transcripts. The PCR products were analysed by gel electrophoreses (2% agarose), stained with ethidiumbromide and visualized in an UV-transluminator (Vilber Lourmat, New Ark, NJ, USA). As size marker, 1kb DNA marker was used (BioLabs, Frankfurt am Main).

2.2.10 Immunoblotting

GzmB and perforin in lysates of CD8⁺ T cells, were quantified by western blot analysis. Cell lysates of wt and ASMase^{-/-} CD8⁺ T cells (**2.2.2**) were diluted in 5-fold SDS sample buffer and boiled for 5 min at 100°C with 10% β-ME. The samples were centrifuged for 1 min at 9000 rpm and equal volumes of supernatants were loaded on a 10% polyacrylamid gel and run under standard conditions. A commercial protein-marker was used (SeeBluePlus2 pre-stained standard, Invitrogen or prestained protein ladder 10-180 kD, Fermentas) for the identification of protein sizes. After gel electrophoresis, proteins were transferred to nitrocellulose membrane (Protran 0.2 μm; Schleicher and Schuell). Free protein binding sites were blocked for 1 h with blocking buffer and perf or gzmB labelled with the primary antibodies anti-perf (KM585, Kamiya Biomedical, Seattle, USA), anti-gzmB (R&D Systems) or anti-mouse β-actin monoclonal antibody, respectively. After three times washing with TBS-T, membranes were then incubated with the appropriate horseradish peroxidase-conjugated secondary antibodies for 1 h (**2.1.7, p 9-10**), followed by washing in TBS-T and once with TBS. The immune complex was visualised by an enhanced chemiluminescence system (ECL western blotting reagent, Amersham) and detected by hyper film (Amersham ECL hyperfilm, GE healthcare).

2.2.11 Immunological synapse formation

Granule polarisation and synapse formation were studied in dextran-pulsed (**2.2.8**) or untreated CD8⁺ T cells co-incubated at 1:1 ratios with L1210.3 target cells in the presence of 3 μg/ml anti-CD3 in 1 ml complete medium. Cells were centrifuged at 500 rpm for 3 min at room temperature for synchronisation of cell contact and incubated for 10 min at 37°C. Conjugates were fixed for 30 min with 2.5% PFA by

adding the same volume 5% PFA into the sedimented cell culture and resuspended carefully after 10 min with a 1 ml pipette. Cells were washed and further processed for EM (2.2.13) or IFM (2.2.12).

2.2.12 Immunofluorescence microscopy

Fixed wt or ASMase^{-/-} CD8⁺ T cells alone or conjugated to target cells were washed with permeabilising buffer for 20 min. Cells were incubated with blocking buffer for 30 min and incubated for 30 min with primary antibodies specific for Lamp1, RANTES or IFN- γ or antisera specific for gzmA or ASMase, followed by staining with corresponding fluorescence-labelled secondary antibodies (2.1.7, p 9-10) in blocking buffer for 30 min. Nuclei were stained with DAPI (Invitrogen), mounted on glass microscopic slides in ProLong Gold anti-fading reagent (Invitrogen) and examined by fluorescence microscopy (Olympus IX81) or confocal laser scanning microscope (Leica DMIRE2). Individual cells were photographed in the focus plane with the highest fluorescence intensity. The mean number of gzmA-positive granules per cell was determined by counting multiple optical planes.

2.2.13 Electron Microscopy

For immunogold labelling, enriched CD8⁺ T cells were fixed with 4% paraformaldehyde and 0.4% glutaraldehyde in 0.2 M PHEM buffer, pH 7.4 for 2 h at room temperature. Afterwards, the cells were spun down at 3500 rpm for 10 min, resuspended in 1 ml storage solution and subsequently further processed by Eric Bos and Peter J. Peters, The Netherlands Cancer Institute, Amsterdam. The cells were processed for cryo-ultramicrotomy, embedded in 12% gelatine and infiltrated for 3 h in 2.3 M sucrose and subsequently plunge-frozen in liquid nitrogen as described (Peters, Bos et al. 2006). Ultrathin cryosections of 50 nm thickness were prepared from the frozen sections with a cryo-ultramicrotome using a 35° angle knife (Ultracut FCS, Leica). The frozen sections were allowed to thaw on a droplet of 2.3 M sucrose and transferred to a formvar-coated copper grid. Then the sections were labelled with rabbit anti mouse gzmB-specific serum for 1 h and with protein A conjugated gold particles of 10 nm in diameter (Amersham Biosciences) overnight. The labelled sections were embedded and air-dried in 2% methylcellulose containing 0.6% uranyl

acetate. Analysis was performed with a Philips CM120 microscope and digital images were made with a Keen View camera (Soft Imaging System).

Conjugates of CD8⁺ T cells and target cells were fixed in 2.5% glutaraldehyde buffered with sodium cacodylate after 10 min of co-incubation. Osmification, dehydration, embedding and sectioning were performed as described (Zentgraf and Franke 1984). Micrographs were taken with a Zeiss EM-10A electron microscope at 80 kV at the German Cancer Research Center in Heidelberg by Hans-Walter Zentgraf. A grating replica was used as a scale bar.

2.2.14 Measurement of ASMase activity

ASMase activity was determined in cooperation with Katja Wiegmann, Institute for Medical Microbiology, Immunology and Hygiene, Cologne. CD8⁺ T cells were washed twice with PBS. The pellet was resuspended in 200 µl of 0.2% triton-X-100 and incubated for 15 min at 4°C. To prepare cellular lysates, cells were homogenized and spun at 14.000 rpm. From the supernatants, 30-50 µg of protein was incubated for 2 h at 37°C in a buffer (50 µl final volume) containing 250 mM sodium acetate, 1 mM EDTA (ph 5.0) and 2.25 µl of [N-methyl-¹⁴C]-sphingomyelin (Amersham). Thereafter, the amount of radioactive phosphorylcholine produced was measured as described (Wiegmann, Schütze et al. 1994).

2.2.15 Thin-layer chromatography

The following preparations were done by Katja Wiegmann, Institute for Medical Microbiology, Immunology and Hygiene, Cologne as described (Krut, Wiegmann et al. 2006). CD8⁺ T cells were washed twice with PBS. Pellets were resuspended in 1.825 ml water and the supernatants were transferred into glass tubes. Subsequently, 6 ml of chloroform/methanol/1 N acidic acid (100/100/1, v/v/v) were added. Tubes were sonicated for 5 min in a water bath sonicator and then centrifuged for 10 min at 6000 x g. The lower organic phase was dried down under nitrogen. The dry samples were resuspended in 2 ml of 0.1 N potassium hydroxide and incubated for 1 h at 37°C (alkaline hydrolysis). 6 ml chloroform/methanol/1 N acidic acid (100/100/1, v/v/v), 1 ml of chloroform and 2.25 ml of water were added. After vortexing, the samples were centrifuged for 10 min at 6000 x g. The lower organic phase was dried down under nitrogen and resuspended in 100 µl of

chloroform followed by transfer into Eppendorf tubes. From this point, the diacylglycerol-kinase assay kit protocol was followed according to the manufacturer (GE Healthcare).

For TLC, plates were pre-run in a solvent system composed of methanol/chloroform (1:1, v/v). Plates were removed from the tank and air-dried. The TLC chambers were pre-equilibrated for 1 h at room temperature with chloroform/methanol/acidic acid (65:15:5, v/v/v). Dried samples were resuspended in 20 μ l chloroform/methanol (95:5 v/v). Samples were streaked onto 10 x 10 silica gel thin layer plate. The plates were placed in a paper-lined TLC developing tank and the solvent was allowed to migrate to the top of the plate.

2.2.16 Measurement of the intracellular calcium-response

Intracellular calcium response was analysed in cooperation with Julian Pardo, MPI Freiburg by flow cytometry. 1×10^7 splenocytes were labelled with anti-CD8 monoclonal antibody conjugated to phycoerythrin (PE) and subsequently with the calcium sensitive fluorescence dye Indo-1 according to the instructions of the manufacturer (Invitrogen) in the presence of Pluronic Acid[®] for 45 min. The calcium-response was measured for 10 min at 37°C and analysed in a LSRII FACS (Becton Dickinson) with FACS Diva software (Becton Dickinson). Release of calcium was induced by thapsigargin at a concentration of 1 μ M. To assess the total amount of intracellularly stored Ca^{2+} , thapsigargin was added at a concentration of 1 μ M. TCR was ligated with CD3-specific mAb cross-linked with anti-hamster IgG.

2.2.17 Measurement of intragranular pH

On day 8 p.i., CD8^+ T cells were enriched and cytotoxic granules were pulsed with 10 μ M FITC- and TRITC-conjugated dextrans for 2 h, washed and chased 2 h in fresh culture medium. FITC- was used as pH-dependent and TRITC-dextran as pH-independent sensor. The fluorescence intensities of test samples and samples of a standard curve were measured by flow cytometry (Vergne, Constant et al. 1998).

To acquire a pH calibration curve, cells were incubated in ice-cold MES calibration buffers of graded pH from 3 to 8 for 20 min in the presence of the ion transporters nigericin (10 μ M) and monensin (10 μ M) to equilibrate the intracellular and extracellular pH (Diwu, Chen et al. 1999; Holopainen, Saarikoski et al. 2001).

Granular pH of samples was determined by comparison with the standard curve (see Fig. 12).

2.2.18 Two-Photon vital microscopy

Two-photon Extracellular Polar-tracer (TEP) life-cell imaging was performed in cooperation with Elmon Schmelzer, MPI Cologne as described (Kasai, Hatakeyama et al. 2005). Briefly, day 8-immune splenocytes were stimulated *in vitro* for 2 days with recombinant IL-2 (10 units/ml). CD8⁺ T cells were negatively enriched using CD8⁺ T cell Isolation Kit (2.2.2), suspended in complete medium containing 25 µM FM1-43 and 500 µM sulforhodamin B (SRB; Invitrogen) and seeded into LabTek-chamber slides (Nunc) previously coated with each 3 µg/ml anti-CD3 and anti-CD28 mAb or isotype control. Microscopy was performed with a Zeiss LSM 510 microscope adjusted to laser power of 8-10 mW at an excitation wavelength of 850 nm. The fluorescence of SRB was detected at 569-665 nm and that of FM1-43 at 400-550 nm. Acquisition and image analysis were performed using Metamorph or Zeiss LSM Image Analyser software.

2.2.19 Radiolabeling of CD8⁺ T cells with [³⁵S]-sulfate

Splenic CD8⁺ T cells were labelled with [³⁵S]-sulfate according to Masson *et al.* (Masson, Peters et al. 1990). At day 30 p.i., immune splenocytes were restimulated with LCMV infected C57BL/6-SV at an effector to target ratio of 10:1 in the presence of 10% ConA SN. After three days, 3 x 10⁷ cells were biosynthetically labelled for 24 hours in 10 ml of sulphate-free RPMI medium containing 10% FCS, 1% PS and β-ME and 1 mCi of carrier-free [³⁵S]-sulfate (Hartmann Analytics, Braunschweig). Afterwards, cells were washed twice in PBS, CD8⁺ T cells were immunomagnetically enriched and chased for 2 h in fresh medium. CD8⁺ T cells were stimulated with PMA/ionomycin and the supernatants were collected at different time points. Total amounts of incorporated [³⁵S]-sulfate were determined in aliquots harvested before stimulation, lysed by adding 100 µl lysis buffer for 30 min. [³⁵S] radioactivity was quantified by scintillation counting.

2.2.20 Patch-clamp technique

CD8⁺ T cells were enriched on day 8 p.i. and subsequently further processed by Elza Kuzmenkina and Stefan Herzig, Pharmacology, University of Cologne. Briefly, cells were washed and placed in bath solution containing 145 mM NaCl, 10 mM KCl, 10 mM HEPES, 2.5 mM CaCl₂, 1mM MgCl₂ adjusted to pH 7.4 with NaOH. Patch pipettes were filled with the same solution and had resistance of 5-8 MΩ. Capacitance measurements were performed in the cell-attached configuration using Axopatch 200A amplifier (Axon Instruments, Union City, CA), controlled by PClamp6 software. The holding potential was 0 mV. Short voltage steps of 100 mV were applied with a frequency of 20 or 100 Hz. The resulting capacitive currents were filtered at 50 kHz with a four-pole low-pass Bessel filter and sampled at 200 kHz. Similar measurement parameters were used by Powell and Marrion (Powell and Marrion 2007). Exocytosis was initiated by simultaneous addition of 10 ng PMA and 500 ng ionomycin per ml, respectively. Averaged currents elicited before the exocytosis was subtracted from all recordings.

Changes in the membrane capacitance (C) were calculated by integration of the

$$\text{measured capacitive currents } (I_m): C = 1/V \int I_m dt, \quad (\text{eq. 1})$$

where V is the amplitude of the voltage step, t is the time after the voltage step, and I_m is the convolution of the evoked capacitive currents (I) and the impulse response function (IRF) of the filter: $I_m = I * IRF = \int I(t - t') IRF(t') dt'$. (eq. 2)

Because of low-pass filtering, $\int IRF(t) dt = 1$, and $C = 1/V \int I dt$. We confirmed the validity of our approach experimentally by comparing capacitance values obtained from voltage-step and voltage-ramp protocols. The characteristic time (the first moment) of the measured capacitive currents (τ_m) was defined as follows:

$$\tau_m = \int I_m t dt / \int I_m dt. \quad (\text{eq. 3})$$

$$\text{It is convenient to introduce a } C\tau_m \text{ integral, } C\tau_m = 1/V \int I_m t dt. \quad (\text{eq. 4})$$

$$\text{Thus, } \tau_m = C\tau_m / C. \quad (\text{eq. 5})$$

To reduce noise and avoid division by zero, we calculated τ_m from equation 5, using average values of C and $C\tau_m$ integrals. Because the first moment of the convolution is the sum of the first moments of the convoluted functions (Laury-Micoulaut 1976),

$$\tau_m = \tau + \tau_{IRF}, \quad (\text{eq. 6})$$

$$\text{and, thus, } \tau = \tau_m - \tau_{IRF}, \quad (\text{eq. 7})$$

where τ is our quantity of interest, the characteristic time of the evoked capacitive currents, and τ_{IRF} is the characteristic time of the IRF,

$$\tau_{IRF} = \int IRF t dt / \int IRF dt . \quad (\text{eq. 8})$$

The IRF for our 50 kHz Bessel filter was obtained as follows. We measured capacitive currents using 5 kHz filtering and 20 kHz time resolution, and then rescaled abscissas and ordinates by dividing and multiplying, respectively, by 10. With equation 8, we obtained τ_{IRF} of $5.7 \pm 0.1 \mu\text{s}$. Finally, we used C to characterize size and amount of granules, and τ to address size of fusion pores. When a single fused granule is represented by an RC circuit, $\tau = R C = C / G$, (eq. 9) where R and $G = 1/ R$ are resistance and conductance of the fusion pore, respectively. For multiple fused granules, τ is the average of τs from individual granules, weighted by their $C\text{s}$.

2.2.21 Statistical analysis

For statistical analysis, the data were subjected to two-tailed Student's t -test. P-values of $p < 0.05$, $p < 0.01$ or $p < 0.001$ are indicated by *, ** or *** respectively.

3. Results

3.1 CD8⁺ T cells of ASMase-deficient mice are severely impaired in perforin-dependent but not in Fas Ligand-mediated cytotoxicity

Based on the above summarized findings of my diploma, this study aimed at elucidating the specific function of ASMase in CTL. To confirm the impaired effector function of CTL, the LCMV-specific cytotoxic activity was determined on day 8 p.i., when the cytotoxic activity in wt mice reaches the peak level (Moskophidis, Assmann-Wischer et al. 1987). LCMV-specific CD8⁺ T cells were immunomagnetically enriched from spleens of wt and ASMase^{-/-} mice and incubated for 4 hours with C57BL/6-SV fibroblasts as target cells loaded with the viral glycoprotein 33-41 peptide (gp₃₃). This D^b-restricted gp-derived peptide induces the majority of LCMV-immune CD8⁺ T cells in C57BL/6 mice (Gairin, Mazarguil et al. 1995; Butz and Bevan 1998). Gp₃₃-specific cytotoxic activity of ASMase^{-/-} CD8⁺ T cells was significantly reduced compared to wt CD8⁺ T cells. As shown in **Fig. 4A**, ASMase^{-/-} CTL required a 4-fold higher effector to target ratio than wt CD8⁺ T cells to achieve the same degree of target cell lysis. This equals a 4-fold reduced cytotoxic activity of ASMase^{-/-}CTL.

CTL induce target cell death by two distinct pathways: (i) the granule exocytosis pathway, which results in induction of cell death via secretion of perforin and granzymes within less than 5 h or (ii) the induction of target cell apoptosis via the Fas Ligand-mediated pathway, detectably after about 8 h (Lowin, Mattman et al. 1996). To identify the effector mechanism affected by deficiency in ASMase, perforin-deficient (perf^{-/-}) and ASMase^{-/-}/perf^{-/-} mice were used. Neither perf^{-/-} nor ASMase^{-/-}/perf^{-/-} CD8⁺ T cells lysed the Fas-deficient C57BL/6-SV target cells (**Fig. 4A**). In an additional approach, inhibition of the perforin-mediated cytotoxic activity in wt and ASMase^{-/-} CTL by concanamycin A (CMA) completely abolished the lytic activity of wt and ASMase^{-/-} CD8⁺ T cells in 4 h cytotoxicity assays (**Fig. 4B**).

To assess, whether the Fas Ligand-mediated cytotoxicity was also impaired, 9.5 hours-cytotoxicity assays with Fas-deficient and Fas overexpressing target cells were performed. ASMase^{-/-} CTL lysed Fas-deficient C57BL/6-SV target cells to markedly reduced extent within 9.5 h co-incubation, confirming and extending the above described observations. Neither perf^{-/-} nor ASMase^{-/-}/perf^{-/-} lysed these target cells

despite the long incubation time (**Fig. 4C**). In contrast, Fas overexpressing MBL.2 target cells (MBL.Fas) were lysed to similar extents by wt as well as $ASMase^{-/-}$ CTL (**Fig. 4D**). Moreover, $perf^{-/-}$ and $ASMase^{-/-}/perf^{-/-}$ CTL also lysed MBL.Fas target cells effectively, indicating that the Fas Ligand-mediated cytotoxic pathway is not affected by deficiency in $ASMase$.

Together, these observations suggest a selective defect of the granule exocytosis pathway in $ASMase^{-/-}$ CTL.

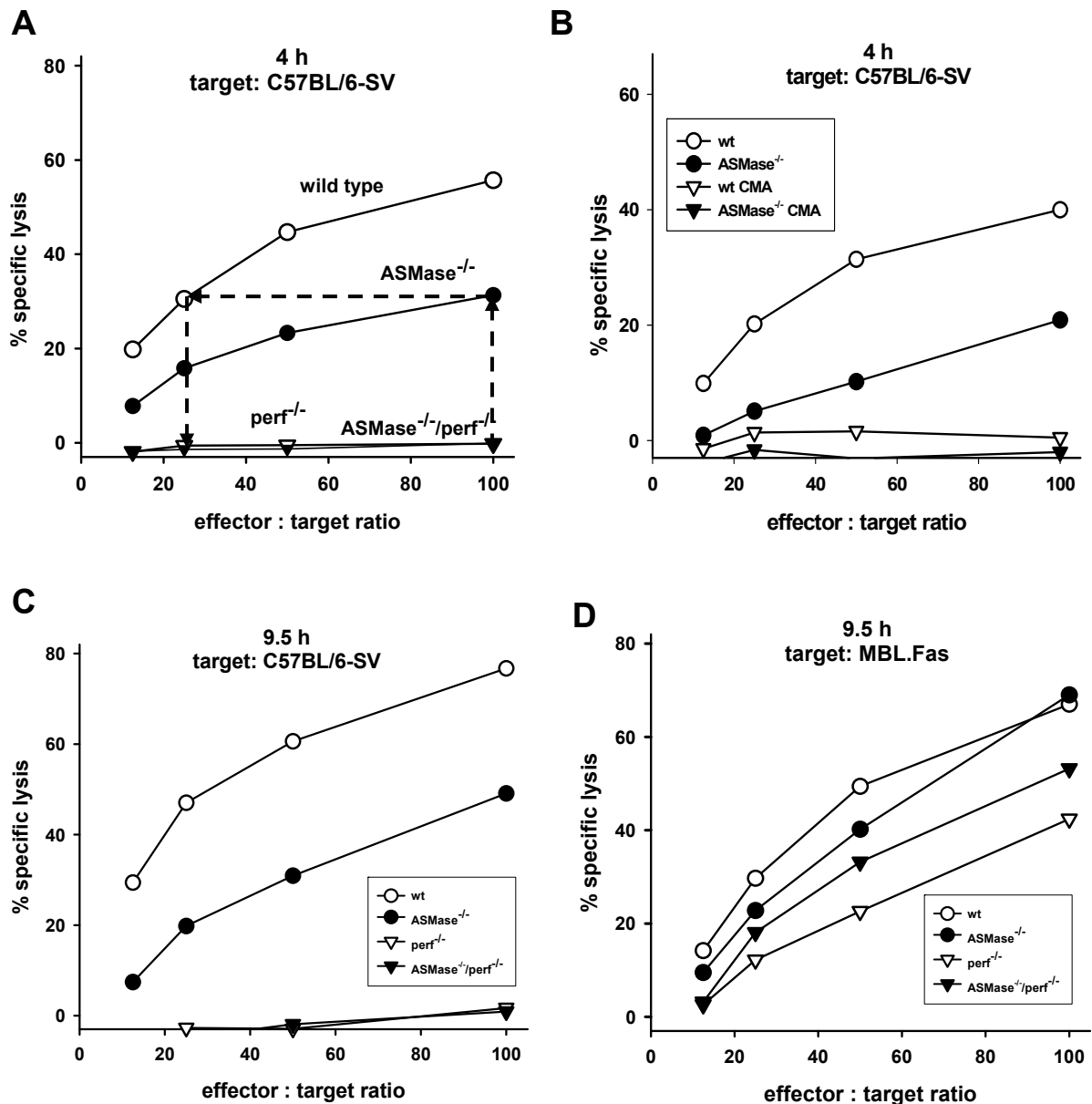


Fig. 4 Perforin-mediated cytotoxicity is severely impaired in ASMase^{-/-} CTL

Wild type (wt), ASMase^{-/-}, per^{-/-} and ASMase^{-/-}/per^{-/-} mice were infected i.v. with 10⁵ IU of the LCMV WE. At day 8 after infection, CD8⁺ T cells were immunomagnetically enriched from splenic single cell suspensions and used as effector cells in Chromium (⁵¹Cr) -release assays against target cells. Target cells were loaded with 10⁻⁶ M gp₃₃ peptide prior to the assay.

(A) Cytotoxic activity of CTL against C57BL/6 fibroblasts in a 4 h standard ⁵¹Cr-release assay.

(B) Inhibition of perforin by 200 nM concanamycin A (CMA) in wt and ASMase^{-/-} CTL in a 4 h standard ⁵¹Cr-release assay against C57BL/6-SV target cells.

(C) Cytotoxic activity of CTL against C57BL/6-SV (D) or Fas-overexpressing MBL.2 target cells in a 9.5 h ⁵¹Cr-release assay.

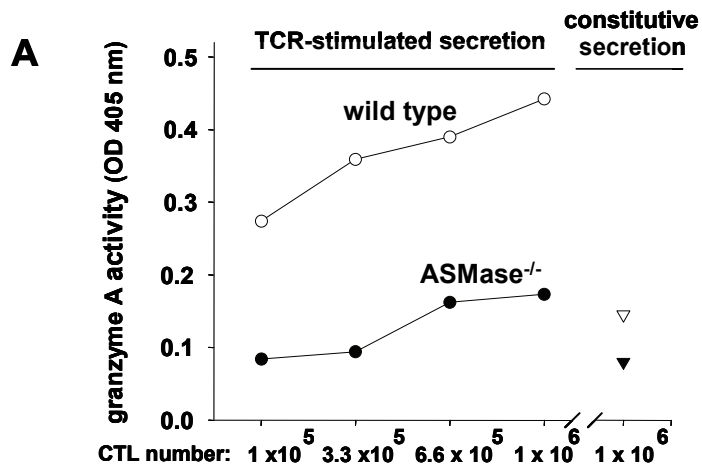
The experiments were repeated five times with similar results. Lysis of non-infected target cells was below 6% (not shown).

3.2 Impaired secretion of cytotoxic effector molecules by ASMase^{-/-} virus-specific CTL

To unravel the molecular mechanism responsible for the decreased cytotoxic activity of ASMase^{-/-} CD8⁺ T cells, the secretion of the cytotoxic effector molecules was measured. Strikingly, the amount of granzyme A (gzmA) secreted by ASMase^{-/-} CD8⁺ T cells in response to T cell receptor (TCR) ligation was drastically reduced compared to wt CD8⁺ T cells. Actually, 1×10^6 ASMase^{-/-} CD8⁺ T cells secreted less gzmA than 1×10^5 wt CD8⁺ T cells (**Fig. 5A**). Moreover, constitutive secretion of gzmA by ASMase^{-/-} CD8⁺ T cells was also reduced as compared to wt CD8⁺ T cells (**Fig. 5A, right**). Quantitative real time PCR revealed that wt and ASMase^{-/-} CD8⁺ T cells contained similar numbers of mRNA copies coding for each of the effector molecules gzmA, gzmB and perforin (**Fig. 5B**). The percentages of CD8⁺ T cells expressing gzmA as well as the mean signal intensities for this cytotoxic effector molecule were similar for wt and ASMase^{-/-} splenocytes as determined by flow cytometry of LCMV-immune CD8⁺ T cells intracellularly stained for gzmA (**Fig. 6A**). In addition, lysates of CD8⁺ T cells from wt and ASMase^{-/-} mice exerted similar gzmA- and gzmB-related proteolytic activity (**Fig. 6B**). The contents of perforin and gzmB as determined by Western blot were comparable in wt and ASMase^{-/-} CD8⁺ T cells (**Fig. 6C**). Moreover, perforin-associated lytic activity was also similar in wt and ASMase^{-/-} CD8⁺ T cells (**Fig. 6D**).

The secretion of β -hexosaminidase activity in response to TCR ligation was investigated to corroborate the impaired secretion of gzmA with a widely used independent marker of cytotoxic granules (Stinchcombe, Barral et al. 2001). As shown in **Fig. 6E**, secretion of β -hexosaminidase activity was strongly reduced in ASMase^{-/-} compared to wt CD8⁺ T cells although lysates of both cell populations contained comparable quantities of hexosaminidase activities.

Taken together, these data indicate that exocytosis of contents from cytotoxic granules is severely impaired in ASMase^{-/-} CD8⁺ T cells although the cells contain similar quantities of cytotoxic effector molecules at the level of mRNA, protein and enzymatic activity.

**B**

	number of mRNA copies per 1×10^4 CD8 ⁺ T cells		
	gzmA	gzmB	perforin
wild type	1.8×10^5	6.4×10^5	1.5×10^4
ASMase ^{-/-}	2.3×10^5	5.9×10^5	1.2×10^4

Fig. 5 Reduced secretion of granzyme A by virus-specific ASMase^{-/-} CTL

At day 8 after i.v. infection of mice with 10^5 IU LCMV, CD8⁺ T cells were immunomagnetically enriched from spleens.

(A) Granzyme A specific proteolytic activity secreted by serial dilutions of wt or ASMase^{-/-} CTL during 6 h co-incubation with L1210.3 target cells in the absence (right; constitutive secretion) and presence of 2 μ g/ml CD3 specific mAb (left; TCR-stimulated secretion). GzmA secretion assays were done in cooperation with Julian Pardo, MPI Freiburg.

(B) Expression of mRNA coding for granzyme A (gzmA), gzmB and perforin in 1×10^4 wt and ASMase^{-/-} CTL as detected by quantitative RT-PCR.

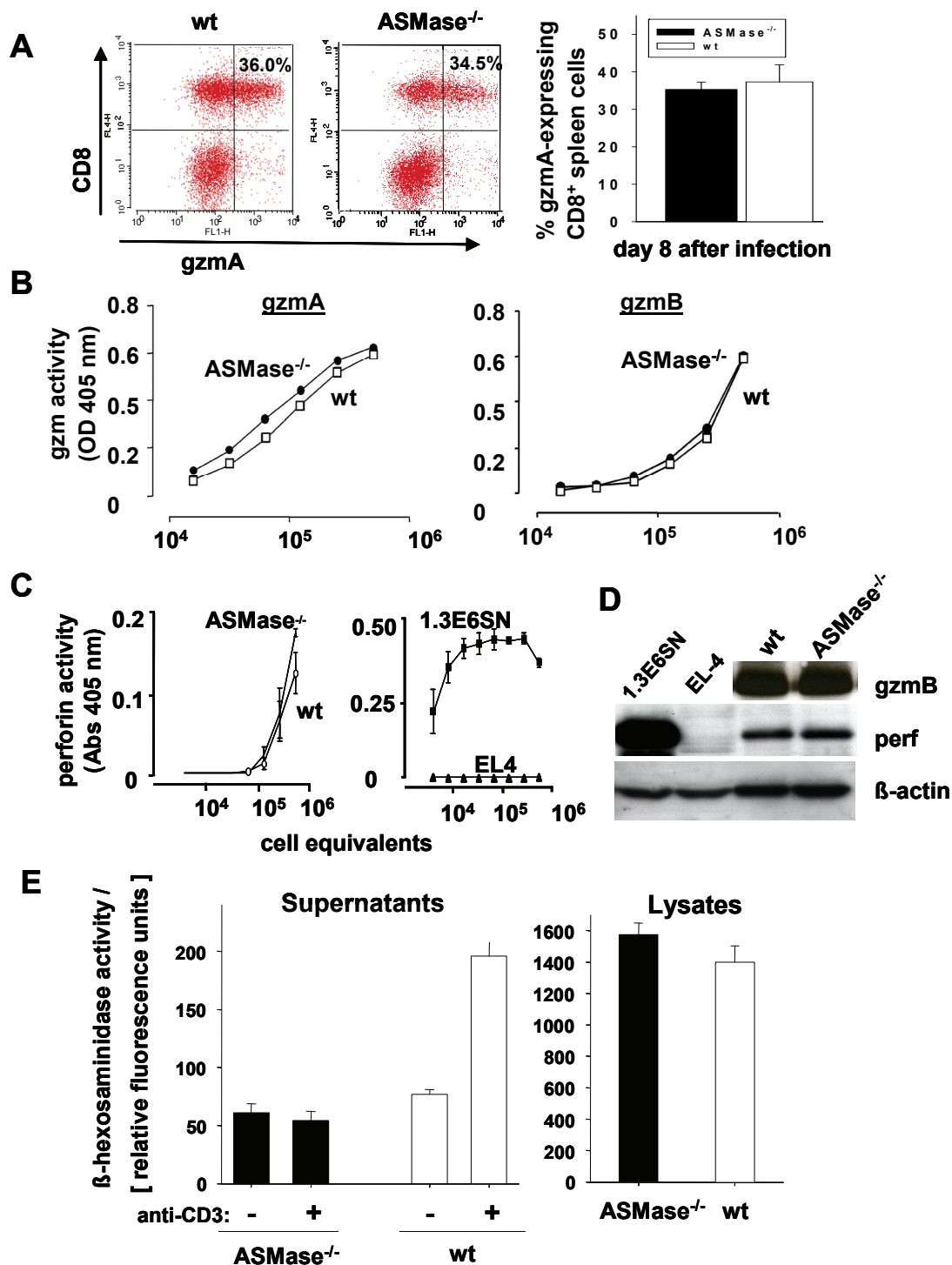


Fig. 6 Severely impaired secretion of cytotoxic effector molecules by virus-specific ASMase^{-/-} CTL

(A) Percentage of gzmA expressing CD8⁺ T cells measured by flow cytometry. Cumulative data of three independent experiments are shown as mean ± standard errors (right).

(B) GzmA- and gzmB-specific proteolytic activity in serial dilutions of lysates of wt and ASMase^{-/-} CTL.

(C) Contents of gzmB and perforin in lysates of wt and ASMase^{-/-} CTL as determined by Western blot using specific mAb. Reprobing for β-actin ensured equal loading of wt and ASMase^{-/-} protein.

(D) Perforin-associated haemolytic activity in serial dilutions of lysates of wt and ASMase^{-/-} CD8⁺ T cells. Lysates of murine CTL clone 1.3E6SN served as positive and of EL4 cells as negative control.

(E) β-hexosaminidase activity in lysates or supernatants from wt and ASMase^{-/-} CD8⁺ T cells. Supernatants were collected after 6 h co-incubation of T cells with L1210.3 target cells with or without 2 μg/ml CD3 specific mAb. Secretion of cytotoxic effector molecules has been done in cooperation with Julian Pardo, MPI Freiburg.

3.3 ASMase localises to lytic granules of CTL

The impaired secretion of cytotoxic effector molecules might be caused by misdirected loading of cytotoxic granules in ASMase^{-/-} CD8⁺ T cells. Therefore, the subcellular localisation of the cytotoxic effector molecules in CTL was determined by confocal immunofluorescence microscopy (IFM). As shown in **Fig. 7**, lysosome-associated membrane glycoprotein 1 (Lamp1/CD107a) co-localises with gzmA in vesicular structures, showing that the effector molecule is properly loaded to these compartments in a similar pattern in wt and ASMase^{-/-} CD8⁺ T cells. In wt CD8⁺ T cell granules, co-localization of gzmA and Lamp1 with ASMase was evident, showing that ASMase localises to secretory lysosomes in CTL. As expected, ASMase staining was not detectable in ASMase^{-/-} CD8⁺ T cells.

As shown in **Fig. 8A**, wt and ASMase^{-/-} CTL both contain the same average number of about five gzmA-positive granules per cell and show non-distinguishable distributions of granule numbers (**Fig. 8B**).

Proper loading of cytotoxic effector molecules was further verified by immunoelectronmicroscopy. GzmB was detectable in both wt and ASMase^{-/-} cells exclusively in membrane-surrounded structures, resembling lysosomes (**Fig. 9**). These structures are alike in wt and ASMase^{-/-} CD8⁺ T cells with regard to the size and intensity of labelling for gzmB.

Altogether, these data strongly argue against an intracellular mislocalisation of cytotoxic effector molecules in ASMase^{-/-} CTL.

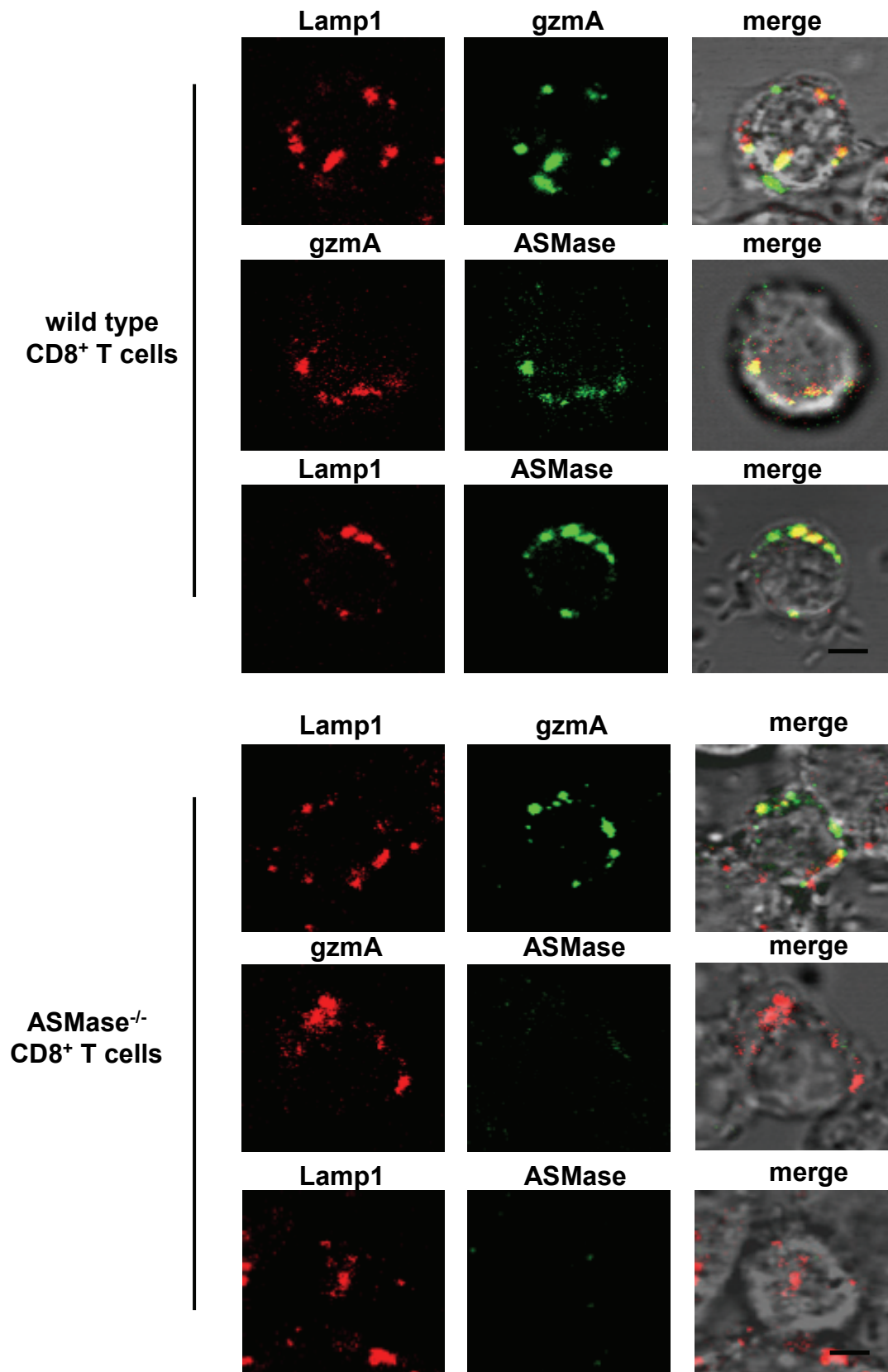


Fig. 7 ASMase localises to cytotoxic granules of CTL

Immunofluorescence microscopical images of virus-induced wt or ASMase^{-/-} CD8⁺ T cells on day 8 p.i. CTL were stained with antisera specific for gzmA or ASMase or with mAb specific for Lamp1. Bars are 5 μm.

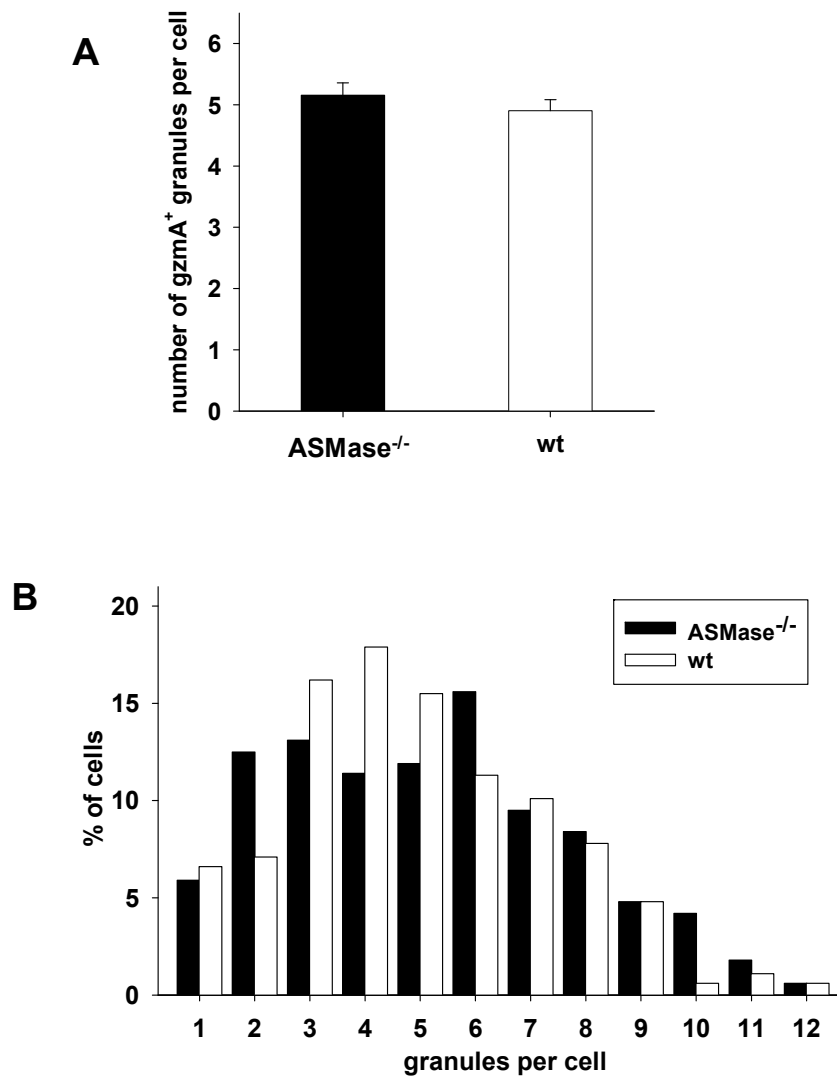


Fig. 8 Analysis of granule-numbers in wt and ASMase^{-/-} CTL

CD8⁺ T cells were intracellularly stained on day 8 after infection with gzmA specific antiserum and FITC-conjugated secondary antibody. Individual cells were photographed in the focus plane with the highest fluorescence intensity. GzmA-positive granules were counted in 167 T cells of each genotype. (A) Shown are the mean \pm standard error and (B) the frequency distribution of the number of granules per CTL as cumulative data from 2 experiments.

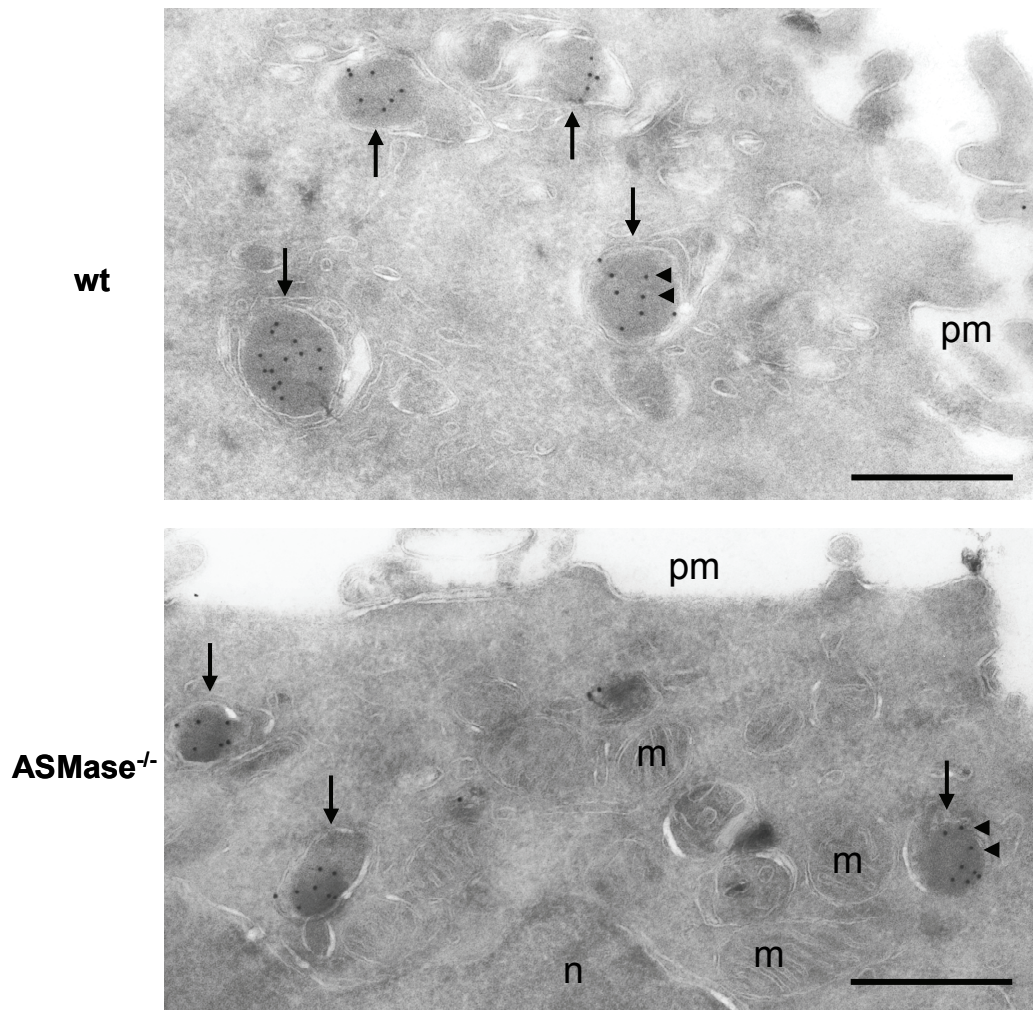


Fig. 9 Ultrastructural studies of cytototoxic granules in wt and ASMase^{-/-} CTL

On day 8 after infection, LCMV-specific CD8⁺ T cells were immunomagnetically enriched from splenic single cell suspensions and further processed by Eric Bos and Peter J. Peters, The Netherlands Cancer Institute, Amsterdam. Electron micrographs of wt and ASMase^{-/-} CTL were stained with gzmB-specific mAb and gold (10 nm)-conjugated secondary mAb.

Cytotoxic granules are indicated by *arrows*, gzmB gold labeling by *arrowheads*, mitochondria: *m*, plasma membrane: *pm* and nucleus: *n*. Scale bar is 500 nm.

3.4 Selective secretory defects of ASMase^{-/-} CD8⁺ T cells

To exclude that ASMase^{-/-} T cells are generally impaired in their secretory capacity, two further secretory pathways independent of cytotoxic granules were studied: The secretion of IFN- γ and RANTES. In ASMase^{-/-} CD8⁺ T cells, secretion of IFN- γ via the constitutive secretion pathway was significantly impaired during incubation with LCMV infected target cells as compared to wt effector cells (**Fig. 10A**). Spontaneous secretion of IFN- γ by either ASMase^{-/-} or wt CD8⁺ T cells was below the limit of detection (data not shown). Remarkably, the frequency of ASMase^{-/-} CD8⁺ T cells secreting IFN- γ was slightly, but not significantly lower, than that of wt CD8⁺ T cells as determined by ELISpot analysis (**Fig. 10B**). However, the percentages of ASMase^{-/-} and wt CD8⁺ T cells containing intracellular IFN- γ were comparable (**Fig. 10C**). This data clearly indicates that ASMase^{-/-} T cells are not impaired in the production or accumulation of IFN- γ but rather in its secretion. Fluorescence microscopy revealed that ASMase co-localises with IFN- γ (**Fig. 10D**).

In contrast, the antigen-induced secretion of RANTES via the RANTES secretory vesicle (RSV)-pathway (Catalfamo, Karpova et al. 2004) was not impaired in ASMase^{-/-} CD8⁺ T cells (**Fig. 11A**). RANTES localises to vesicles clearly distinct from ASMase-positive cytotoxic granules (**Fig. 11B**). Thus, ASMase is selectively involved in the cytotoxic granule as well as in the constitutive secretion pathway of IFN- γ but not in the secretion of RANTES.

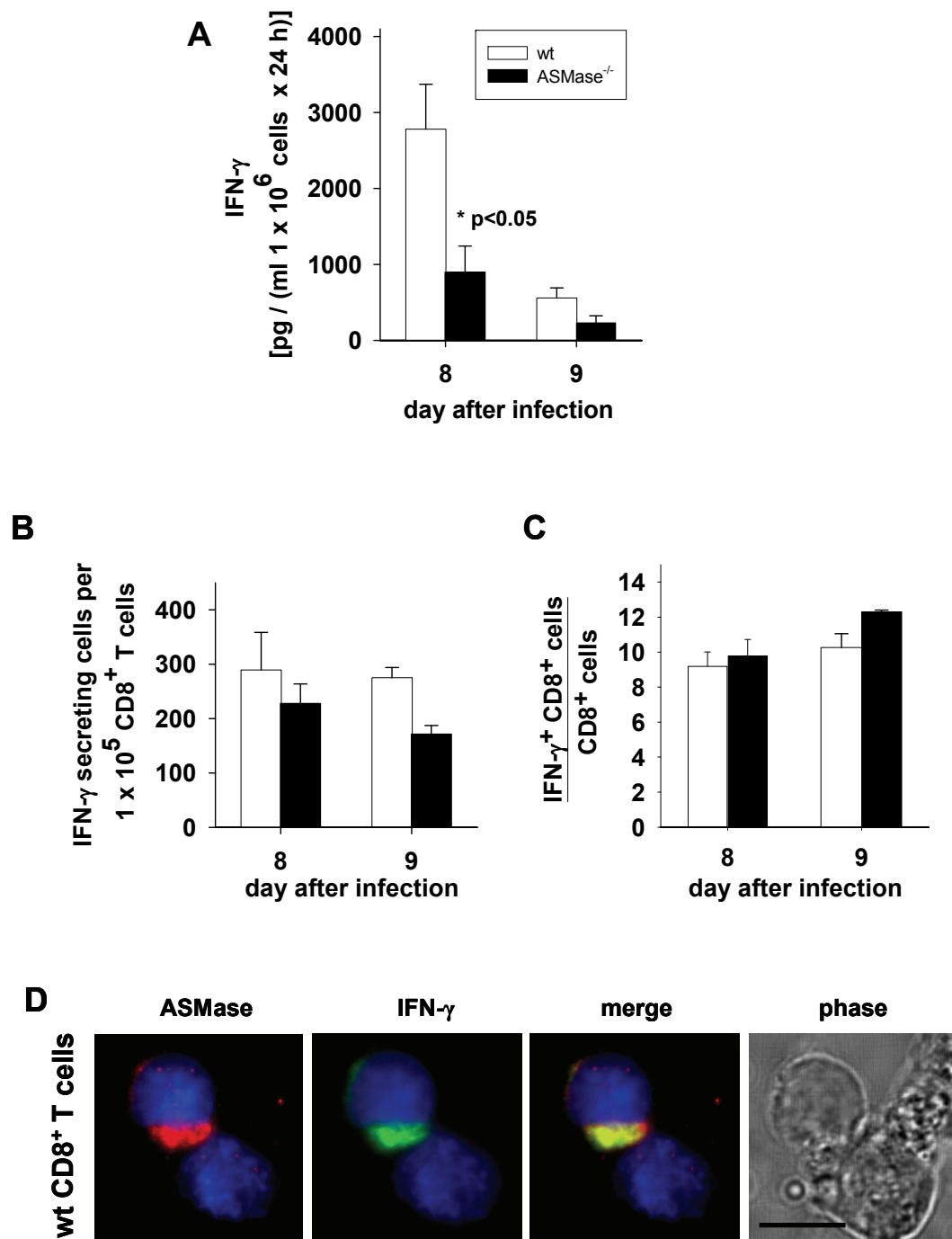


Fig. 10 Impaired secretion of IFN- γ by ASMase^{-/-} CD8⁺ T cells

On day 8 and 9 after i.v. infection of mice with 10⁵ IU LCMV, CD8⁺ T cells were immunomagnetically enriched from spleens and stimulated with LCMV infected C57BL/6-SV target cells (E:T = 10:1).

(A) IFN- γ secreted by 1 x 10⁶ wt or ASMase^{-/-} CTL was measured in the supernatants after 24 h by ELISA. Spontaneous secretion was under the limit of detection (not shown).

(B) The frequency of CD8⁺ T cells secreting IFN- γ was analysed by ELISpot assay in response to LCMV infected C57BL/6-SV fibroblasts.

(C) The percentage of CD8⁺ T cells intracellularly accumulating IFN- γ was analysed by flow cytometry. Cumulative data of four independent experiments are shown as mean \pm standard errors (A-C).

(D) Wt CD8⁺ T cells were stained with antisera specific for ASMase and mAb specific for IFN- γ and analysed by IFM. Scale bar is 10 μ m.

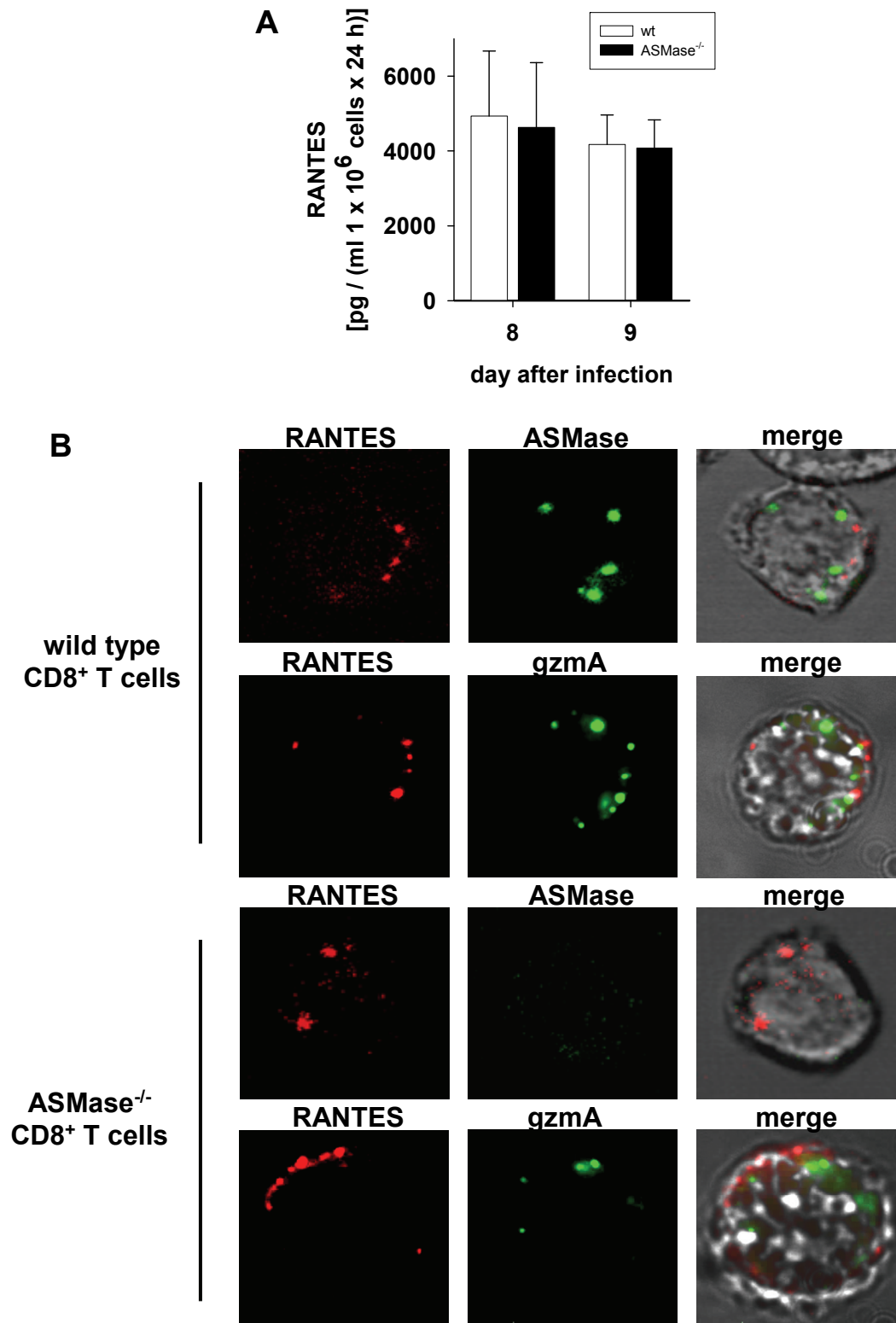


Fig. 11 Normal secretion of RANTES by ASMase^{-/-} CD8⁺ T cells

On day 8 and 9 after i.v. infection of mice with 10⁵ IU LCMV, CD8⁺ T cells were immunomagnetically enriched from spleens. 1 x 10⁶ wt or ASMase^{-/-} CTL were stimulated with LCMV infected C57BL/6-SV target cells (E:T = 10:1) and the supernatants were collected.

(A) RANTES secreted by wt or ASMase^{-/-} CTL was measured after 24 h by ELISA. Spontaneous secretion was under the limit of detection (not shown). Cumulative data of four independent experiments are shown as mean ± standard errors.

(B) Wt and ASMase^{-/-} CTL were stained with mAb specific for RANTES and antisera specific for ASMase or gzMA and analysed by IFM.

3.5 Specific inhibition of ASMase in CD8⁺ T cells with imipramine mimics the phenotype of ASMase^{-/-} CTL

Imipramine is a pharmacologic inhibitor of ASMase (Albouz, Le Saux et al. 1986; Hurwitz, Ferlinz et al. 1994). Imipramine reduced the activity of ASMase in T cells (**Fig. 12A**) in a time- and dose-dependent fashion and inhibited the cytotoxic activity of CD8⁺ T cells (**Fig. 12B, C**). Resembling the phenotype of ASMase^{-/-} T cells, the release of gzmA and hexosaminidase activity was reduced by treatment of CD8⁺ T cells with 25 μM imipramine (**Fig. 12D, E**). Furthermore, pre-treatment of CD8⁺ T cells with imipramine led to reduced secretion of IFN-γ in response to LCMV infected target cells to a comparable degree as ASMase^{-/-} CD8⁺ T cells, while secretion of RANTES was not affected (**Fig. 12F, G**).

Together, the pharmacological inhibition of ASMase in CD8⁺ T cells reproduces the secretory defects of ASMase^{-/-} CTL, suggesting that the phenotype of ASMase^{-/-} CTL is a specific consequence of missing ASMase activity rather than non-specific late sequelae of sphingomyelin storage.

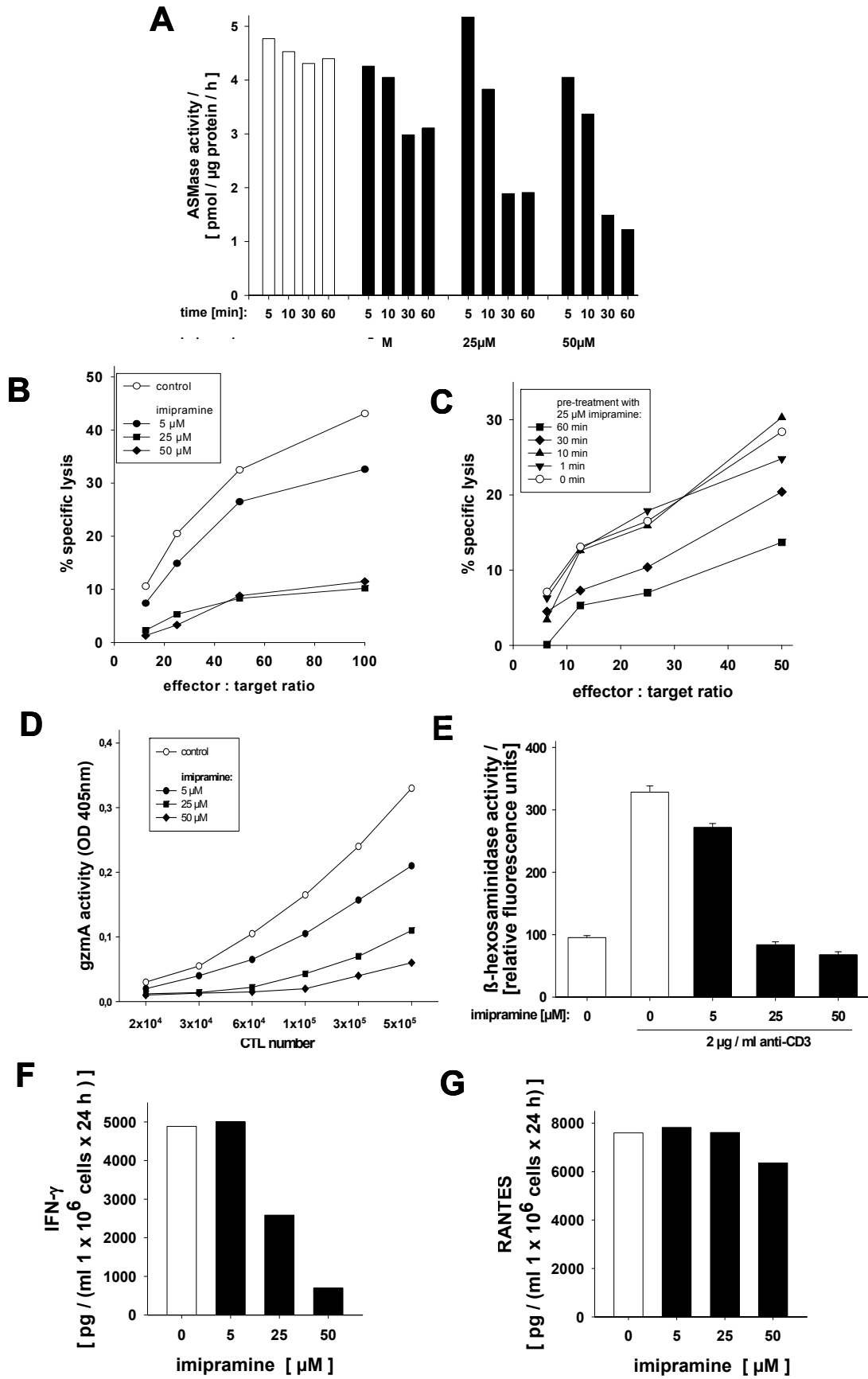


Fig. 12 Pre-treatment of wt CD8⁺ T cells with imipramine mimics the phenotype of ASMase^{-/-} CD8⁺ T cells

(legend on next page)

Fig. 12 Pre-treatment of wt CD8⁺ T cells with imipramine mimics the phenotype of ASMase^{-/-} CD8⁺ T cells

On day 8 after i.v. infection of mice with 10⁵ IU LCMV, CD8⁺ T cells were immunomagnetically enriched from spleens.

(A) ASMase specific activity was measured in CTL that were pre-treated for 5, 10, 30 and 60 min with different concentrations of imipramine. The assay was performed in cooperation with Katja Wiegmann, Institute for Medical Microbiology, Cologne.

(B) Dose- and (C) time-dependency of the cytotoxic activity of wt and ASMase^{-/-} CTL inhibitory effect of imipramine in a 4 h standard ⁵¹Cr-release assay against gp₃₃-loaded C57BL/6-SV target cells. Dose-dependent inhibition of (D) the release of gzmA- and (E) β-hexosaminidase activity was determined after stimulation with L1210.3 target cells in the presence of 2 μg/ml CD3 specific mAb for 6 h.

(F) Inhibitory effect of imipramine on secretion of IFN-γ (G) or RANTES measured by ELISA after 24 h.

3.6 Membrane-lipid composition is not altered in $ASMase^{-/-}$ $CD8^{+}$ T cells

In several cell types, deficiency in $ASMase$ leads to the accumulation of sphingomyelin (Horinouchi, Erlich et al. 1995). A perturbed lipid metabolism might influence cell signalling, e.g. by disrupting sphingomyelin-cholesterol domains of the plasma membrane, i.e. lipid rafts, to which the TCR complex localises (Gulbins and Li 2006). The lipid composition of the plasma membrane of $ASMase^{-/-}$ $CD8^{+}$ T cells was analysed by thin-layer chromatography (TLC) after extracting phospholipids from $CD8^{+}$ T cells. The lipid composition of $ASMase^{-/-}$ $CD8^{+}$ T cells does not show any overt alterations when compared to wt $CD8^{+}$ T cells (**Fig. 13**).

It has been reported that sphingolipid storage is observed predominantly in long-lived, non-proliferating cells of $ASMase^{-/-}$ mice elder than two months, but less pronounced in short-lived, proliferating cells such as T lymphocytes, especially in younger mice (Lozano, Morales et al. 2001). These data argue against the defect in exocytosis being a secondary effect of alterations in lipid membrane composition in $ASMase^{-/-}$ $CD8^{+}$ T cells.

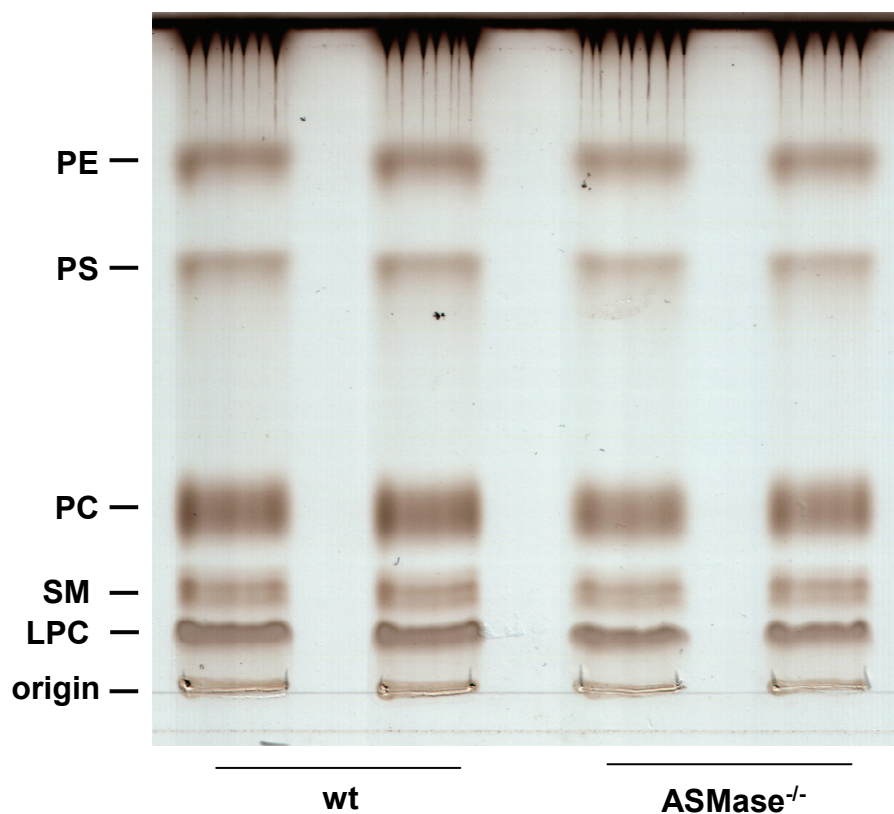


Fig. 13 Lipid composition of the plasma membrane of wt and ASMase^{-/-} CD8⁺ T cells

On day 8 after i.v. infection of mice with 10^5 IU LCMV, CD8⁺ T cells were immunomagnetically enriched from spleens. Phospholipids were extracted from the lysates and analysed by thin-layer-chromatography processed by Katja Wiegmann, Institute for Medical Microbiology, Cologne. On the left, positions of phospho- and sphingolipid- standards are indicated: PE – phosphatidylethanolamine, PS – phosphatidylserine, PC – phosphatidylcholine, SM – sphingomyelin and LPC-lysophosphatidylcholine.

3.7 Calcium-dependent signalling is normal in *ASMase*^{-/-} T cells

Minor changes in membrane lipid composition or subtle alterations of lipid raft architecture might escape detection by the above described TLC analysis. Therefore, assays for the functions of lipid rafts were performed. Release of Ca^{2+} from the endoplasmic reticulum by thapsigargin, an inhibitor of the calcium endoplasmic reticulum-ATPase which increases intracellular calcium in T cells (Gouy, Cefai et al. 1990), resulted in comparable signals in wt and *ASMase*^{-/-} effector cells (**Fig. 14A**). Moreover, crosslinking of the TCR, which co-localises with lipid rafts, resulted in a comparable Ca^{2+} -release in both *ASMase*^{-/-} and wt CD8^+ T cells (**Fig. 14B**). The similar amount of intracellular Ca^{2+} as well as identical TCR-triggered Ca^{2+} signals in wt and *ASMase*^{-/-} CD8^+ T cells rule out that deficiency of *ASMase* affects the intracellular storage of calcium or its release in response to TCR signalling from lipid rafts.

In combination with the normal Fas Ligand-mediated induction of target cell apoptosis and the proper secretion of RANTES, these data rule out any defects in TCR-mediated signalling in *ASMase*^{-/-} CD8^+ T cells.

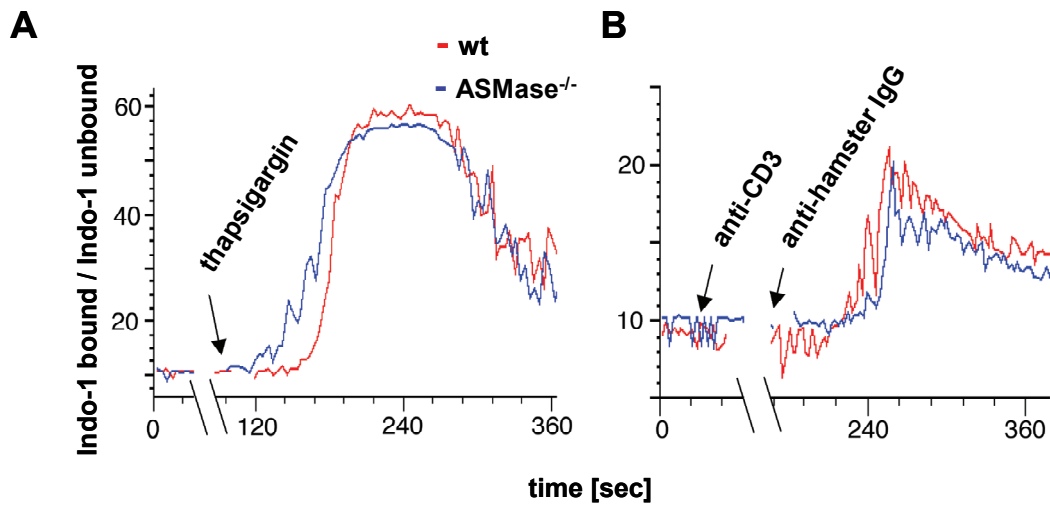


Fig. 14 Release of intracellular Ca²⁺ in CD8⁺ T cells

On day 8 after i.v. infection of mice with 10⁵ IU LCMV, 1 x 10⁷ CD8⁺ T cells were labelled with the calcium sensitive fluorescence dye Indo-1 in the presence of pluronic acid. After 45 min calcium variations were measured for 10 minutes at 37°C by flow cytometry in cooperation with Julian Pardo, MPI Freiburg.

(A) Release of calcium from intracellular stores was induced by thapsigargin (B) or by TCR ligation with anti-CD3 mAb cross-linked with anti-hamster IgG.

3.8 Normal intragranular pH in $ASMase^{-/-}$ $CD8^{+}$ T cells

Proper acidification of cytotoxic granules is a prerequisite for intragranular processing of perforin (Kataoka, Takaku et al. 1994) and for condensation of the granule's matrix (Braga, Grujic et al. 2007). Therefore, acidification of the cytotoxic granule was determined by a method relying on pH-dependent quenching of FITC-fluorescence in comparison to pH-independent TRITC-fluorescence. Cytotoxic granules were pulse-chase labelled with equimolar amounts of FITC- and TRITC-conjugated dextrans. Fluorescence intensities of FITC and TRITC were measured by flow cytometry to calculate the pH of the cytotoxic granules of wt and $ASMase^{-/-}$ $CD8^{+}$ T cells by use of a standard curve (**Fig. 15A**). As shown in **Fig. 15B**, a pH of 5.45 ± 0.35 in cytotoxic granules of wt CTL and of 5.75 ± 0.4 in $ASMase^{-/-}$ CTL did not significantly differ and was in accordance with published data (pH 5.5, (Burkhardt, Hester et al. 1990; Masson, Peters et al. 1990)).

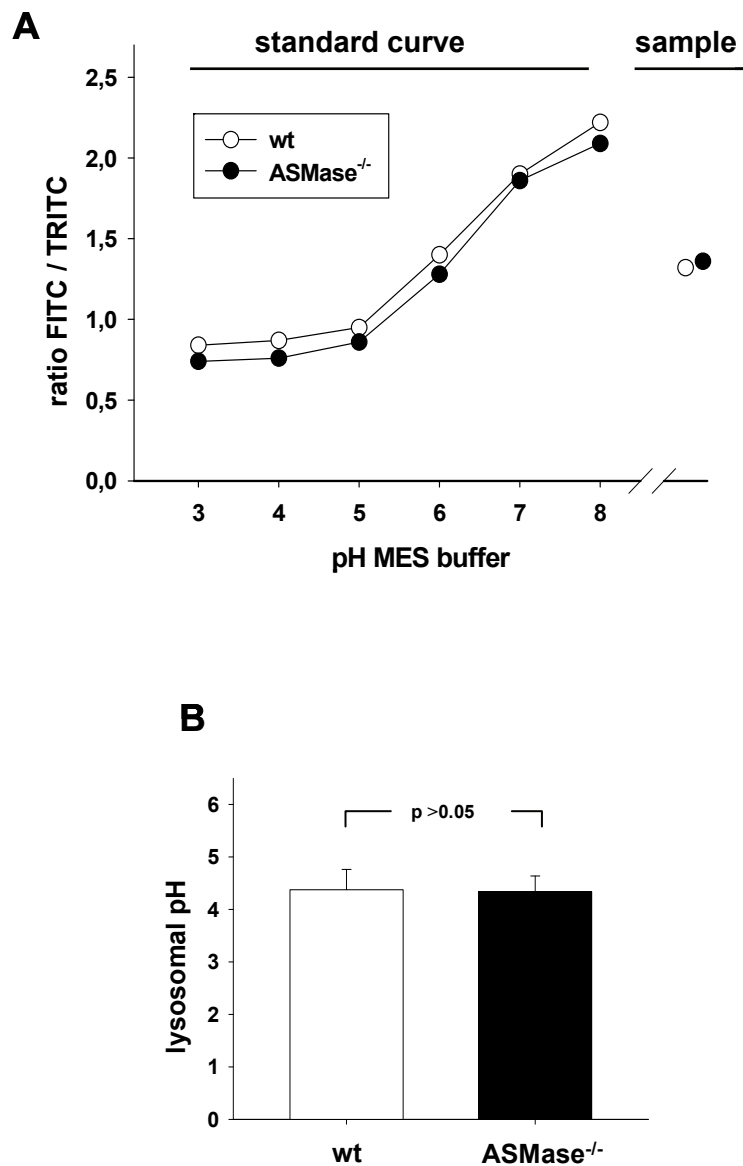


Fig. 15 Lysosomal pH in ASMase^{-/-} CD8⁺ T cells

On day 8 after i.v. infection of mice with 10⁵ IU LCMV, CD8⁺ T cells were immunomagnetically enriched from spleens. Cytotoxic granules were pulsed 2 h with 10 μM FITC- and TRITC- conjugated dextran, washed extensively and chased for 2 h in fresh culture medium.

(A) Fluorescence intensities of test samples and samples of a standard curve covering pH 3-8 were measured by flow cytometry.

(B) Shown are the cumulative data of four experiments as means ± standard error.

3.9 Intracellular transport of cytotoxic granules: Polarisation to the immunological synapse and fusion with the plasma membrane

Crucial steps for cytolysis by CTL are the formation of an immunological synapse with its target cell, the polarisation of cytotoxic granules towards the synapse, the docking of secretory lysosomes to the plasma membrane and the formation of a fusion pore between the granule limiting membrane and the plasma membrane.

Ultra-structural analysis of immunological synapse between CD8⁺ T cells and target cells by electron-microscopy revealed synapses of wt or ASMase^{-/-} CD8⁺ T cells indistinguishable with respect to the size of the contact area, the number of membrane bridges or the morphology of the synaptic cleft between effector and target cell (**Fig. 16A**). Moreover, the percentage of wt and ASMase^{-/-} CD8⁺ T cells conjugated to targets cells determined by immunofluorescence microscopy, was comparable after 10 min of co-incubation (**Fig. 16B**). In response to target cell contact, Lamp1-positive cytotoxic granules, were rapidly polarised toward the immunological synapse in wt as well as ASMase^{-/-} CD8⁺ T cells within less than 20 min (**Fig. 16C**).

Fusion of cytotoxic granules with the plasma membrane of CD8⁺ T cells was determined by monitoring the translocation of Lamp1 from the inner membrane leaflet of cytotoxic granules onto the surface of the T cell. Co-incubation of wt or ASMase^{-/-} CD8⁺ T cells with target cells resulted in a similar time-dependent increase of the percentage of CD8⁺ T cells expressing Lamp1 on the cell surface (**Fig. 17A**). In addition to the kinetics, the signal intensity for Lamp1 was similar on CD8⁺ T cells of both genotypes (**Fig. 17B**). Resembling the phenotype of ASMase^{-/-} T cells by pre-treatment of wt CD8⁺ T cells with imipramine, the exposure of Lamp1 on the plasma membrane in response to target cell contact was not altered (**Fig. 17C**).

These data provide evidence that the prerequisites for the secretion of cytotoxic contents up to the formation of a fusion pore between granule and plasma membrane are fully achieved by wt as well as ASMase^{-/-} CD8⁺ T cells. Thus, ASMase activity has to contribute to the very last steps of the secretion of cytotoxic granules, i.e. the actual release of cytotoxic effector molecules.

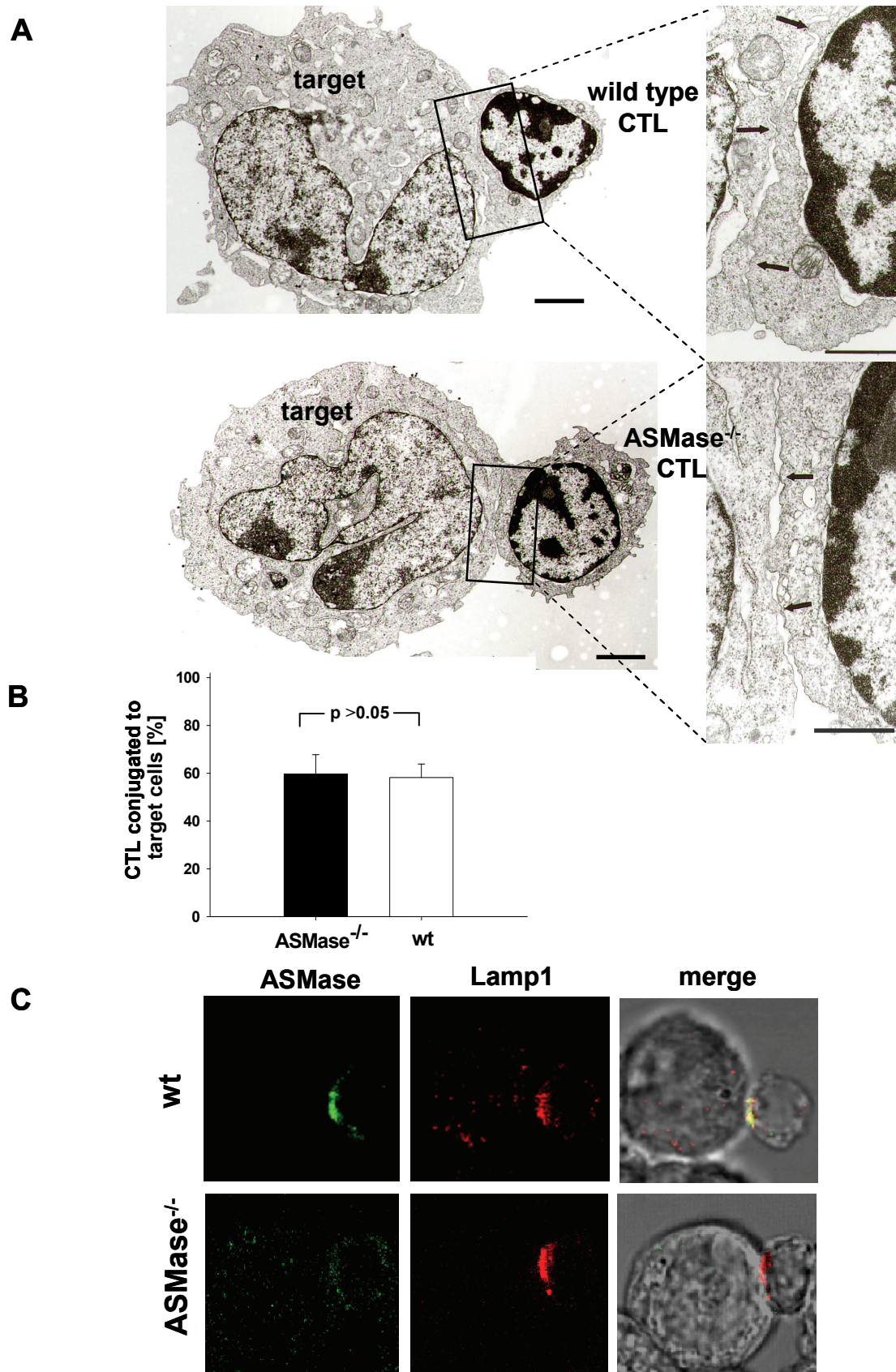


Fig. 16 Proper polarisation of cytotoxic granules at morphologically intact immunological synapse in ASMase^{-/-} CD8⁺ T cells

(legend on next page)

Fig. 16 Proper polarisation of cytotoxic granules at morphologically intact immunological synapse in *ASMase*^{-/-} CD8⁺ T cells

On day 8 after i.v. infection of mice with 10⁵ IU LCMV, CD8⁺ T cells were immunomagnetically enriched from spleens. Wt and *ASMase*^{-/-} CD8⁺ T cells were co-incubated with L1210.3 target cells in the presence of 3 µg/ml anti-CD3 mAb. Effector target cell conjugates were incubated for 10 min, fixed and (A) further processed for immuno-electron microscopy by Hans-Walter Zentgraf, DKFZ, Heidelberg, (B) counted for conjugates of CTL and target cells or (C) stained with antisera specific for *ASMase* and mAb specific for Lamp1.

Scale bar is 500 nm. Arrows indicate membrane bridges between target and effector cells.

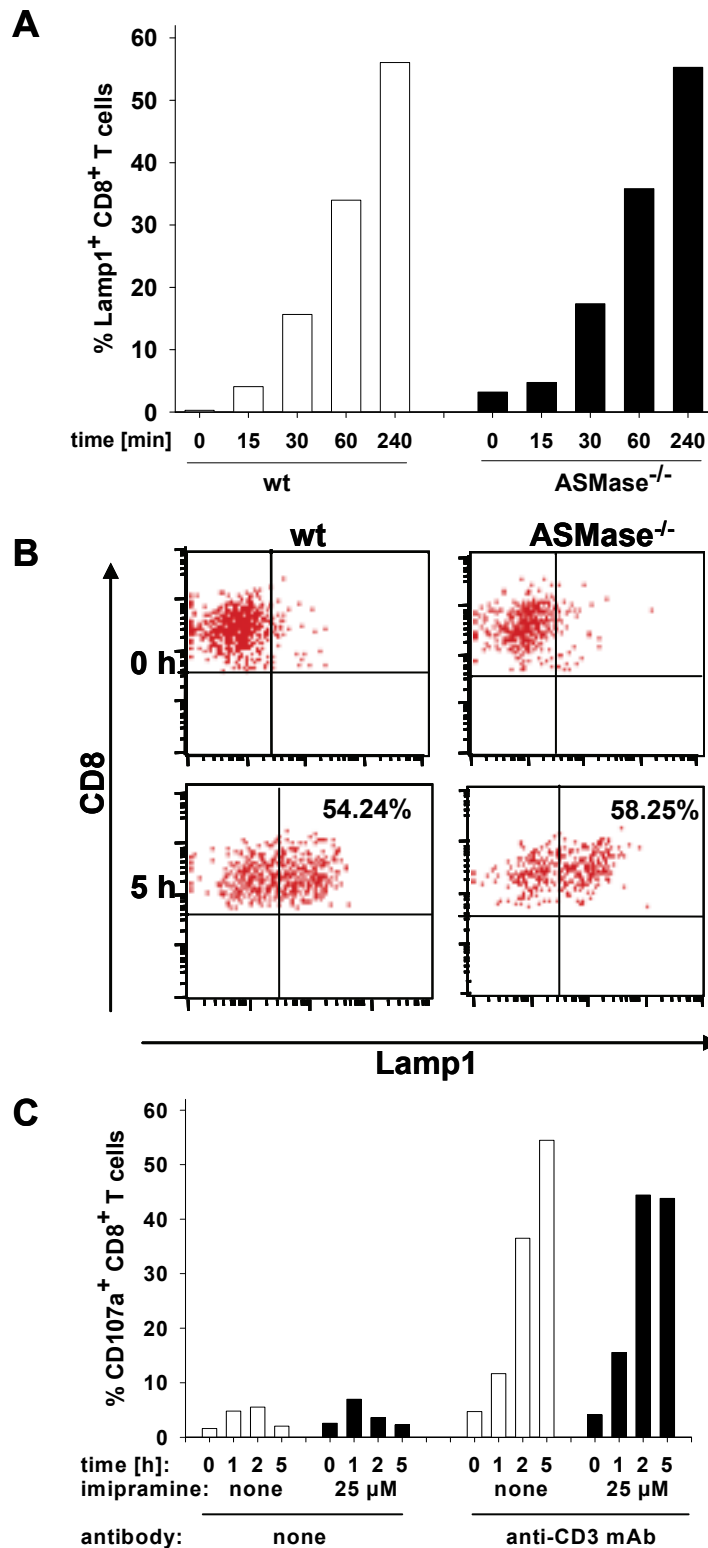


Fig. 17 Exposure of Lamp1 on the surface of the T cell in ASMase^{-/-} CD8⁺ T cells is not altered

On day 8 after i.v. infection of mice with 10⁵ IU LCMV, CD8⁺ T cells were immunomagnetically enriched from spleens. Wt and ASMase^{-/-} CD8⁺ T cells were co-incubated with L1210.3 target cells in the absence or presence of 3 μg/ml anti-CD3 mAb.

(A) Kinetics of the exposure of Lamp1 (CD107a) on the cell surface was determined by flow cytometry on wt and ASMase^{-/-} CTL at the indicated time points after staining the cells for CD8 and Lamp1. The experiment was repeated five times with similar results.

(B) Representative dot plots of one experiment for 0 and 5 h time of co-incubation.

(C) Translocation of Lamp1 to the cell surface of wt CTL pre-treated 60 min with 25 μM imipramine. The experiment was repeated three times with similar results.

3.9 Characterisation of cytotoxic granule exocytosis in *ASMase*^{-/-} CD8⁺ T cells

Secretion of contents from cytotoxic granules was monitored after pulse-chase-labelling of cytotoxic granules with fluorescent dextran of 3, 70 or 500 kDa molecular weight as fluid phase markers. As shown in **Fig. 18A and B**, dextran molecules of each used size were almost quantitatively incorporated into vesicles that were identified as cytotoxic granules by co-staining with *gzmA*. These vesicles were of equal size in wt and *ASMase*^{-/-} CD8⁺ T cells (**Fig. 18C**).

CD8⁺ T cells of both genotypes polarised the dextran-loaded cytotoxic granules readily to the immunologic synapse within 10 min (**Fig. 19A**), suggesting proper intracellular transport of the dextran-loaded cytotoxic granules. In response to co-incubation of CD8⁺ T cells with LCMV infected target cells for 60 min, the number of granules per cell declined similar in both T cell populations (**Fig. 19B**).

Secretion of fluorescent fluid phase markers was monitored by flow cytometry. Fluorescent dextran molecules of either 3 kDa or 70 kDa were released from wt and *ASMase*^{-/-} CD8⁺ T cells in identical quantities and with similar kinetics (**Fig. 19C**). As expected 3 kDa dextran molecules with about 4 nm diameter were secreted a little more rapid and to slightly higher extents than the 70 kDa dextran with about 12 nm diameter. 500 kDa fluorescent dextran of about 20 nm diameter was neither by wt nor by *ASMase*^{-/-} CD8⁺ T cells secreted to significant degrees. Secretion of dextran was fully inhibited by several inhibitors of exocytosis, including cytochalasin D, cyclosporin A or FK-506 to the minimal level of secretion observed in non-stimulated cells (**Fig. 19D**).

Secretion of fluid phase markers by wt as well as *ASMase*^{-/-} CTL further confirms proper formation of a fusion pore between granules and the plasma membrane, as previously observed by exposure of Lamp1 (**Fig. 17A, B**).

However, the normal exposure of Lamp1 on the plasma membrane and the similar secretion of fluorescent dextrans by wt and *ASMase*^{-/-} CD8⁺ T cells is in apparent conflict with the impaired secretion of *gzmA* and β -hexosaminidase (**Fig. 5A, 6E**). An explanation could be that the effector molecules of cytotoxic granules, i.e. perforin and *gzm*, are not stored as soluble molecules but rather as high molecular weight complexes with proteoglycans amounting for about 1300 kDa and a diameter of up to 140 nm (Raja, Metkar et al. 2003). Therefore, further experiments were designed, to assess secretion of these complexed contents.

After conjugation to target cells, $gzmA^+$ cytotoxic granules appear as small distinct dots beneath the immunological synapse of wt CTL. In contrast, much larger clusters of $gzmA^+$ granules accumulate beneath the immunological synapse in $ASMase^{-/-}$ CTL (**Fig. 20A**). The resolution of IFM does not allow discriminating whether the $gzmA^+$ clusters are lying within the CTL or are adhering to the outside of the cell. Flow cytometry analysis of CTL extracellularly stained with $gzmB$ -specific monoclonal Ab with or without use of a signal intensifying antibody did not reveal any sign for granzyme adhering to the outside of the plasma membrane during PMA/ionomycin-stimulated secretion (**Fig. 20B**). Thus, large clusters of $gzmA$ appear to resemble granules which were not able to extrude their granule contents.

By two-photon microscopy of viable cells the events during secretion of cytotoxic granules were further characterised. $CD8^+$ T cells were stimulated by solid-phase-bound anti-CD3 and anti-CD28 mAb in medium containing the polar fluorescent tracer sulforhodamine-B (SRB) and the water-soluble membrane marker FM1-43. When the cells were stimulated, exocytic events of individual cytotoxic granules could be identified as the appearance of small red-fluorescent spots in wt CTL, due to the entry of extracellular SRB into the fused granule (**Fig. 21A**). Remarkably, significantly larger vesicles were stained with SRB in $ASMase^{-/-}$ CTL (**Fig. 21B**). These exocytic events were not seen in unstimulated control cells.

FM1-43 is soluble in water and becomes fluorescent after integration into bio-membranes. It cannot penetrate the cell membrane so that it stains membranes with access to the surrounding medium. After formation of the fusion pore, FM1-43 stains the granular membrane as well as the contents. This has been reported previously for the content of lactotrophic granules in rat pituitary (Angleon, Cochilla et al. 1999). Comparable to staining with SRB, large FM1-43 vesicles were detected in $ASMase^{-/-}$ $CD8^+$ T cells. These concordant observations suggest that a fusion pore is formed in both, wt and $ASMase^{-/-}$ CTL, but the granular content cannot be properly extruded from the cytotoxic granules of $ASMase^{-/-}$ CTL.

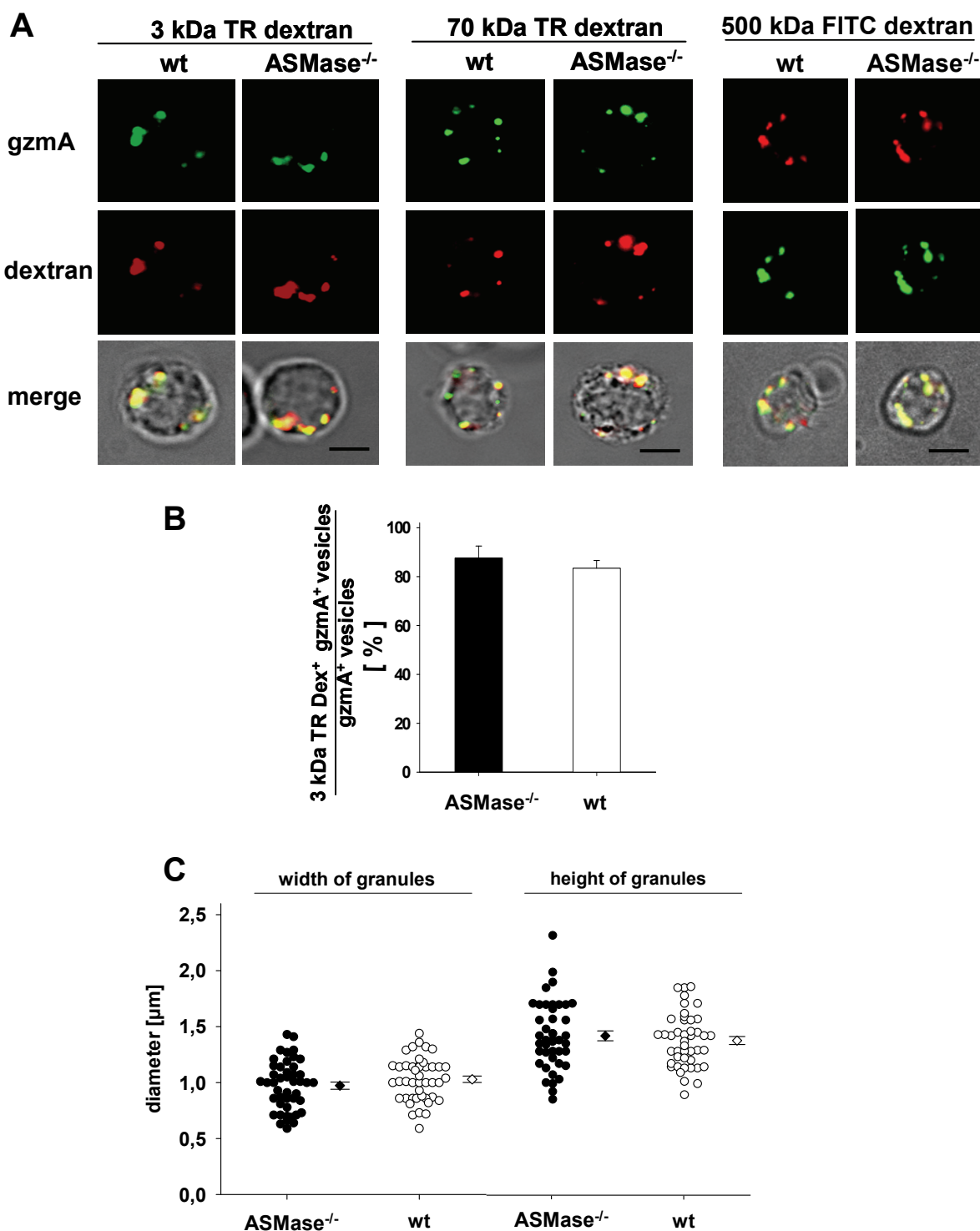


Fig. 18 Fluorescent dextran molecules by wt and ASMase^{-/-} CD8⁺ T cells

On day 8 after i.v. infection of mice with 10⁵ IU LCMV, CD8⁺ T cells were immunomagnetically enriched from spleens. Wt and ASMase^{-/-} CD8⁺ T cells were pulsed for 2 h in medium containing 10 µM 3, 70 or 500 kDa dextrans conjugated to Texas Red (TR) or FITC. Cells were washed three times and chased for 2 h in fresh culture medium.

(A) CD8⁺ T cells were stained intracellularly for gzmA. Scale bar is 5 µm.

(B) CTL loaded with 3 kDa Texas-Red dextran and intracellularly stained for gzmA were analysed for the proportion of gzmA⁺ vesicles additionally positive for dextran. Shown are mean ± standard errors from two experiments including n=126 wt and n=136 ASMase^{-/-} cytotoxic granules.

(C) 3 and 70 kDa dextran loaded CTL were measured in micrograph from 2PM. Shown are mean ± standard errors of two experiments including n=45 cells

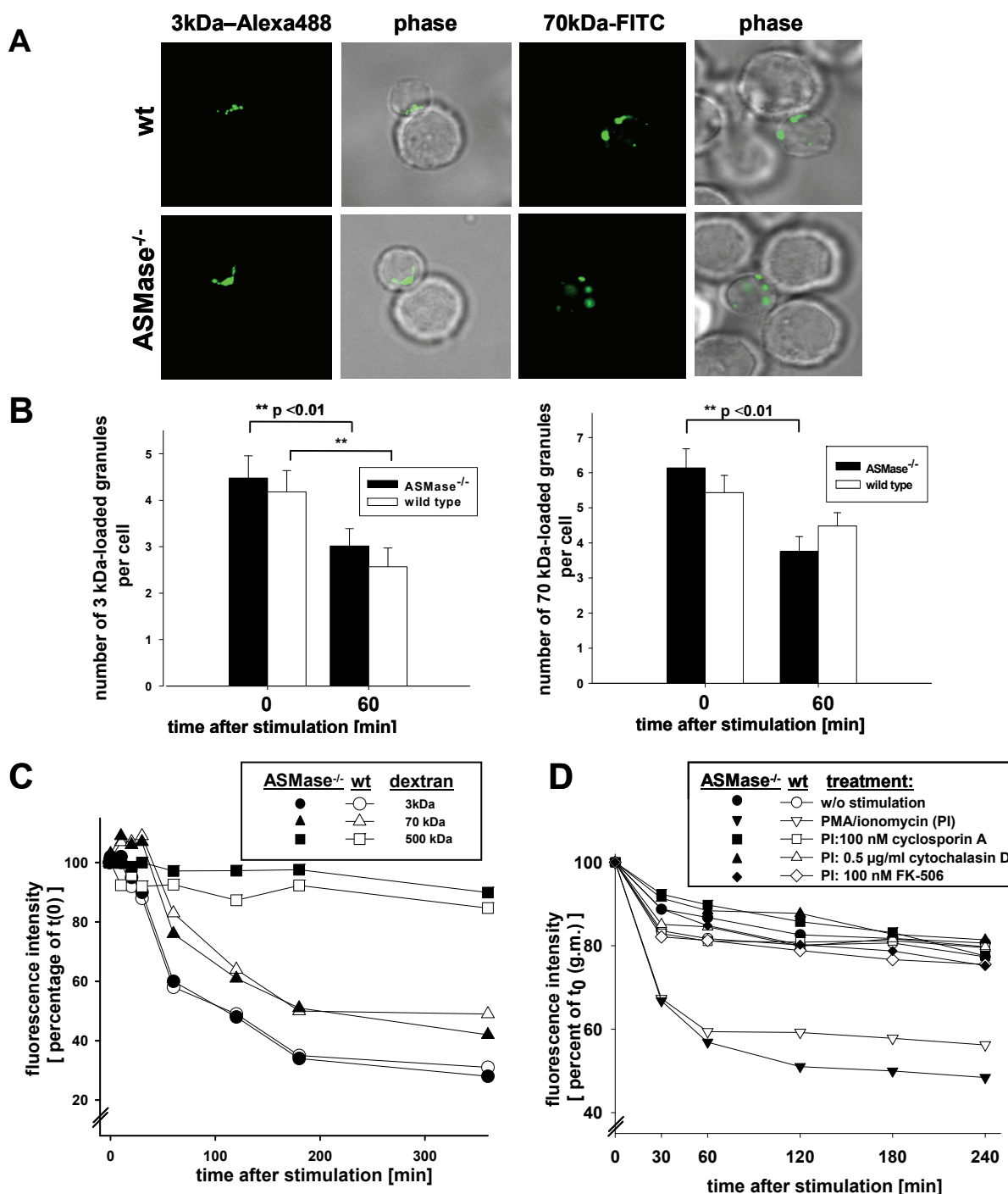


Fig. 19 Identical secretion of fluorescent fluid phase markers in wt and ASMase^{-/-} CD8⁺ T cells
 On day 8 after i.v. infection of mice with 10⁵ IU LCMV, CD8⁺ T cells were immunomagnetically enriched from spleens and pulsed for 2 h in medium containing 10 µM 3, 70 or 500 kDa dextran conjugated to fluorescent dyes. Cells were washed and chased for 2 h in fresh culture medium.
 (A) CD8⁺ T cells loaded with Alexa488-labelled 3 or FITC-labelled 70 kDa dextran were co-incubated with L1210.3 target cells in the presence of 3 µg/ml anti-CD3 and anti-CD28 mAb for 10 min.
 (B) Cytotoxic granules of CD8⁺ T cells loaded with 3 or 70 kDa dextran conjugated to Texas Red were counted before and after 60 min of stimulation with 10 ng/ml PMA and 500 ng/ml ionomycin. For each time point, dextran size and genotype, n=60 cells were counted.
 (C) CD8⁺ T cells loaded with Alexa488-labelled 3 kDa, Oregon Green-labelled 70 kDa or FITC-labelled 500 kDa dextran were stimulated with 10 ng/ml PMA and 500 ng/ml ionomycin and fluorescence intensity was measured by flow cytometry at the indicated time points. Shown are the relative fluorescence intensities normalized for the values at t=0. (D) Secretion of 3 kDa Alexa488-dextran labelled cytotoxic granules was inhibited by cytochalasin D, cyclosporin A and FK-506.

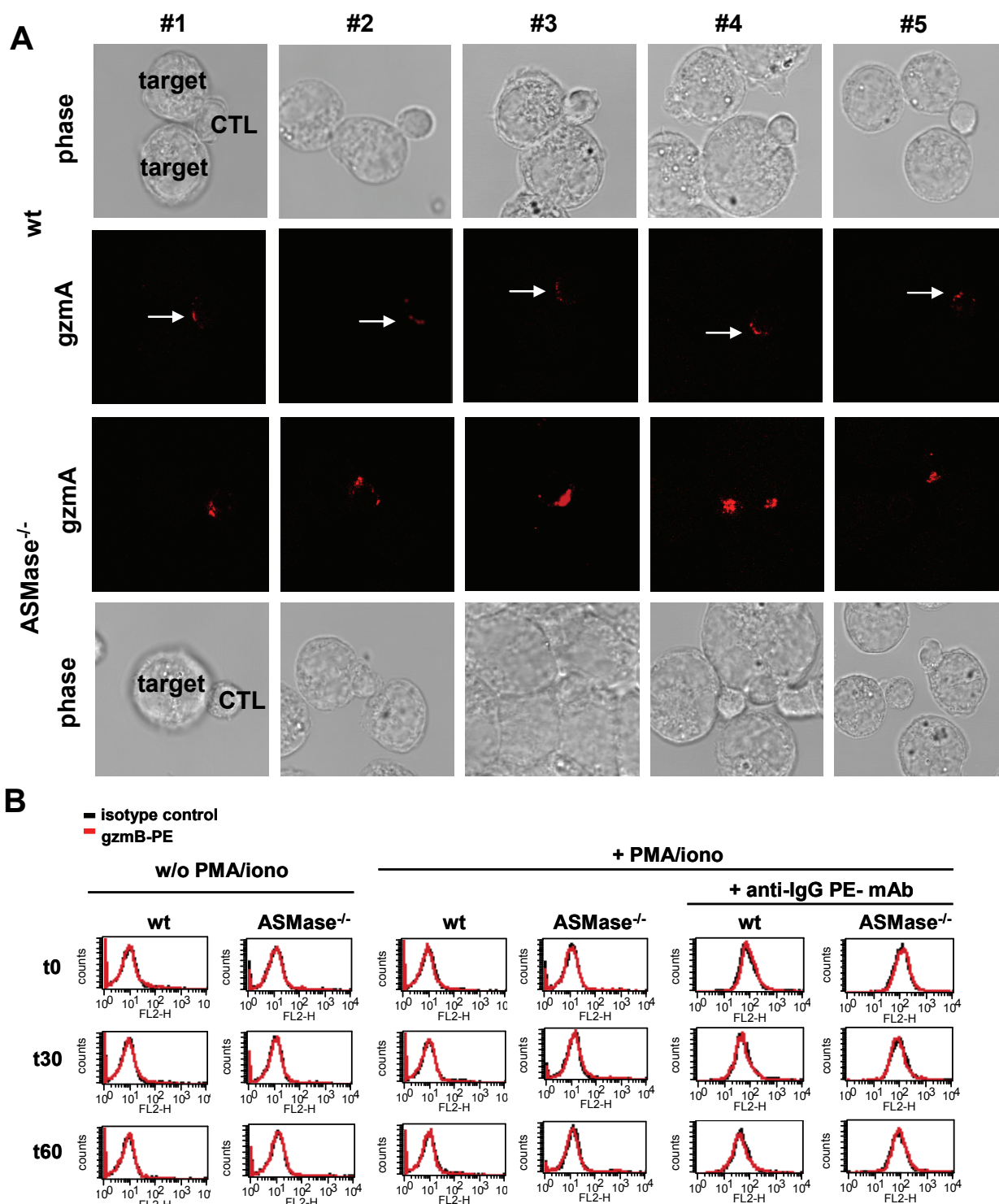


Fig. 20 In ASMase^{-/-} CD8⁺ T cells large clusters of gzmA-positive cytotoxic granules persist beneath the immunological synapse

On day 8 after i.v. infection of mice with 10^5 IU LCMV, CD8⁺ T cells were immunomagnetically enriched from spleens.

(A) CD8⁺ T cells (indicated “CTL”) were co-incubated with L1210.3 cells (indicated “target”) in the presence of CD3 and CD28 specific mAb for 10 min. The cells were fixed, permeabilised and stained with gzmA-specific antiserum and analysed by confocal microscopy. Five representative CTL/target conjugates, either wt or ASMase^{-/-} CTL are shown. The small gzmA-positive vesicles are indicated in wt CTL by white solid arrows.

(B) Flow cytometry analysis of CD8⁺ T cells stained with gzmB specific mAb for extracellular gzmB during PMA/ionomycin stimulation. One set of samples was stained by additional use of a PE-conjugated amplifier mAb against mouse-IgG.

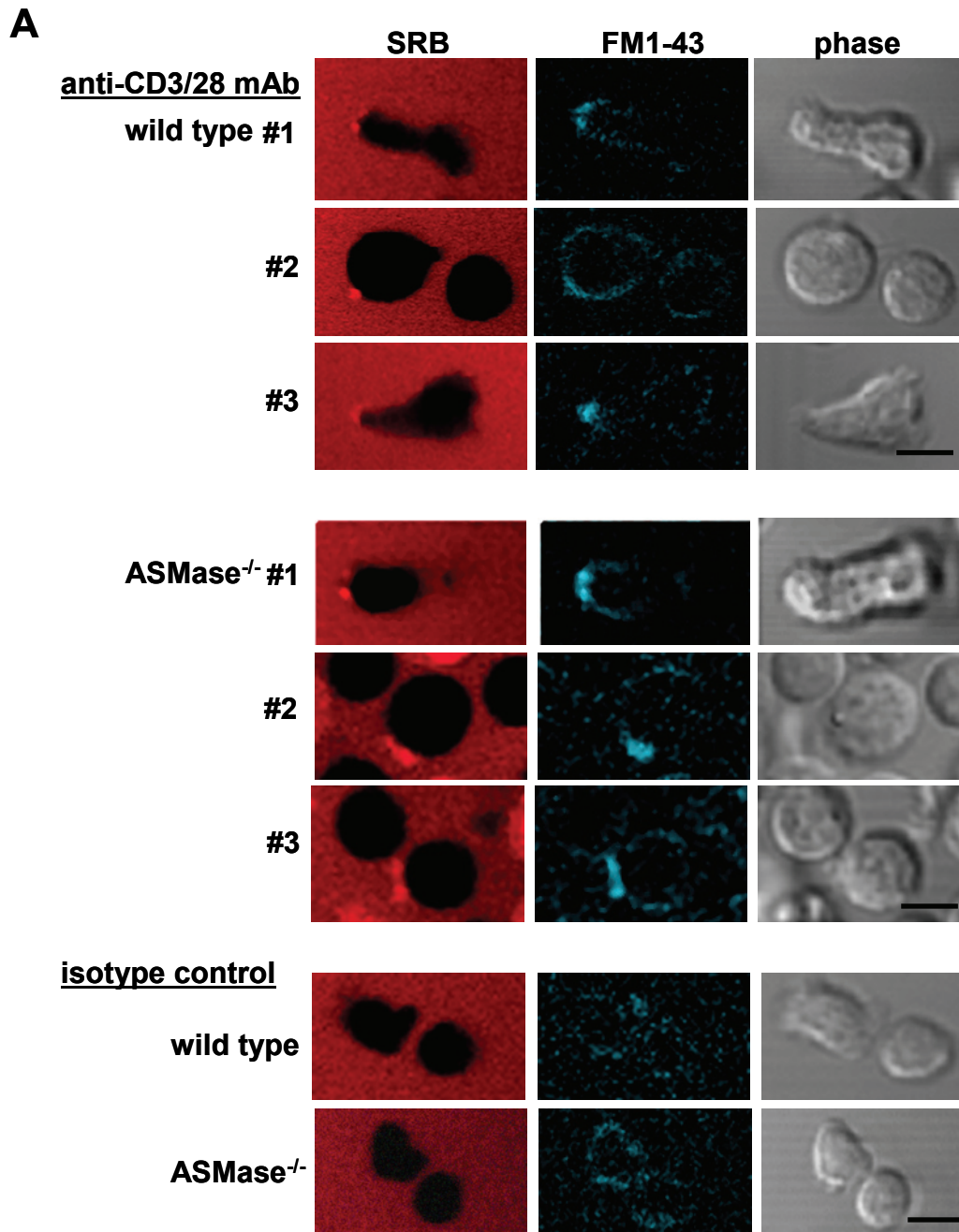


Fig. 21 Vital microscopy of CD8⁺ T cells during secretion: staining of granule clusters in ASMase^{-/-} CD8⁺ T cells

On day 8 after i.v. infection of mice with 10⁵ IU LCMV, splenocytes were restimulated with 10 U/ml recombinant mouse IL-2 *in vitro*. Two days later, wt and ASMase^{-/-} CD8⁺ T cells were immunomagnetically enriched and immersed in medium containing 500 μM of the polar tracer sulforhodamine B (SRB) and 25 μM of the membrane dye FM1-43 in chamber slides coated with anti-CD3 and anti-CD28-specific mAb or isotype control. Influx of extracellular medium into cytotoxic granules after stimulation was visualized via two-photon vital microscopy.

(A) Three representative CD8⁺ T cells stimulated with anti-CD3 and CD28 mAb are shown for each genotype.

(continued on next page)

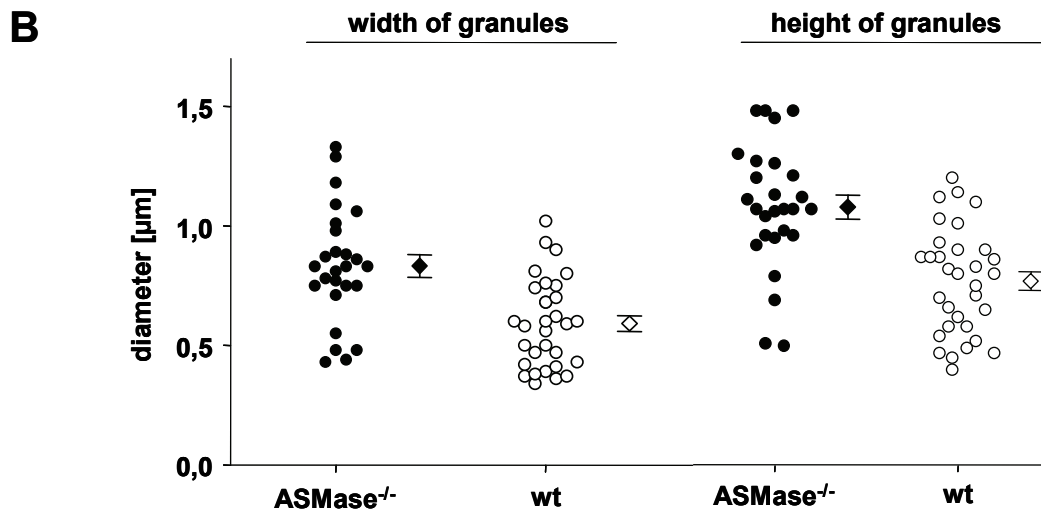


Fig. 21 Vital microscopy of CD8⁺ T cells during secretion: staining of granule clusters in ASMase^{-/-} CD8⁺ T cells

(B) The size of SRB stained cytototoxic granules from cells shown in (A) was determined in the plane focus with the highest fluorescence intensity. 40 cells for each genotype and the mean \pm standard errors are shown.

3.10 Deficiency in ASMase impairs cytotoxicity of CTL independent of the molecular size of granular matrix

The extrusion of cytotoxic granules might be facilitated in wt CTL by ASMase activity contributing to dissolve the high molecular weight matrix of granules. This hypothesis was experimentally addressed by using mice deficient for serglycin ($SG^{-/-}$), the core protein of the high molecular weight proteoglycan matrix. $SG^{-/-}$ $CD8^{+}$ T cells generate cytotoxic granules of lower electron density with a matrix consisting of only short glycosaminoglycan (GAG) chains.

The lack of serglycin itself does not affect the cytotoxic activity of CTL (Grujic, Braga et al. 2005). On the contrary, $SG^{-/-}$ $CD8^{+}$ T cells lysed target cells slightly more effectively than wt CTL (**Fig. 22A**).

The disturbance in proteoglycan synthesis in $SG^{-/-}$ T cells was indicated by a 10-fold reduced incorporation of [^{35}S] into $SG^{-/-}$ $CD8^{+}$ T cells as compared to wt $CD8^{+}$ T cells (**Fig. 22B**). This decreased incorporation of [^{35}S] into $SG^{-/-}$ CTL is in agreement with data of Grujic *et al.* (Grujic, Braga et al. 2005). As might be expected, the relative release of low molecular weight [^{35}S]-labelled material was slightly increased in $SG^{-/-}$ as compared to wt $CD8^{+}$ T cells (**Fig. 22C**).

A possible requirement for ASMase in dissolving the high molecular weight matrix of granules was investigated in $CD8^{+}$ T cells deficient for both SG and ASMase. While $SG^{-/-}$ $CD8^{+}$ T cells lysed their target cells slightly more effectively than wt CTL (**Fig. 23A, left, 21A**), the cytotoxic activity of $ASMase^{-/-}/SG^{-/-}$ $CD8^{+}$ T cells was as low as that of $ASMase^{-/-}$ CTL (**Fig. 23A, right**). Additionally, pre-treatment of $SG^{-/-}$ CTL with the ASMase inhibitor imipramine strongly reduces the cytotoxicity of $SG^{-/-}$ and wt CTL to the same levels observed in $ASMase^{-/-}$ CTL (**Fig. 23B**).

These data show that ASMase is required for effective cytotoxic activity of CTL, regardless whether the effector molecules are bound to the high molecular weight proteoglycan-matrix or low molecular weight glycosaminoglycan matrix. This argues against ASMase dissolving the granule's matrix.

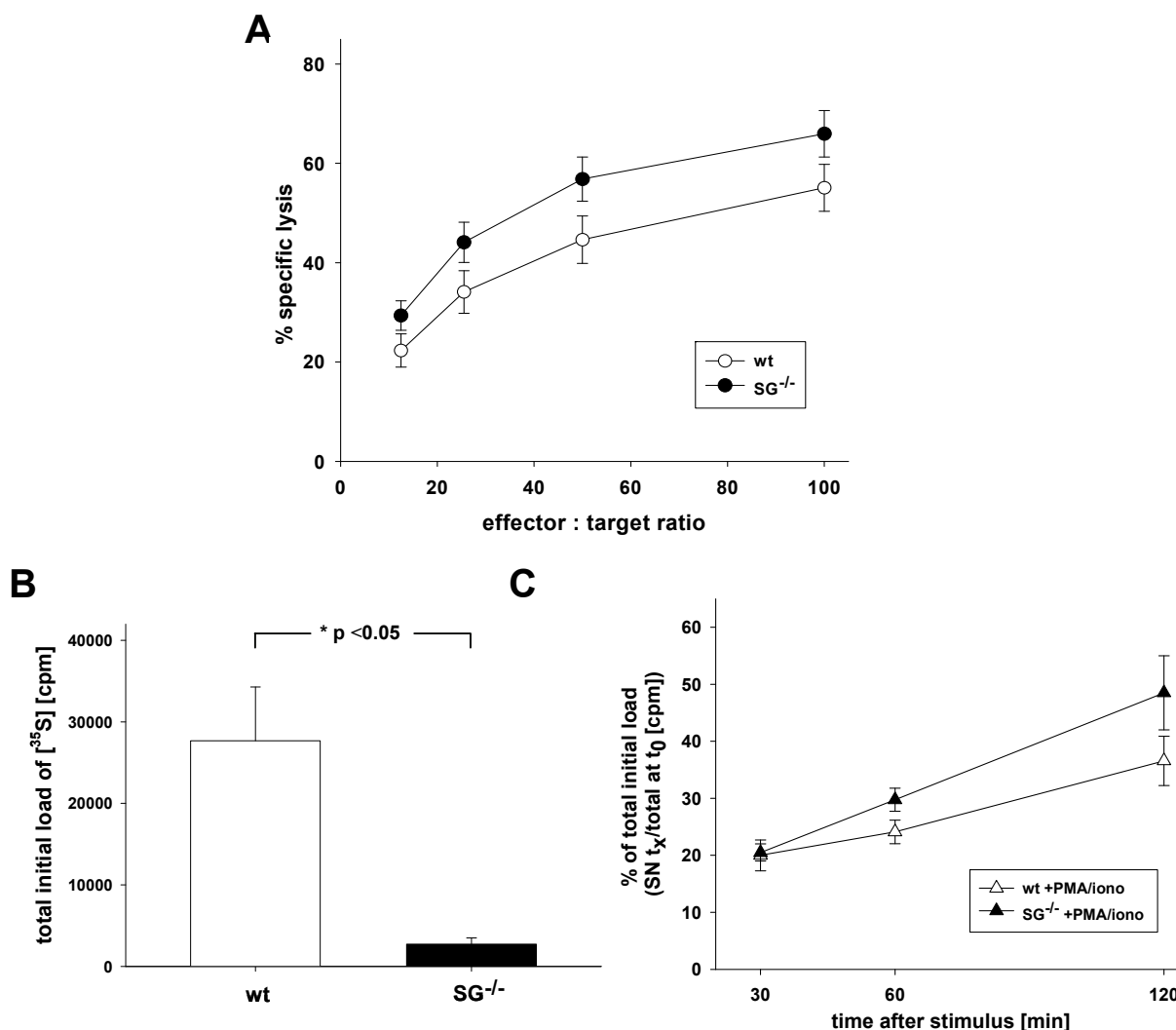


Fig. 22 Characterization of SG^{-/-} CTL

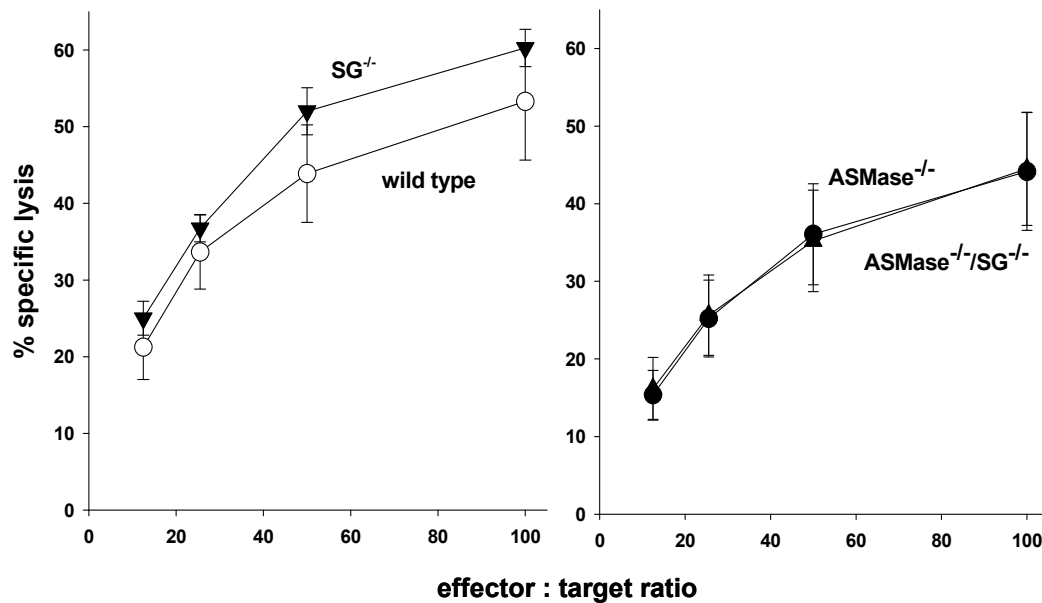
Wild type and SG^{-/-} mice were infected i.v. with 10⁵ IU of the LCMV-WE.

(A) At day 8 after infection, CD8⁺ T cells were immunomagnetically enriched from splenic single cell suspensions and used as effector cells in a 4 h standard [⁵¹Cr]-release assay against C57BL/6-SV target cells loaded with 10⁻⁶ M gp₃₃ peptide. Shown are mean and standard error of cumulative data from 11 experiments (wt: n=21; SG^{-/-}: n=17).

(B) At day 30 p.i., immune splenocytes were *in vitro* stimulated with LCMV infected C57BL/6-SV target cells (E:T=10:1) in the presence of 10% ConA SN for 3 days. A total of 3 x 10⁷ cells were incubated in 10 ml sulphate-free RPMI supplemented with 1 mCi [³⁵S] for 24 h. CD8⁺ T cells were immunomagnetically enriched and chased for 2 h in fresh RPMI medium. Shown is the total [³⁵S] incorporation quantified by liquid scintillation counting of cell lysates from four experiments (wt n=9; SG^{-/-} n=4).

(C) Secretion of [³⁵S]-labelled wt and SG^{-/-} CD8⁺ T cells was induced by PMA/ionomycin stimulation. Shown are mean ± standard errors of percentages of [³⁵S] in cell-free supernatants normalised to the total initial load of [³⁵S] material from 4 experiments (wt n=9; SG^{-/-} n=4). Unstimulated CD8⁺ T cells did not secrete significant amounts of radioactivity (data not shown).

A



B

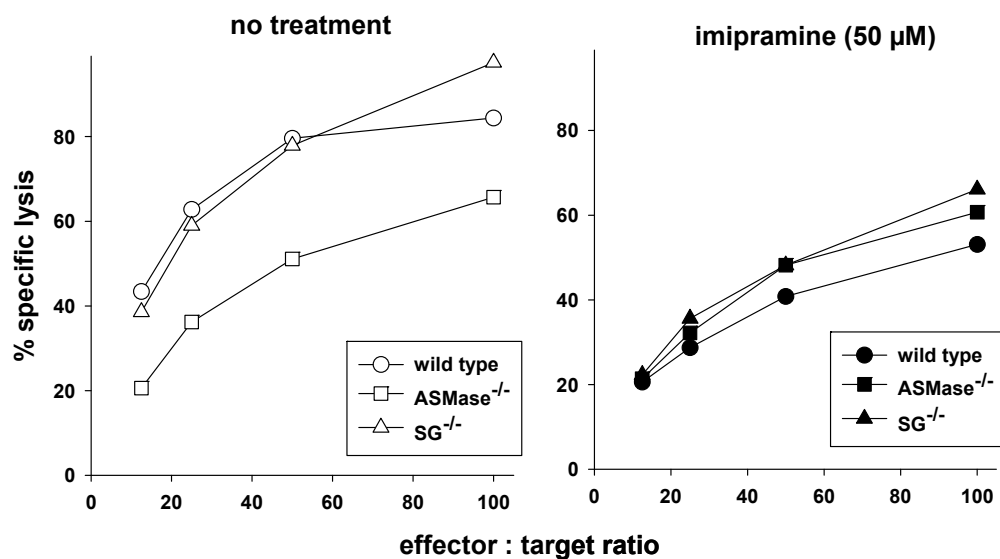


Fig. 23 Similarly impaired cytotoxic activity of $ASMase^{-/-}$ and $ASMase^{-/-}/SG^{-/-}$ CTL

Wild type, $SG^{-/-}$, $ASMase^{-/-}$ and $ASMase^{-/-}/SG^{-/-}$ mice were infected i.v. with 10^5 IU of the LCMV-WE.

(A) At day 8 after infection, $CD8^+$ T cells were immunomagnetically enriched from splenic single cell suspensions and used as effector cells in a 4 h standard [^{51}Cr]-release assay against C57BL/6-SV target cells loaded with 10^{-6} M gp₃₃ peptide. Shown are mean \pm standard errors of 6 experiments (wt n=6; $SG^{-/-}$ n=6; $ASMase^{-/-}$ n=8; $ASMase^{-/-}/SG^{-/-}$ n=7).

(B) The cytotoxic activity was measured in CTL that were pre-treated with 25 μ M imipramine against C57BL/6-SV in a 4 h standard [^{51}Cr]-release assay.

3.11 Monitoring exocytosis by patch-clamp experiments reveals in *ASMase*^{-/-} CD8⁺ T cells larger gains in membrane area than in wt T cells

Electrophysiological patch-clamp experiments were designed to monitor secretion of cytotoxic granules of *ASMase*^{-/-} CD8⁺ T cells.

ASMase^{-/-} CD8⁺ T cells responded with larger increases in capacitance for exocytotic events compared to wt CD8⁺ T cells (**Fig. 24A, B**). The capacitance is proportional to the area of vesicular membrane added by fusion to the plasma membrane. Therefore, post-fusion vesicles are larger in *ASMase*^{-/-} than in wt CD8⁺ T cells.

These data correspond with the larger size of cytotoxic granules stained with SRB after influx from the extracellular medium in *ASMase*^{-/-} T cells during secretion determined by TEP-microscopy (**Fig. 21**). This suggests that the deficiency in *ASMase* leads to defective extrusion of cytotoxic granule contents and might be due to a decrease in contractile tension of the vesicle membrane as discussed below.

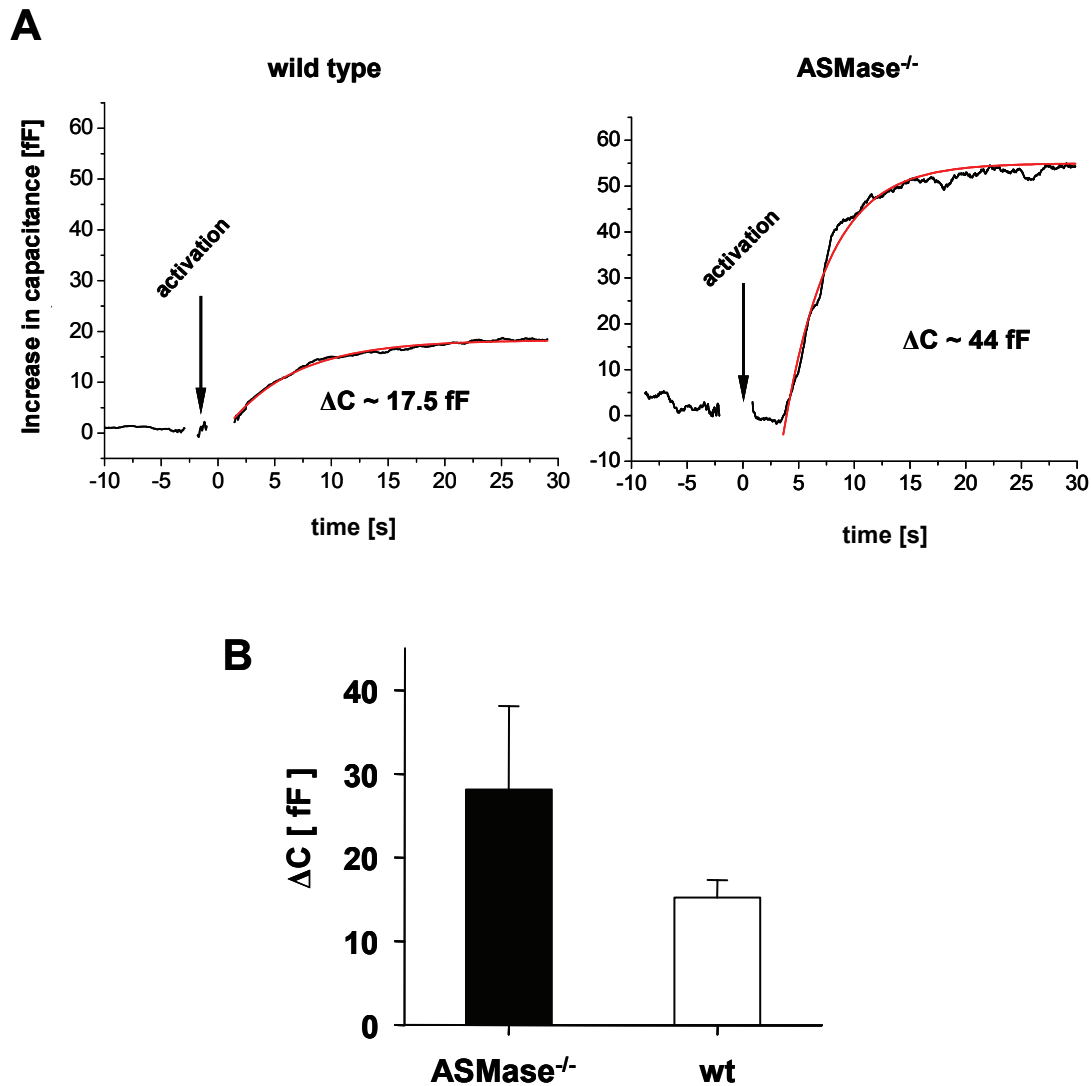


Fig. 24 Enhanced increases of capacitance observed by patch-clamp analysis of secretion in ASMase^{-/-} CD8⁺ T cells

Wild type and ASMase^{-/-} mice were infected i.v. with 10⁵ IU of the LCMV-WE. At day 8 after infection, CD8⁺ T cells were immunomagnetically enriched from splenic single cell suspensions and used in patch-clamp experiments that have been carried out by Elza Kuzmenkina and Stefan Herzig, Department of Pharmacology, Cologne.

(A) Capacitance diagram of one representative for each genotype and (B) corresponding mean \pm standard errors.

4. Discussion

ASMase-induced sphingomyelin hydrolysis has been implicated in many cellular responses to external stimuli. However, in many instances the precise mode of action remained unresolved. Deficiency of mice in ASMase severely affects the course of the immune response during acute LCMV infection. The clearance of the virus by ASMase^{-/-} mice is significantly impaired and virus-specific delayed type hypersensitivity (DTH) reaction is reduced (Diplom). To control acute infection with LCMV, CD8⁺ T cells are necessary and sufficient in mice (Moskophidis, Cobbold et al. 1987). Corresponding to the impaired control of the virus in ASMase^{-/-} mice, the cytotoxic activity of ASMase^{-/-} CD8⁺ T lymphocytes (CTL) *in vitro* was reduced. This work aimed at elucidating the ASMase-dependent mechanism in the cytotoxic machinery of CD8⁺ T cells.

The loading of cytotoxic granules both, with respect to biochemical and to morphological parameters is properly achieved in CTL of ASMase^{-/-} mice: wt and ASMase^{-/-} CTL were indistinguishable regarding a) mRNA copy numbers for gzmA, gzmB and perf, b) protein expression levels, c) their confinement to cytotoxic granules, d) their size and number per cell, e) the acidification of cytotoxic granules and f) enzymatic activity of gzms and perf, which clearly excludes any interference of transcription, translation, intracellular storage and processing of cytotoxic effector molecules by the absence of ASMase.

The accumulation of sphingomyelin in ASMase^{-/-} cells may impair the secretion of cytotoxic effector molecules by a lack of lipid rafts or alterations in the lipid composition of the plasma membrane as observed in various cell types of another strain of ASMase^{-/-} mice (Nix and Stoffel 2000). However, it has been reported that sphingolipid storage is observed predominantly in long-lived, non-proliferating cells of ASMase^{-/-} mice older than two months, but less pronounced in short-lived, proliferating cells such as T lymphocytes, especially in younger mice (Lozano, Morales et al. 2001). In the strain of ASMase^{-/-} mice used for this study, originally generated by Schuchmann and co-workers, none of the alterations described by Stoffel *et al.* (Nix and Stoffel 2000) were detectable (Lozano, Morales et al. 2001) and Diplom).

The lipid composition of the plasma membrane of ASMase^{-/-} CD8⁺ T cells does not show any alterations in comparison to wt CD8⁺ T cells. Furthermore, TCR-triggered release of calcium from intracellular storages is not altered in ASMase^{-/-}

CD8⁺ T cells. These findings exclude that deficiency in ASMase by affecting the composition of membrane lipids in general or specifically in lipid rafts impairs TCR-signalling as a possible cause of reduced secretion of cytotoxic granules.

It is also important to note that ASMase^{-/-} CD8⁺ CTL do not have a general secretory defect, because the secretion of the chemokine RANTES was not affected in these cells. RANTES is stored in and secreted via a specialized subcellular compartment of microvesicles, for which the term “RANTES secretory vesicle” was coined (Catalfamo, Karpova et al. 2004). In contrast, secretion of IFN- γ was impaired in ASMase^{-/-} CTL, which is not surprising, because we showed that IFN- γ localises to ASMase-positive vesicles in wt CTL.

Importantly, the phenotype of ASMase-deficiency is recapitulated by short term pharmacologic inhibition of ASMase by imipramine. Incubation of cells with imipramine leads to proteolytic degradation of ASMase (Hurwitz, Ferlinz et al. 1994). Short-term inhibition of ASMase activity does not allow accumulation of sphingomyelin. Therefore, selectively impaired secretion of cytotoxic granules and IFN- γ , but not of RANTES and imipramine-induced reduction of the cytolytic activity of CTL mimicking the effects of genetic absence of ASMase and preclude that the secretory defects of ASMase^{-/-} CTL are secondary to generally impaired vesicular traffic caused by sphingomyelin storage.

At the level of cellular organelles, the structural reorganization of a CTL required for granule exocytosis, i.e. 1) polarisation of granules towards the immunological synapse, 2) the release of cytotoxic granules from microtubules, 3) tethering, 4) docking to and 5) fusion with the plasma membrane were found to be intact in ASMase^{-/-} CD8⁺ CTL. This is shown by similar kinetics and extent of exposure of Lamp1 (CD107a) on the cell-surface after stimulation. Lamp1 localises to the inner membrane of the cytotoxic granule. After fusion of the granule with the plasma membrane, a fusion pore is formed, which allows Lamp1 to translocate to the plasma membrane. Similar kinetics and extent of Lamp1 expression in wt and ASMase^{-/-} CTL, indicate that the first four stages of exocytosis are intact in ASMase^{-/-} CD8⁺ T cells. In this respect, the ASMase dependent mechanism can be clearly distinguished from that of Rab27a and Munc13-4 which are required for the release of cytotoxic granules from microtubules and for the induction of SNARE-mediated fusion with the plasma membrane, respectively (Menasche, Pastural et al. 2000; Haddad, Wu et al. 2001; Feldmann, Callebaut et al. 2003).

By stepwise analysing the process of cytotoxic granules exocytosis this study revealed that ASMase impairs the final step of granule secretion after a fusion pore between the granule membrane and the plasma membrane has been formed.

Despite the exposure of Lamp1 on the surface of CTL, the release of gzm and other proteins from cytotoxic granules is reduced in ASMase-deficient CTL. Two independent lines of evidence suggest that cytotoxic effector molecules are retained within fused cytotoxic granules beneath the immunologic synapse in ASMase^{-/-} CTL and refrained from release. First, confocal microscopy of immunological synapses consistently revealed larger areas with gzmA positive granules adjacent to the immunologic synapse in ASMase^{-/-} CTL compared to wt CD8⁺ T cells. Second, two photon-microscopy showed that, post-fusion granules stained with the polar tracer SRB in the extracellular medium in ASMase^{-/-} CTL are significantly larger than in wt CD8⁺ T cells.

In CD8⁺ CTL, perf and gzms are stored in cytotoxic granules previously recognised as secretory lysosomes (Peters, Borst et al. 1991), which impose as dense-core vesicles in electron microscopy. Secretion of the contents of dense-core vesicles has been studied in greater detail in cells of the nervous system and of endocrine glands. In these cells, transmitters are bound to a condensed matrix, which reduces the osmolarity to allow storage of the transmitter at high concentrations within the vesicle (Artalejo, Elhamdani et al. 1998; Rutter and Tsuboi 2004). After complete degranulation of these vesicles the matrix is presumably dissolved to release the biologic active transmitter. In analogy, the acidified proteoglycan matrix allows CTL to store perforin and gzms at high concentrations required for cytolysis of target cells (Smyth, Kelly et al. 2001). Serglycin is the protein backbone to which the chondroitin sulfate glycosaminoglycans are covalently linked giving rise to high molecular weight serglycin-proteoglycans. Within cytotoxic granules up to 32 molecules of gzmB are complexed to one serglycin-proteoglycan molecule (Raja, Wang et al. 2002). With a molecular weight of about 300 kDa for serglycin-proteoglycan and 32 kDa for a single gzmB molecule, large supramolecular complexes of up to 1300 kDa arise. By dynamic laser light scattering analysis the hydrodynamic diameter of serglycin-proteoglycan itself has been determined to reach about 140 nm (Raja, Wang et al. 2002). Thus, CTL do not secrete effector molecules as soluble monomers but rather as large stable complexes with a size in the order of

viruses. Apparently, the matrix complexed with cytotoxic proteins has to be dissolved by influx of fluid from the extracellular environment or expelled its entirety for release of the effector molecules within the cleft of the immunological synapse. Therefore, a possible requirement for ASMase in dissolving the high molecular weight matrix of granules was investigated in CD8⁺ T cells by using mice deficient for serglycin (SG^{-/-}). Importantly, deficiency of the matrix core protein serglycin results in the lack of the electron dense core in cytotoxic granules of CTL, while these cells are otherwise not morphologically impaired. CTL of SG^{-/-} mice do not exert at least as effective cytotoxic activity as wt CD8⁺ T cells (Grujic, Braga et al. 2005) and exhibit slightly increased release of low molecular weight [³⁵S]-labelled matrix as compared to wt CD8⁺ T cells. Remarkably, additional deficiency in ASMase impairs the cytotoxic activity of serglycin^{-/-} CD8⁺ T cells to the same extent as observed in ASMase^{-/-} CD8⁺ T cells, which are competent to synthesize serglycin-proteoglycans. This argues against ASMase contributing to dissolve the dense core material during secretion of cytotoxic granules.

Decisive insight into the mechanistic effect of ASMase was provided by electrophysiological analysis of secretory events in CD8⁺ T cells: In ASMase^{-/-} T cells a considerable fraction of individual secretory events was characterised by larger increases of capacitance than those observed in wt T cells. Since the increase in capacitance is proportional to the area of vesicular membrane added by fusion to the plasma membrane these data are in accordance with the larger diameters of granules in ASMase^{-/-} CTL after fusion with the plasma membrane as detected by influx of extracellular tracers in vital microscopy. Prior to stimulation, the size of cytotoxic granules does not differ between ASMase^{-/-} and wt CD8⁺ T cells. The detection of larger post-fusion granules suggests that the granules fused with the plasma membrane do not properly collapse in ASMase^{-/-} CD8⁺ T cells. The effects of ASMase activity upon the biophysical properties of cytotoxic granules facilitate the collapse of fused granules as follows. The removal of the head group phosphorylcholine from sphingomyelin generates ceramide in the luminal leaflet of the granule's membrane. Ceramide requires less space within the luminal surface of the membrane so that the surface tension increases within this leaflet. Due to the asymmetric distribution of sphingomyelin in the membrane and the localization of ASMase exclusively in the lumen of the granule, the outer leaflet of the membrane is not altered, thereby preventing the granule from shrinking as long as its membrane is

not fused to the plasma membrane. After fusion, however, the contractile surface tension can be released by the granule collapsing into the plasma membrane. In granules of ASMase^{-/-} CD8⁺ T cells, the lack of surface tension leads to an impaired collapse of the granule resulting in reduced extrusion of its contents. This explanation is supported by Laplace's law describing the transmural pressure (p) of contractile spherical bodies as a function of the radius of the body (r), the tension (t) and thickness (d) of the surrounding membrane as: $p = 2t / (r * d)$. We determined the radius (r) of granules in wt and ASMase^{-/-} CD8⁺ T cells to be identical and the thickness (d) of biomembranes is constant. Thus, the transmural pressure of cytotoxic granules is directly proportional to the tension of its membrane, which is increased by ASMase activity as described above.

It has been shown recently, that neutral SMase activity suffices to initiate inside budding of microvesicles into artificial giant unilamellar vesicles (Trajkovic, Hsu et al. 2008). Mechanistically, the generation of cone-shaped ceramide on the surface of those giant vesicles creates an area difference between its outer and inner membrane leaflet, i.e. surface tension that generates stretches of negative curvature resulting in inward budding. The opposite effects of budding in the giant vesicles and collapsing in CTL, both are due to the asymmetrical localization of the substrate, sphingomyelin and the distinct subcellular localisation.

5. References

- Albouz, S., F. Le Saux, et al. (1986). "Modifications of sphingomyelin and phosphatidylcholine metabolism by tricyclic antidepressants and phenothiazines." Life Sci **38**(4): 357-63.
- Angleson, J. K., A. J. Cochilla, et al. (1999). "Regulation of dense core release from neuroendocrine cells revealed by imaging single exocytic events." Nat Neurosci **2**(5): 440-6.
- Artalejo, C. R., A. Elhamdani, et al. (1998). "Secretion: dense-core vesicles can kiss-and-run too." Curr Biol **8**(2): R62-5.
- Assenmacher, M., J. Schmitz, et al. (1994). "Flow cytometric determination of cytokines in activated murine T helper lymphocytes: expression of interleukin-10 in interferon-gamma and in interleukin-4-expressing cells." Eur J Immunol **24**(5): 1097-101.
- Barry, M. and R. C. Bleackley (2002). "Cytotoxic T lymphocytes: all roads lead to death." Nat Rev Immunol **2**(6): 401-9.
- Bollinger, C. R., V. Teichgraber, et al. (2005). "Ceramide-enriched membrane domains." Biochim Biophys Acta **1746**(3): 284-94.
- Braga, T., M. Grujic, et al. (2007). "Serglycin proteoglycan is required for secretory granule integrity in mucosal mast cells." Biochem J **403**(1): 49-57.
- Brunner, K. T., J. Mauel, et al. (1968). "Quantitative assay of the lytic action of immune lymphoid cells on 51-Cr-labelled allogeneic target cells in vitro; inhibition by isoantibody and by drugs." Immunology **14**(2): 181-96.
- Buchmeier, M. J., R. M. Welsh, et al. (1980). "The virology and immunobiology of lymphocytic choriomeningitis virus infection." Adv Immunol **30**: 275-331.
- Burkhardt, J. K., S. Hester, et al. (1990). "The lytic granules of natural killer cells are dual-function organelles combining secretory and pre-lysosomal compartments." J Cell Biol **111**(6 Pt 1): 2327-40.
- Butz, E. and M. J. Bevan (1998). "Dynamics of the CD8+ T cell response during acute LCMV infection." Adv Exp Med Biol **452**: 111-22.
- Butz, E. A. and M. J. Bevan (1998). "Massive expansion of antigen-specific CD8+ T cells during an acute virus infection." Immunity **8**(2): 167-75.
- Catalfamo, M., T. Karpova, et al. (2004). "Human CD8+ T cells store RANTES in a unique secretory compartment and release it rapidly after TcR stimulation." Immunity **20**(2): 219-30.

- Chalfant, C. E., Z. Szulc, et al. (2004). "The structural requirements for ceramide activation of serine-threonine protein phosphatases." J Lipid Res **45**(3): 496-506.
- Cifone, M. G., P. Roncaioli, et al. (1995). "Multiple pathways originate at the Fas/APO-1 (CD95) receptor: sequential involvement of phosphatidylcholine-specific phospholipase C and acidic sphingomyelinase in the propagation of the apoptotic signal." Embo J **14**(23): 5859-68.
- Clark, R. H., J. C. Stinchcombe, et al. (2003). "Adaptor protein 3-dependent microtubule-mediated movement of lytic granules to the immunological synapse." Nat Immunol **4**(11): 1111-20.
- Diwu, Z., C. S. Chen, et al. (1999). "A novel acidotropic pH indicator and its potential application in labeling acidic organelles of live cells." Chem Biol **6**(7): 411-8.
- Ebnet, K., M. Hausmann, et al. (1995). "Granzyme A-deficient mice retain potent cell-mediated cytotoxicity." Embo J **14**(17): 4230-9.
- Feldmann, J., I. Callebaut, et al. (2003). "Munc13-4 is essential for cytolytic granules fusion and is mutated in a form of familial hemophagocytic lymphohistiocytosis (FHL3)." Cell **115**(4): 461-73.
- Fruth, U., M. Prester, et al. (1987). "The T cell-specific serine proteinase TSP-1 is associated with cytoplasmic granules of cytolytic T lymphocytes." Eur J Immunol **17**(5): 613-21.
- Futerman, A. H. and Y. A. Hannun (2004). "The complex life of simple sphingolipids." EMBO Rep **5**(8): 777-82.
- Futerman, A. H. and H. Riezman (2005). "The ins and outs of sphingolipid synthesis." Trends Cell Biol **15**(6): 312-8.
- Gairin, J. E., H. Mazarguil, et al. (1995). "Optimal lymphocytic choriomeningitis virus sequences restricted by H-2Db major histocompatibility complex class I molecules and presented to cytotoxic T lymphocytes." J Virol **69**(4): 2297-305.
- Goni, F. M. and A. Alonso (2002). "Sphingomyelinases: enzymology and membrane activity." FEBS Lett **531**(1): 38-46.
- Gouy, H., D. Cefai, et al. (1990). "Ca²⁺ influx in human T lymphocytes is induced independently of inositol phosphate production by mobilization of intracellular Ca²⁺ stores. A study with the Ca²⁺ endoplasmic reticulum-ATPase inhibitor thapsigargin." Eur J Immunol **20**(10): 2269-75.
- Grassme, H., E. Gulbins, et al. (1997). "Acidic sphingomyelinase mediates entry of *N. gonorrhoeae* into nonphagocytic cells." Cell **91**(5): 605-15.
- Grassme, H., J. Jin, et al. (2006). "Regulation of pulmonary *Pseudomonas aeruginosa* infection by the transcriptional repressor Gfi1." Cell Microbiol **8**(7): 1096-105.

- Grassme, H., H. Schwarz, et al. (2001). "Molecular mechanisms of ceramide-mediated CD95 clustering." Biochem Biophys Res Commun **284**(4): 1016-30.
- Griffiths, G. M. and S. Isaacs (1993). "Granzymes A and B are targeted to the lytic granules of lymphocytes by the mannose-6-phosphate receptor." J Cell Biol **120**(4): 885-96.
- Grujic, M., T. Braga, et al. (2005). "Serglycin-deficient cytotoxic T lymphocytes display defective secretory granule maturation and granzyme B storage." J Biol Chem **280**(39): 33411-8.
- Gulbins, E. and P. L. Li (2006). "Physiological and pathophysiological aspects of ceramide." Am J Physiol Regul Integr Comp Physiol **290**(1): R11-26.
- Haddad, E. K., X. Wu, et al. (2001). "Defective granule exocytosis in Rab27a-deficient lymphocytes from Ashen mice." J Cell Biol **152**(4): 835-42.
- Heinrich, M., M. Wickel, et al. (2000). "Ceramide as an activator lipid of cathepsin D." Adv Exp Med Biol **477**: 305-15.
- Henkart, P. A., M. S. Williams, et al. (1997). "Do CTL kill target cells by inducing apoptosis?" Semin Immunol **9**(2): 135-44.
- Hofmann, K. and V. M. Dixit (1998). "Ceramide in apoptosis--does it really matter?" Trends Biochem Sci **23**(10): 374-7.
- Hofmann, K. and V. M. Dixit (1999). "Reply to kolesnick and hannun, and perry and hannun." Trends Biochem Sci **24**(6): 227.
- Holopainen, J. M., M. I. Angelova, et al. (2000). "Vectorial budding of vesicles by asymmetrical enzymatic formation of ceramide in giant liposomes." Biophys J **78**(2): 830-8.
- Holopainen, J. M., J. Saarikoski, et al. (2001). "Elevated lysosomal pH in neuronal ceroid lipofuscinoses (NCLs)." Eur J Biochem **268**(22): 5851-6.
- Holopainen, J. M., M. Subramanian, et al. (1998). "Sphingomyelinase induces lipid microdomain formation in a fluid phosphatidylcholine/sphingomyelin membrane." Biochemistry **37**(50): 17562-70.
- Holthuis, J. C. and T. P. Levine (2005). "Lipid traffic: floppy drives and a superhighway." Nat Rev Mol Cell Biol **6**(3): 209-20.
- Horinouchi, K., S. Erlich, et al. (1995). "Acid sphingomyelinase deficient mice: a model of types A and B Niemann-Pick disease." Nat Genet **10**(3): 288-93.
- Hurwitz, R., K. Ferlinz, et al. (1994). "The tricyclic antidepressant desipramine causes proteolytic degradation of lysosomal sphingomyelinase in human fibroblasts." Biol Chem Hoppe Seyler **375**(7): 447-50.

- Huwiler, A., D. Fabbro, et al. (1998). "Selective ceramide binding to protein kinase C- α and - δ isoenzymes in renal mesangial cells." Biochemistry **37**(41): 14556-62.
- Jahn, R., T. Lang, et al. (2003). "Membrane fusion." Cell **112**(4): 519-33.
- Kägi, D., B. Ledermann, et al. (1994). "Cytotoxicity mediated by T cells and natural killer cells is greatly impaired in perforin-deficient mice." Nature **369**(6475): 31-7.
- Kanfer, J. N., O. M. Young, et al. (1966). "The metabolism of sphingomyelin. I. Purification and properties of a sphingomyelin-cleaving enzyme from rat liver tissue." J Biol Chem **241**(5): 1081-4.
- Kasai, H., H. Hatakeyama, et al. (2005). "A new quantitative (two-photon extracellular polar-tracer imaging-based quantification (TEPIQ)) analysis for diameters of exocytic vesicles and its application to mouse pancreatic islets." J Physiol **568**(Pt 3): 891-903.
- Kataoka, T., K. Takaku, et al. (1994). "Acidification is essential for maintaining the structure and function of lytic granules of CTL. Effect of concanamycin A, an inhibitor of vacuolar type H(+)-ATPase, on CTL-mediated cytotoxicity." J Immunol **153**(9): 3938-47.
- Kolesnick, R. and Y. A. Hannun (1999). "Ceramide and apoptosis." Trends Biochem Sci **24**(6): 224-5; author reply 227.
- Krönke, M. (1999). "Biophysics of ceramide signaling: interaction with proteins and phase transition of membranes." Chem Phys Lipids **101**(1): 109-21.
- Krut, O., K. Wiegmann, et al. (2006). "Novel tumor necrosis factor-responsive mammalian neutral sphingomyelinase-3 is a C-tail-anchored protein." J Biol Chem **281**(19): 13784-93.
- Lehmann-Grube, F. and J. Ambrassat (1977). "A new method to detect lymphocytic choriomeningitis virus-specific antibody in human sera." J Gen Virol **37**(1): 85-92.
- Lehmann-Grube, F., J. Lohler, et al. (1993). "Antiviral immune responses of lymphocytic choriomeningitis virus-infected mice lacking CD8+ T lymphocytes because of disruption of the beta 2-microglobulin gene." J Virol **67**(1): 332-9.
- Levade, T. and J. P. Jaffrezou (1999). "Signalling sphingomyelinases: which, where, how and why?" Biochim Biophys Acta **1438**(1): 1-17.
- Lowin, B., C. Mattman, et al. (1996). "Comparison of Fas(Apo-1/CD95)- and perforin-mediated cytotoxicity in primary T lymphocytes." Int Immunol **8**(1): 57-63.
- Lozano, J., A. Morales, et al. (2001). "Niemann-Pick Disease versus acid sphingomyelinase deficiency." Cell Death Differ **8**(1): 100-3.

- Martin, P., R. Wallich, et al. (2005). "Quiescent and activated mouse granulocytes do not express granzyme A and B or perforin: similarities or differences with human polymorphonuclear leukocytes?" Blood **106**(8): 2871-8.
- Masson, D., P. J. Peters, et al. (1990). "Interaction of chondroitin sulfate with perforin and granzymes of cytolytic T-cells is dependent on pH." Biochemistry **29**(51): 11229-35.
- Menasche, G., E. Pastural, et al. (2000). "Mutations in RAB27A cause Griscelli syndrome associated with haemophagocytic syndrome." Nat Genet **25**(2): 173-6.
- Moskophidis, D., U. Assmann-Wischer, et al. (1987). "The immune response of the mouse to lymphocytic choriomeningitis virus. V. High numbers of cytolytic T lymphocytes are generated in the spleen during acute infection." Eur J Immunol **17**(7): 937-42.
- Moskophidis, D., S. P. Cobbold, et al. (1987). "Mechanism of recovery from acute virus infection: treatment of lymphocytic choriomeningitis virus-infected mice with monoclonal antibodies reveals that Lyt-2+ T lymphocytes mediate clearance of virus and regulate the antiviral antibody response." J Virol **61**(6): 1867-74.
- Nix, M. and W. Stoffel (2000). "Perturbation of membrane microdomains reduces mitogenic signaling and increases susceptibility to apoptosis after T cell receptor stimulation." Cell Death Differ **7**(5): 413-24.
- Oldstone, M. B. (2002). "Biology and pathogenesis of lymphocytic choriomeningitis virus infection." Curr Top Microbiol Immunol **263**: 83-117.
- Otterbach, B. and W. Stoffel (1995). "Acid sphingomyelinase-deficient mice mimic the neurovisceral form of human lysosomal storage disease (Niemann-Pick disease)." Cell **81**(7): 1053-61.
- Perry, D. K. and Y. A. Hannun (1999). "The use of diglyceride kinase for quantifying ceramide." Trends Biochem Sci **24**(6): 226-7.
- Peters, P. J., J. Borst, et al. (1991). "Cytotoxic T lymphocyte granules are secretory lysosomes, containing both perforin and granzymes." J Exp Med **173**(5): 1099-109.
- Peters, P. J., E. Bos, et al. (2006). "Cryo-immunogold electron microscopy." Curr Protoc Cell Biol **Chapter 4**: Unit 4 7.
- Powell, A. D. and N. V. Marrion (2007). "Resolution of fusion pore formation in a cell-attached patch." J Neurosci Methods **162**(1-2): 272-81.
- Raja, S. M., S. S. Metkar, et al. (2003). "Cytotoxic granule-mediated apoptosis: unraveling the complex mechanism." Curr Opin Immunol **15**(5): 528-32.

- Raja, S. M., B. Wang, et al. (2002). "Cytotoxic cell granule-mediated apoptosis. Characterization of the macromolecular complex of granzyme B with serglycin." J Biol Chem **277**(51): 49523-30.
- Rubio, V., T. B. Stuge, et al. (2003). "Ex vivo identification, isolation and analysis of tumor-cytolytic T cells." Nat Med **9**(11): 1377-82.
- Rutter, G. A. and T. Tsuboi (2004). "Kiss and run exocytosis of dense core secretory vesicles." Neuroreport **15**(1): 79-81.
- Schneider-Brachert, W., V. Tchikov, et al. (2004). "Compartmentalization of TNF receptor 1 signaling: internalized TNF receptosomes as death signaling vesicles." Immunity **21**(3): 415-28.
- Schütze, S., K. Potthoff, et al. (1992). "TNF activates NF-kappa B by phosphatidylcholine-specific phospholipase C-induced "acidic" sphingomyelin breakdown." Cell **71**(5): 765-76.
- Shresta, S., T. A. Graubert, et al. (1999). "Granzyme A initiates an alternative pathway for granule-mediated apoptosis." Immunity **10**(5): 595-605.
- Shresta, S., C. T. Pham, et al. (1998). "How do cytotoxic lymphocytes kill their targets?" Curr Opin Immunol **10**(5): 581-7.
- Smyth, M. J., J. M. Kelly, et al. (2001). "Unlocking the secrets of cytotoxic granule proteins." J Leukoc Biol **70**(1): 18-29.
- Stinchcombe, J. C., D. C. Barral, et al. (2001). "Rab27a is required for regulated secretion in cytotoxic T lymphocytes." J Cell Biol **152**(4): 825-34.
- Stinchcombe, J. C., G. Bossi, et al. (2001). "The immunological synapse of CTL contains a secretory domain and membrane bridges." Immunity **15**(5): 751-61.
- Stinchcombe, J. C. and G. M. Griffiths (1999). "Regulated secretion from hemopoietic cells." J Cell Biol **147**(1): 1-6.
- Stinchcombe, J. C. and G. M. Griffiths (2007). "Secretory mechanisms in cell-mediated cytotoxicity." Annu Rev Cell Dev Biol **23**: 495-517.
- Trajkovic, K., C. Hsu, et al. (2008). "Ceramide triggers budding of exosome vesicles into multivesicular endosomes." Science **319**(5867): 1244-7.
- Utermöhlen, O., U. Karow, et al. (2003). "Severe impairment in early host defense against *Listeria monocytogenes* in mice deficient in acid sphingomyelinase." J Immunol **170**(5): 2621-8.
- Vergne, I., P. Constant, et al. (1998). "Phagosomal pH determination by dual fluorescence flow cytometry." Anal Biochem **255**(1): 127-32.

-
- Vyas, Y. M., H. Maniar, et al. (2002). "Visualization of signaling pathways and cortical cytoskeleton in cytolytic and noncytolytic natural killer cell immune synapses." Immunol Rev **189**: 161-78.
- Watts, J. D., R. Aebersold, et al. (1999). "Ceramide second messengers and ceramide assays." Trends Biochem Sci **24**(6): 228.
- Wiegmann, K., S. Schütze, et al. (1994). "Functional dichotomy of neutral and acidic sphingomyelinases in tumor necrosis factor signaling." Cell **78**(6): 1005-15.
- Zentgraf, H. and W. W. Franke (1984). "Differences of supranucleosomal organization in different kinds of chromatin: cell type-specific globular subunits containing different numbers of nucleosomes." J Cell Biol **99**(1 Pt 1): 272-86.
- Zhang, Y., B. Yao, et al. (1997). "Kinase suppressor of Ras is ceramide-activated protein kinase." Cell **89**(1): 63-72.
- Zinkernagel, R. M. (2002). "Lymphocytic choriomeningitis virus and immunology." Curr Top Microbiol Immunol **263**: 1-5.

6. Abstract

The acid sphingomyelinase (ASMase) hydrolyses the membrane lipid sphingomyelin into ceramide and phosphorylcholine. ASMase localises to phagosomes, endosomes, lysosomes and the plasma membrane, i.e. those subcellular sites which are at the crossroads of many immunological processes. One of these is granule-mediated cytotoxicity as the major effector mechanism of CD8⁺ cytotoxic T lymphocytes (CTL). Cytotoxic granules have been characterized previously as secretory lysosomes. This raised the question, whether ASMase contributes to granule-mediated cytotoxicity of CD8⁺ T cells. In my diploma project, I have already shown that ASMase is required for the effective control of the acute infection with the Lymphocytic Choriomeningitis Virus (LCMV) in mice. More specifically, ASMase-deficient (ASMase^{-/-}) CTL were shown to be severely impaired in their virus-specific cytotoxicity. This project aimed at elucidating the ASMase-dependent mechanism contributing to effective cytotoxicity of CD8⁺ CTL.

Analysis of ASMase^{-/-} CD8⁺ T cells revealed that the transcription, translation, intracellular storage and processing of cytotoxic effector molecules proceed without defects. Moreover, in ASMase^{-/-} CD8⁺ T cells no hints for the accumulation of sphingomyelin were detected. These findings excluded excessive sphingomyelin as the cause for impaired cytotoxicity. The specificity of the ASMase-dependent mechanism was shown by a strongly reduced T cell receptor-triggered release of cytotoxic effector molecules while secretion of the chemokine RANTES was not impaired in ASMase^{-/-} CTL.

In ASMase^{-/-} T cells, cytotoxic granules were shown to fuse properly with the plasma membrane at the immunological synapse. The very last step of granule exocytosis, i.e. the extrusion of granular contents, is impaired by deficiency in ASMase. Even in CTL unable to generate high molecular weight granule matrix, the secretion of low molecular weight granule contents was strongly impaired by ASMase-deficiency.

Biomorphometry revealed that cytotoxic granules are of identical size in wt and ASMase^{-/-} CTL prior to fusion with the plasma membrane. However, after fusion with the plasma membrane, in ASMase^{-/-} CD8⁺ T cells the granules remain significantly larger than in wt cells. This phenomenon can be explained by the biophysical consequences of ASMase activity: Generation of ceramide in wt cells increases the surface tension within the inner leaflet of cytotoxic granules. According to Laplace's law this facilitates the collapse of the fused granule, thus leading to effective extrusion of the granules contents.

7. Zusammenfassung

Die saure Sphingomyelinase (ASMase) hydrolysiert das Membranlipid Sphingomyelin zu Ceramid und Phosphorylcholin. ASMase ist in Phagosomen, Endosomen, Lysosomen und an der Plasmamembran lokalisiert, d.h. an den subzellulären Orten, die Schnittstelle vieler immunologischer Prozesse sind. Einer hiervon ist die Granula-vermittelte zytotoxische Aktivität als wichtigster zytotoxischer Effektormechanismus von CD8⁺ zytotoxischen T Lymphozyten (CTL). Zytotoxische Granula wurden bereits als sekretorische Lysomen charakterisiert. Daraus entstand die Frage, ob die ASMase an der Granula-vermittelten Zytotoxizität von CD8⁺ T Zellen mitwirkt. In meiner Diplomarbeit habe ich bereits gezeigt, dass die ASMase für die effektive Elimination des Virus der Lymphozytären Choriomeningitis (LCMV) aus akut infizierten Mäusen notwendig ist. ASMase-defiziente CTL sind in ihrer virus-spezifischen Zytotoxizität stark beeinträchtigt. Ziel dieser Arbeit ist die Aufklärung der ASMase-abhängigen Mechanismen, die zu einer effektiven Zytotoxizität von CD8⁺ T Zellen beitragen. Die Spezifität des ASMase-abhängigen Mechanismus wurde nachgewiesen durch eine stark reduzierte Ausschüttung der zytotoxischen Effektormoleküle nach Stimulation des T-Zell Rezeptors, wohingegen die Sekretion von RANTES nicht beeinträchtigt war.

Die Analyse von ASMase^{-/-} CTL zeigte, dass die Transkription, Translation, intrazelluläre Speicherung und Prozessierung der zytotoxischen Effektormoleküle ungestört ist. Außerdem wurden in ASMase^{-/-} CTL keine Hinweise auf die Akkumulation von Sphingomyelin gefunden. Diese Daten schließen die übermäßige Speicherung von Sphingomyelin als Ursache für die beeinträchtigte Zytotoxizität aus.

Überraschenderweise fusionieren in ASMase^{-/-} CTL die zytotoxischen Granula unbeeinträchtigt mit der Plasmamembran. Allerdings ist der letzte Schritt der Exozytose zytotoxischer Granula, die Extrusion des Granulainhalts, in ASMase^{-/-} T-Zellen gestört. Sogar in CTL, die keine hochmolekulare Granulamatrix synthetisieren können, war die Sekretion von niedermolekularem Granulainhalt durch den Defekt der ASMase stark gestört.

Biomorphometrische Messungen zeigten, dass zytotoxische Granula vor der Fusion mit der Plasmamembran in ASMase^{-/-} CTL genauso groß sind wie in wt CTL. Allerdings bleiben die Granula nach der Fusion mit der Plasmamembran in ASMase^{-/-} T-Zellen signifikant größer als in wt Zellen. Dieses Phänomen kann über die biophysikalischen Eigenschaften der ASMase Aktivität erklärt werden: die Bildung von Ceramid in wt CD8⁺ T-Zellen erhöht die Oberflächenspannung der inneren Membrane des zytotoxischen Granulum. In Übereinstimmung mit Laplace's Gesetz, ermöglicht dies den Kollaps des fusionierten Granulums, was zu einer effektiven Ausschüttung des Granulainhalts führt.

Curriculum Vitae

Jasmin Herz

geboren am 04. Juli 1979

in Bergisch Gladbach

deutsche Staatsangehörigkeit

Hochschulausbildung:

- | | |
|-------------|--|
| seit 2004 | Promotionsstudium am Institut für Medizinische Mikrobiologie, Immunologie und Hygiene der Uniklinik Köln |
| 2003 – 2004 | Diplomarbeit in Biologie am Institut für Medizinische Mikrobiologie, Immunologie und Hygiene der Uniklinik Köln bei Prof. Dr. Martin Krönke unter der Anleitung von Olaf Utermöhlen
Thema: „Die akute Infektion von Saure Sphingomyelinase-defizienten Mäusen mit dem Virus der Lymphozytären Choriomeningitis“ |
| 1998 – 2003 | Studium der Biologie an der Universität zu Köln
Hauptfach: Genetik
Nebenfächer: Biochemie und Pharmakologie |

Schulbildung:

- | | |
|-------------|--|
| 1995 – 1998 | Allgemeine Hochschulreife
Paul-Klee-Gymnasium in Overath |
| 1989 – 1995 | Realschulabschluss
Johannes-Gutenberg-Realschule in Bergisch Gladbach |
| 1985-1989 | Gemeinschaftsgrundschule Kippekausen |

Danksagung

Für die wertvollen Diskussionen, die bedeutenden wissenschaftlichen Ideen und die engagierte Leitung während der gesamten Arbeit möchte ich mich bei Herrn Prof. Dr. Martin Krönke bedanken.

Besonders danke ich PD Dr. Olaf Utermöhlen für seine begeisternd kreativen Anregungen, die ausgezeichnete wissenschaftliche Anleitung und letztendlich die kritische Korrektur dieser Arbeit.

Bei Ulrike Karow, Tina Tosetti, Nikola Baschuk, Eva Glowalla, Daniela Grumme, Zeinab Abdullah und allen anderen Mitarbeitern des Institutes bedanke ich mich herzlich sowohl für die fachliche als auch private Unterstützung und Hilfsbereitschaft, sowie die gute Zusammenarbeit in den letzten Jahren.

Die Durchführung dieser Arbeit wurde zudem erst durch die Kooperationspartner ermöglicht, denen ich auf diesem Weg noch einmal meinen Dank aussprechen möchte: Hamid Kashkar, Michael Schramm und Katja Krönke-Wiegmann aus unserem Institut, Julian Pardo und Markus M. Simon des MPI für Immunbiologie in Freiburg, Eric Bos und Peter J. Peters vom NCRZ, Amsterdam, Elmon Schmelzer vom MPI für Züchtungsforschung, Elza Kuzmenkina und Stefan Herzig aus dem Institut für Pharmakologie in Köln. Danke, für die ertragsreiche und exzellente wissenschaftliche Zusammenarbeit.

Mein Dank gilt meinen Eltern und meinen Freunden, besonders meiner Schwester Nadine, Damian und Tina die mich nach unbegrenzten Kräften liebevoll unterstützt und mir so die Durchführung dieser Arbeit ermöglicht haben.

Erklärung

Ich versichere, dass ich die von mir vorgelegte Dissertation selbständig angefertigt, die benutzten Quellen und Hilfsmittel vollständig angegeben und die Stellen der Arbeit – einschließlich Tabellen, Karten und Abbildungen –, die anderen Werken im Wortlaut oder dem Sinn nach entnommen sind, in jedem Einzelfall als Entlehnung kenntlich gemacht habe; dass diese Dissertation noch keiner anderen Fakultät oder Universität zur Prüfung vorgelegen hat; dass sie – abgesehen von unten angegebenen Teilpublikationen - noch nicht veröffentlicht worden ist sowie, dass ich eine solche Veröffentlichung vor Abschluss des Promotionsverfahrens nicht vornehmen werde.

Die Bestimmungen der Promotionsordnung sind mir bekannt. Die von mir vorgelegte Arbeit ist von Herrn Prof. Dr. Martin Krönke betreut worden.

Fusogenicity of membranes: The impact of acid sphingomyelinase on innate immune response

Olaf Utermöhlen, Jasmin Herz, Michael Schramm, Martin Krönke
Immunobiology (2008) 213, 307-314

Acid sphingomyelinase is required for efficient phago-lysosomal fusion

Michael Schramm, Jasmin Herz, Albert Haas, Martin Krönke, Olaf Utermöhlen
Cellular Microbiology (2008) 10, 9, 1839-1853

Acid sphingomyelinase is a critical regulator of cytotoxic granule secretion by primary T lymphocytes

Jasmin Herz* , Julian Pardo* , Hamid Kashkar, Michael Schramm, Elza Kuzmenkina, Erik Bos, Katja Wiegmann, Reinhard Wallich, Peter J. Peters, Stefan Herzig, Elmon Schmelzer, Martin Krönke, Markus M. Simon and Olaf Utermöhlen
- In review by *Nature Immunology* -